Journal of Molecular Structure 1316 (2024) 139381

Contents lists available at ScienceDirect

Journal of Molecular Structure

journal homepage: www.elsevier.com/locate/molstr

Synthesis, characterization, biological evaluation and molecular docking study of some novel phenoxy methyl linked 1,2,3-triazole derivatives bridged with amide functionalities via 'click chemistry' approach

Rahul V. Parmar [a,*], Milan S. Vadodaria [a], Seema N. Kher [b], Nutan P. Vishwakarma [c]

[a] Chemical Research Laboratory, Shree M. & N. Virani Science College, Rajkot 360005, Gujarat India
[b] Department of Chemistry, Monark University, Ahmedabad 382330, Gujarat India
[c] Department of Biotechnology, Atmiya University, Rajkot 360005, Gujarat India

ARTICLE INFO

Keywords:
ADME
Antimicrobial activity
Click chemistry
CuAAC
1,4-disubstituted 1,2,3-triazoles
Minimal inhibitory concentrations
Molecular docking
Phenoxy Methyl

ABSTRACT

Herein, a new series of phenoxy methyl linked 1,4-disubstituted 1,2,3-triazole derivatives **(SR1–SR16)** was synthesized by click reaction and copper-catalyzed Huisgen [3 + 2] cycloaddition in the presence of copper sulphate and sodium ascorbate. All the newly synthesized compounds were characterized *via* Mass, ^{1}H NMR, ^{13}C NMR, FT-IR spectroscopy, and elemental analysis and evaluated for their antimalarial and antimicrobial activities. Among the synthesized compounds, **SR12** containing naphthyl substituent is found to be the most active compound with IC_{50} of 18.60 μM in antimalarial activities and **SR7** and **SR9** were found to exhibit good antimicrobial activity at 600.83 μM and 614.12 μM concentration respectively. The antimalarial activity of the synthesized compounds was further supplemented by molecular docking studies against the PfDHFR (PDB ID-3QGT) receptor, revealing that the remarkable binding affinity values and key interactions as compared to the standard reference Chloroquine. The drug-likeness properties of these compounds were supported by predicted pharmacokinetics.

1. Introduction

According to the report of WHO (2023), there are predictable 249 million malaria cases worldwide in 2022 in 85 malaria-endemic countries, reported hike of 5 million cases compared to 2021 [1]. Malaria: a parasitic disease which is spread by the female mosquitos: *Anopheles* genus and *Plasmodium* spp., the etiological agents of the disease with 5 species that can infect humans. P. *falciparum* has the uppermost dispersion and severity of the infection which is typically found in Sub-Saharan Africa. In Africa, the infections spread by this parasite, are accountable for most of death-rate in children. P. *vivax*, which is typically endemic of Asia [2] and South America [3] has now been recognized as malignant. In consideration of 15 million infections every year, and up to 2500 million people at peril, P. *vivax* is a valuable threat for all emerging nations in tropical and sub-tropical regions [4]. The strengthening of anticipation and controller measures led to 29% decrease in mortality rates by malarial disease around the world since 2010. Sub-Saharan-Africa is having highly irregular share of the world's malarial disease cases and deaths [5]. However, AMR (antimicrobial resistance) is also one of the chief health crises disturbing the health care system globally [6]. After COVID-19 pandemic further amplified antimicrobial resistance risk due to uncontrolled use of antibiotics; especially in developing countries [7]. Hence, to encounter against drug resistance and increase the ammunition against the scrounger, novel chemotherapeutic agents are required that can efficiently target a sexual stage of the parasite and assist in reaching our goal of malaria elimination and decrease microbial infection.

Heterocyclic scaffolds having nitrogen are significant class of the

Abbreviations and notation: ADME, Absorption, distribution, metabolism, and excretion; TLC, thin layer chromatography; ^{1}HNMR, Proton nuclear magnetic resonance; ^{13}CNMR, Carbon-13 nuclear magnetic resonance; FT-IR, Fourier transform infrared; MS, mass spectra; M.P, melting point; °C, Celsius;%, percentage; RT, room temperature; Pd/C, Palladium on carbon; H, hydrogen; N, nitrogen; HATU, 1-[Bis(dimethylamino)methylene]-1H-1,2,3-triazolo[4,5-b]pyridinium 3-oxide hexafluorophosphate; DIPEA, N,N-Diisopropylethylamine; DMSO, dimethyl sulfoxide; TMS, tetramethyl silat; K_2CO_3, Potassium carbonate; KBr, Potassium Bromide; Br, Bromine.

* Corresponding author.
E-mail address: rahulparmar1313@gmail.com (R.V. Parmar).

https://doi.org/10.1016/j.molstruc.2024.139381
Received 4 April 2024; Received in revised form 9 July 2024; Accepted 18 July 2024
Available online 24 July 2024

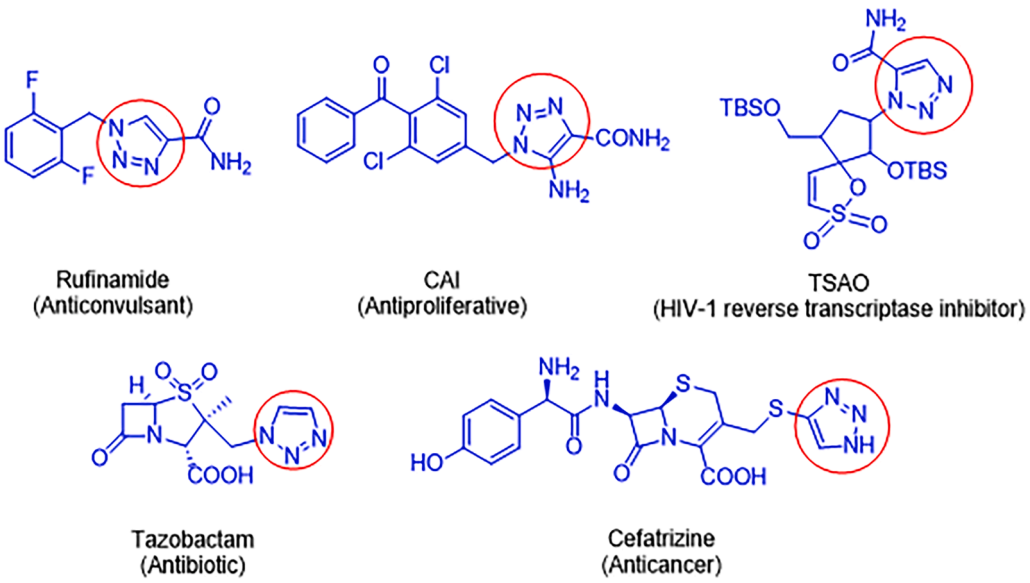

Fig. 1. 1,2,3-Triazole having marketed drugs.

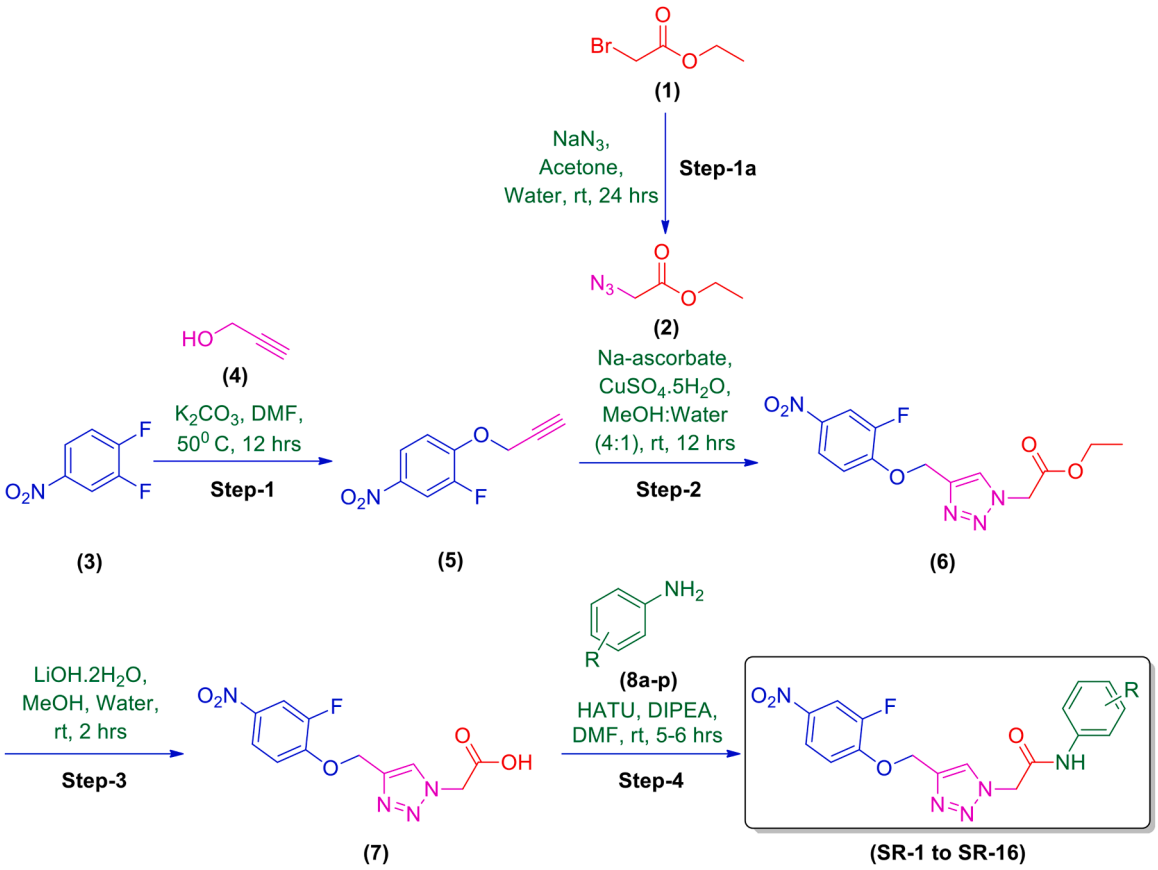

Scheme 1. The synthesis of amide derivatives of 2-(4-((2-fluoro-4-nitrophenoxy)methyl)−1*H*-1,2,3-triazol-1-yl) (**SR1-SR16**).

drug compounds, that exhibits miscellaneous targets and therapeutic properties. Because of their applications in medicinal chemistry with multivarious pharmaceutical actions and therapeutic index, the triazoles measured as one of the essential *N*-heterocyclic building blocks, which have received a unique interest [8]. Amongst them, 1,2,3-triazole scaffolds as a major pharmacophore, is one of the most significant class of nitrogen-rich heterocyclic moiety, that attracted substantial consideration with the help of 'click chemistry' approach owing to two prevalent contributions to the synthesis of 1,4-disubstituted-1,2,3-triazoles followed by the Ru-catalyzed synthesis of the 1,5-disubstituted isomer [9]. The azide-alkyne cycloaddition reaction in the presence of Cu(I)-catalyst (CuAAC) offers an adaptable root to the 1,2,3-triazoles moiety, that might form various non-covalent interactions, such as van der Waals forces, H-bonds, and dipole–dipole bonds with diverse

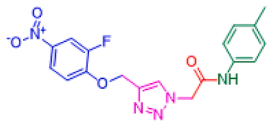

SR1 (5 h, 82%)

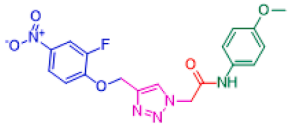

SR2 (6 h, 79%)

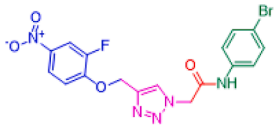

SR3 (5 h, 80%)

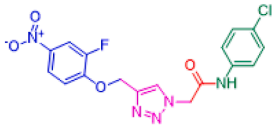

SR4 (5 h, 85%)

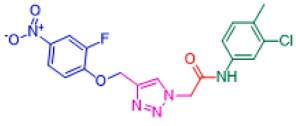

SR5 (5 h, 81%)

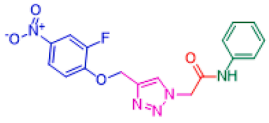

SR6 (6 h, 78%)

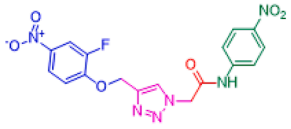

SR7 (6 h, 72%)

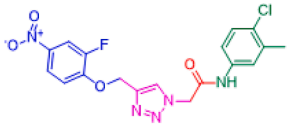

SR8 (5 h, 83%)

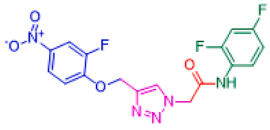

SR9 (6 h, 80%)

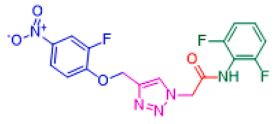

SR10 (6 h, 73%)

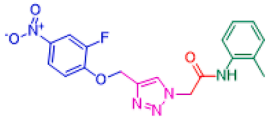

SR11 (5 h, 85%)

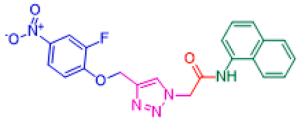

SR12 (6 h, 82%)

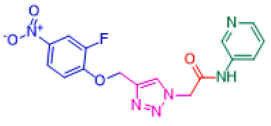

SR13 (6 h, 78%)

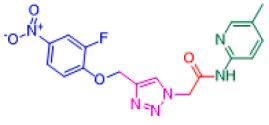

SR14 (6 h, 76%)

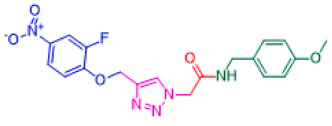

SR15 (5 h, 10%)

SR16 (6 h, 79%)

Fig. 2. Structure of 1,4-disubstituted 1,2,3-triazole amide derivatives (**SR1**–**SR16**).

Table 1
Docking Results and Key Interactions of Compounds with *Plasmodium falciparum* dihydrofolate reductase (PfDHFR).

Ligand	Binding Affinity (kcal/mol)	RMSD/ub*	RMSD/lb*
3QGT_A_Chloroquine_uff_E = 237.05	−7.1	0	0
3QGT_A_SR1_uff_E = 587.51	−8.8	0	0
3QGT_A_SR2_uff_E = 452.45	−8.9	0	0
3QGT_A_SR3_uff_E = 461.51	−9.1	0	0
3QGT_A_SR4_uff_E = 467.35	−9.2	0	0
3QGT_A_SR5_uff_E = 562.01	−8.7	0	0
3QGT_A_SR6_uff_E = 480.08	−8.2	0	0
3QGT_A_SR7_uff_E = 597.49	−9.4	0	0
3QGT_A_SR8_uff_E = 538.31	−8.9	0	0
3QGT_A_SR9_uff_E = 522.87	−8.8	0	0
3QGT_A_SR10_uff_E = 508.28	−9.2	0	0
3QGT_A_SR11_uff_E = 484.76	−9.2	0	0
3QGT_A_SR12_uff_E = 682.48	−10.7	0	0
3QGT_A_SR13_uff_E = 603.95	−8.7	0	0
3QGT_A_SR14_uff_E = 491.95	−8.5	0	0
3QGT_A_SR15_uff_E = 609.06	−9.5	0	0
3QGT_A_SR16_uff_E = 468.93	−9.7	0	0

* RMSD/lb (Root Mean Square Deviation/lower bound) and RMSD/ub (Root Mean Square Deviation/upper bound).

proteins, receptors, and enzymes with high resistance to enzymatic degradation, which permits their potential use in medicinal chemistry. From the last two decades, 1,2,3-triazoles moiety has been emerged as the one of the most potential pharmacophores having vital biological activities such as antibacterial [10], anti-cancer [11], antifungal [12], anti-human immunodeficiency virus (anti-HIV) [13], antidiabetic [14], and antimalarial [15]. In addition to that, a few medications linked 1,2,3-triazoles derivative based potential pharmaceuticals include the Rufinamide, Carboxy amido triazole (CAI), tert-butyl dimethyl silyl spiroamino oxathiole dioxide (TSAO), Tazobactam, Cefatrizine and I-A09 (Fig. 1).

Molecular docking is a computational method which aims to detect the preferred orientation of a ligand to its macromolecular receptor (target). Hence, ligands and receptors are bound to each other to produce a stable complex [16] which is a cost-effective, reliable, and time-saving technique in the field of drug discovery [17]. Various docking tools are available for commercial and academic purpose, such as DOCK [18], Autodock [19], Autodock Vina [20], PyRx [21], etc. Amongst them, the Autodock Vina of PyRx tool is an open-source software program used for present molecular docking study and Autodock Vina was utilized as an empirical scoring function to calculate the binding affinity of the protein-ligand complex [22].

However, based on all the prior information available in the literature with reference to the synthesis of new biologically active agents, our research aims the study of the 1,2,3-triazole nucleus in view of its significance of the biological properties. To develop the biological active moiety, diverse phenoxy methyl-1,2,3-triazoles were synthesized *via* "click chemistry" approach using CuAAC [23]. In view of the significant importance and with the aim of future biological study, we synthesized a new series of 1,4-disubstituted-1,2,3-triazoles moiety. The synthesized triazole derivatives were characterized through various spectroscopic techniques such as ^{1}H and ^{13}C NMR, FT-IR and mass spectra (MS). In addition to that, they were analyzed for their biological activities such as antimalarial, antimicrobial. Molecular docking computational study has been carried out. In this study, SwissADME web-server was utilized to compute ADME parameters, pharmacokinetic properties, druglike nature and medicinal chemistry friendliness of one or multiple small molecules to support drug discovery [24].

2. Experimental

2.1. Chemistry

All the solvents and reagents used for the synthesis were purchased from Sigma-Aldrich, Rankem India Ltd. and Spectrochem Pvt. Ltd. with 98–99% purity and used without further purification. A thin layer chromatography (TLC) on alumina plates coated with silica gel 60 F254, having 0.25 mm thickness (Merck) through which the reaction progress was monitored. Open glass capillary melting point was identified using fisher-johns melting point equipment. ^{1}HNMR spectra were recorded at 400 MHz and ^{13}CNMR spectra were recorded at 101 MHz on Bruker Avance III (400 MHz) spectrometer using DMSO-d^{6} as a solvent and tetramethylsilane (TMS) used as a domestic standard. Coupling constant which is denoted as a "*J*" is given in hertz (Hz) and "δ" is chemical shift is given in parts per million (ppm). ^{1}HNMR data were announced as multiplicity (singlet (s), doublet (d), triplet (t), quartet (q), quintet (quint), septet (sept), doublet or doubles (dd), doublet or triplet (dt), broad singlet (bs)). FT-IR analysis was carried out with FTIR 8400, CE Shimadzu instrument and it demonstrated the data in cm^{-1} (KBr). Mass spectral data were measured by Shimadzu GCMS–-QP-2010 mass spectrometer in ESI model through direct inlet probe technique and m/z is reported in atomic units per elementary charge.

2.2. General process for the synthesis of amide derivatives of 2-(4-((2-fluoro-4-nitrophenoxy)methyl)−1H-1,2,3-triazol-1-yl) (SR1-SR16)

Mixture of compound **(12)** (200 mg, 0.67 mol, 1 equiv.), DMF (2 mL) was added in HATU (381 mg, 1.00 mol, 1.5 equiv.) and stirred for 30 min. at RT. To this solution, different amines **(8a-p)** (0.74 mol, 1.1 equiv.) were added followed by the addition of DIPEA (259 mg, 2.01 mmol, 3 equiv.). The resulting solution was stirred at room temperature for 5–6 h until TLC showed the completion of the reaction. The mixture was poured into ice-water (40 mL) and resulting solid was filtered through Wattman filter paper. The resulting solid was triturated with MTBE and hexane to get pure derivatives **(SR1-SR16)** (Yield 72–85%).

2.2.1. 2-(4-((2-fluoro-4-nitrophenoxy)methyl)−1H-1,2,3-triazol-1-yl)-N-(p-tolyl)acetamide (SR1)

Compound **SR1** was obtained via 1,3-dipolar cycloaddition reaction between alkyne (**5**) and azide (**2**) and the resulting solution was further reacted with amine (**8a**) for 5 h lead to off-white solid; Yield: 82%; M.P.: 263 °C; **FT-IR** (KBr), cm^{-1}: 3263.66 (NH), 3093.92 (Ar-H), 2939.61 (C—H), 1666.55 (C = O), 1519.96 (C = C-Ar), 1350.22 (NO_2), 1219.05 (F-Ar), 1057.03 (C—O).; **^{1}H NMR** (400 MHz, DMSO-d^{6}) δ: 10.43 s (1H, -NH), 8.35 s (1H, H_{arom}), 8.20–8.17 d (2H_{arom}, *J* = 8.5 Hz), 7.68 s (1H, H_{arom}), 7.47–7.46 d (2H_{arom}, *J* = 7.5 Hz), 7.14–7.13 d (2H_{arom}, *J* = 9.5 Hz), 5.46 s (2H, CH_2), 5.36 s (2H, CH_2), 2.76 s (3H, CH_3).; **^{13}C NMR** (101 MHz, DMSO-d^{6}): 163.816, 151.866, 151.610, 149.140, 141.018, 140.360, 135.845, 132.746, 129.260, 126.996, 121.330, 119.179, 114.633, 112.203, 111.974, 62.519, 52.195, 20.410.; **Mass**: Calculated: 385.12, Found: 384.9; **Elemental Analysis:** Calculated for $C_{18}H_{16}FN_5O_4$: C-56.10, H-4.19, N-18.17 Found: C-56.08, H-4.17, N-18.15%

2.2.2. 2-(4-((2-fluoro-4-nitrophenoxy)methyl)−1H-1,2,3-triazol-1-yl)-N-(4-methoxyphenyl)acetamide (SR2)

Compound **SR2** was obtained via 1,3-dipolar cycloaddition reaction between alkyne (**5**) and azide (**2**) and the resulting solution was further reacted with amine (**8b**) for 6 h lead to the dark grey solid; Yield: 79%; M.P.: 241 °C; **FT-IR** (KBr), cm^{-1}: 3264.60 (NH), 3073.82 (Ar-H), 2940.64 (C—H), 1666.55 (C = O), 1524.98 (C = C-Ar), 1340.12 (NO_2), 1249.05 (F-Ar), 1090.03 (C—O).; **^{1}H NMR-d^{6}** (400 MHz, DMSO-d^{6}) δ: 10.32 s (1H, NH), 8.37 s (1H, H_{arom}), 7.80–7.79 d (1H_{arom}, *J* = 9.5 Hz), 7.72–7.70 d (1H_{arom}, *J* = 5.5 Hz), 7.65 s (1H, H_{arom}), 7.31–7.29 d (2H_{arom}, *J* = 6.5 Hz), 7.17–7.16 d (2H_{arom}, *J* = 7.5 Hz), 5.46 s (2H,

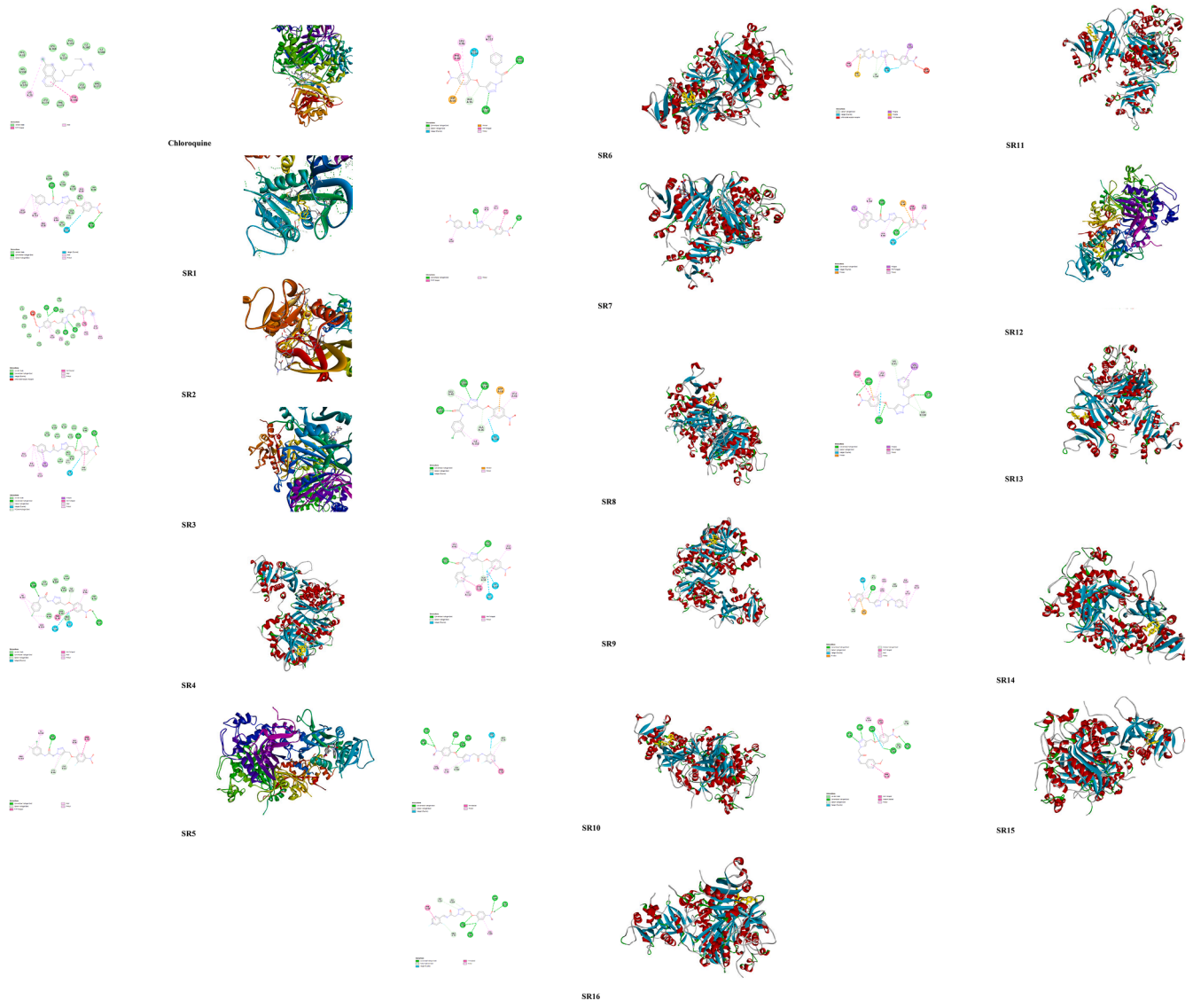

Fig. 3. Interaction of pfDHFR with the Chloroquine and **SR1**–**SR16**.

Table 2
Drug-likeness properties of compounds **SR1**–**SR16**.

Comp.	Molecular weight (range ≤ 500)	Rotatable bonds (range 1–10)	H-bond acceptors (range ≤ 10)	H-bond donors (range ≤ 5)	Molar refractivity (Range 40–130)	TPSA	Log Po/w (range ≤ 5)	Log S (Solubility)	Lipinski violations	Bio-availability Score (range 0.4–0.6)	Synthetic Accessibility
SR1	385.35	8	7	1	99.84	114.86	1.85	−4.55	0	0.55	2.95
SR2	401.35	9	8	1	101.37	124.09	1.7	−4.33	0	0.55	3.04
SR3	450.22	8	7	1	102.58	114.86	2.37	−4.88	0	0.55	2.93
SR4	405.77	8	7	1	99.89	114.86	2.28	−4.82	0	0.55	2.89
SR5	419.79	8	7	1	104.85	114.86	2.39	−5.2	0	0.55	2.98
SR6	371.32	8	7	1	94.88	114.86	1.78	−4.16	0	0.55	2.89
SR7	416.32	9	9	1	103.7	160.68	0.99	−4.95	1	0.55	2.97
SR8	419.79	8	7	1	104.85	114.86	2.39	−5.2	0	0.55	2.97
SR9	407.3	8	9	1	94.79	114.86	2.41	−4.37	0	0.55	2.94
SR10	407.3	8	9	1	94.79	114.86	2.36	−4.37	0	0.55	2.95
SR11	385.35	8	7	1	99.84	114.86	1.9	−4.55	0	0.55	2.96
SR12	421.38	8	7	1	112.38	114.86	2.64	−5.46	0	0.55	3.11
SR13	372.31	8	8	1	92.67	127.75	1.01	−3.32	0	0.55	2.91
SR14	386.34	8	8	1	97.64	127.75	1.3	−4.05	0	0.55	3
SR15	415.38	10	8	1	104.64	124.09	1.75	−4.26	0	0.55	3.08
SR16	421.33	9	9	1	98.06	114.86	2.4	−4.31	0	0.55	3.01

Table 3
in vitro antimalarial activity of phenoxy methyl-1,2,3-triazoles (**SR1** to **SR16**) against *P. falciparum* (CQ-resistant strain RKL-9) strain.

Entry	Compounds	Yield (%)	Antimalarial activity after (48 h) IC_{50} (μM)
1	SR1	56	45.43259
2	SR2	54	42.64416
3	SR3	53	36.72301
4	SR4	52	39.96198
5	SR5	57	43.07769
6	SR6	61	51.26112
7	SR7	48	36.09556
8	SR8	55	41.19023
9	SR9	56	42.82696
10	SR10	50	38.30697
11	SR11	51	41.25467
12	SR12	24	18.60515
13	SR13	57	47.64643
14	SR14	59	48.42661
15	SR15	43	32.99207
16	SR16	42	22.15863
17	CQ[a]	–	67.26753

[a] CQ= Chloroquine (act as positive control).

CH_2), 5.36 s (2H, CH_2), 2.78 s (3H, CH_3).; **^{13}C NMR** (101 MHz, DMSO-d^6): 163.832, 151.750, 151.614, 149.142, 141.076, 140.315, 135.831, 132.738, 129.212, 126.912, 121.332, 119.164, 114.616, 112.216, 111.964, 62.519, 55.195, 52.410.; **Mass**: Calculated: 401.11, Found: 401.3; **Elemental Analysis:** Calculated for $C_{18}H_{16}FN_5O_5$: C-53.87, H-4.02, N-17.45 Found: C-53.89, H-4.04, N-17.47%

2.2.3. N-(4-bromophenyl)−2-(4-((2-fluoro-4-nitrophenoxy)methyl)−1H-1,2,3-triazol-1-yl)acetamide (SR3)

Compound **SR3** was obtained via 1,3-dipolar cycloaddition reaction between alkyne (**5**) and azide (**2**) and the resulting solution was further reacted with amine (**8c**) for 5 h lead to the white solid; Yield: 80%; M.P.: 283 °C; **FT-IR** (KBr), cm^{-1}: 3263.66 (NH), 3101.64 (Ar-H), 2947.33 (C—H), 1658.84 (C = O), 1512.24 (C = C-Ar), 1342.50 (NO_2), 1288.49 (F-Ar), 1064.74 (C—O).; **^{1}H NMR** (400 MHz, DMSO-d^6) δ: 10.64 s (1H, NH), 8.35 s (1H, H_{arom}), 8.32 m (1H, H_{arom}), 8.14 m (1H, H_{arom}), 8.19 m (1H, H_{arom}), 8.17 m (1H, H_{arom}), 7.67 s (1H, H_{arom}), 7.56–7.54 d (1H_{arom}, J = 5.5 Hz), 7.53–7.51 d (1H_{arom}, J = 3.5 Hz), 5.46 s (2H, CH_2), 5.43 s (2H, CH_2).; **^{13}C NMR** (101 MHz, DMSO-d^6): 165.394, 151.885, 151.609, 149.139, 141.065, 140.343, 137.727, 131.739, 126.968, 121.324, 121.114, 115.395, 114.640, 112.203, 111.975, 62.559, 52.224.; **Mass**: Calculated: 449.01, Found: 448.6; **Elemental Analysis:** Calculated for $C_{17}H_{13}BrFN_5O_4$: C-45.35, H-2.91, N-15.56 Found: C-45.33, H-2.89, N-15.54%

2.2.4. N-(4-chlorophenyl)−2-(4-((2-fluoro-4-nitrophenoxy)methyl)−1H-1,2,3-triazol-1-yl)acetamide (SR4)

Compound **SR4** was obtained via 1,3-dipolar cycloaddition reaction between alkyne (**5**) and azide (**2**) and the resulting solution was further reacted with amine (**8d**) for 5 h lead to the off-white solid; Yield: 85%; M.P.: 278 °C; **FT-IR** (KBr), cm^{-1}: 3262.56 (NH), 3103.34 (Ar-H), 2957.32 (C—H), 1668.14 (C = O), 1542.04 (C = C-Ar), 1322.96 (NO_2), 1292.43 (F-Ar), 1073.74 (C—O).; **^{1}H NMR** (400 MHz, DMSO-d^6) δ: 10.72 s (1H, NH), 8.40 s (1H, H_{arom}), 8.34–8.33 d (1H_{arom}, J = 9.5 Hz), 8.18–8.16 d (2H_{arom}, J = 5.5 Hz), 8.14–8.13 d (1 H_{arom}, J = 9.5 Hz), 7.66 s (1H, H_{arom}), 7.56–7.54 d (1H_{arom}, J = 7.5 Hz), 7.45–7.43 d (1H_{arom}, J = 6.5 Hz), 5.39 s (2H, CH_2), 5.32 s (2H, CH_2).; **^{13}C NMR** (101 MHz, DMSO-d^6): 165.364, 151.872, 151.620, 149.153, 141.070, 140.361, 137.732, 131.743, 126.976, 121.332, 121.121, 115.380, 114.653, 112.213, 111.932, 62.561, 52.232.; **Mass**: Calculated: 405.06, Found: 405.20; **Elemental Analysis:** Calculated for $C_{17}H_{13}ClFN_5O_4$: C-50.32, H-3.23, N-17.26 Found: C-50.34, H-3.25, N-17.28%

2.2.5. N-(3-chloro-4-methylphenyl)−2-(4-((2-fluoro-4-nitrophenoxy)methyl)−1H-1,2,3-triazol-1-yl)acetamide (SR5

Compound **SR5** was obtained via 1,3-dipolar cycloaddition reaction between alkyne (**5**) and azide (**2**) and the resulting solution was further reacted with amine (**8e**) for 5 h lead to the cream solid; Yield: 81%; M.P.: 302 °C; **FT-IR** (KBr), cm^{-1}: 3356.25 (NH), 3093.92 (Ar-H), 2955.04 (C—H), 1681.98 (C = O), 1512.24 (C = C-Ar), 1342.50 (NO_2), 1288.49 (F-Ar), 1057.03 (C—O).; **^{1}H NMR** (400 MHz, DMSO-d^6) δ 10.63 s (1H, NH), 8.36 s (1H, H_{arom}), 8.19–8.17 d (2H_{arom}, J = 5.5 Hz), 7.76 s (1H, H_{arom}), 7.68 s (1H, H_{arom}), 7.35–7.31 d (1H_{arom}, J = 2.5 Hz), 6.94–6.93 d (1H_{arom}, J = 8.5 Hz), 5.46 s (2H, CH_2), 5.39 s (2H, CH_2), 2.27 s (3H, CH_3).; **^{13}C NMR** (101 MHz, DMSO-d^6): 164.310, 151.862, 151.609, 149.139, 141.065, 140.358, 137.445, 133.184, 130.479, 127.004, 121.289, 119.189, 114.618, 112.190, 111.961, 62.513, 52.183, 18.914.; **Mass**: Calculated: 419.08, Found: 419.5; **Elemental Analysis:** Calculated for $C_{18}H_{15}ClFN_5O_4$: C-51.50, H-3.60, N-16.68 Found: C-51.52, H-3.62, N-16.70%

2.2.6. 2-(4-((2-fluoro-4-nitrophenoxy)methyl)−1H-1,2,3-triazol-1-yl)-N-phenylacetamide (SR6)

Compound **SR6** was obtained via 1,3-dipolar cycloaddition reaction

Table 4
Antibacterial and antifungal activity of newly synthesised scaffolds (**SR1** to **SR16**).

	MIC, μM				
	S. epidermidis	*B. subtilis*	*E. coli*	*S. enterica*	*A. brasiliensis*
Streptomycin[a]	–	-	171.947	171.947	–
Chloramphenicol[a]	309.471	309.471	–	–	–
Nystatin[a]	–	–	–	–	107.98
S1	2596.59	2596.59	2596.59	2596.59	2596.59
S2	2493.08	2493.08	2493.08	2493.08	2493.08
S3	2227.12	2227.12	1113.56	1113.56	2227.12
S4	2468.77	2468.77	1234.38	1234.38	2468.77
S5	596.54	596.54	596.54	1193.08	1193.08
S6	2694.69	2694.69	1347.34	2694.69	2694.69
S7	600.83	600.83	240.33	1201.66	1201.66
S8	1193.08	1193.08	596.54	596.54	2386.17
S9	614.12	614.12	245.65	614.12	614.12
S10	614.12	614.12	614.12	1228.25	1228.25
S11	1298.29	649.14	2596.59	1298.29	2596.59
S12	2374.62	1187.31	1187.31	1187.31	2374.62
S13	2686.72	2686.72	1343.36	1343.36	2686.72
S14	1294.96	1294.96	1294.96	1294.96	2589.93
S15	2408.88	2408.88	2408.88	2408.88	2408.88
S16	1187.36	1187.36	593.68	1187.36	2374.73

[a] Streptomycin, Chloramphenicol and Nystatin acts as positive control for Gram-positive, Gram-negative bacteria and Fungi.

Table 5
Minimum inhibitory concentration (MIC in μM) of synthesised scaffolds (**SR1** to **SR16**)[a].

SR1	PC	2596.59 μM	1298.29 μM	649.14 μM	259.65 μM
S. epidermidis	0.489	0.502	0.556	0.642	0.724
B. subtilis	0.560	0.569	0.569	0.555	0.560
E. coli	0.110	0.147	0.211	0.274	0.348
S. enterica	0.213	0.244	0.305	0.345	0.409
A. brasiliensis	0.245	0.308	0.388	0.467	0.576
SR2	PC	2493.08 μM	1246.54 μM	623.27 μM	249.30 μM
S. epidermidis	0.489	0.577	0.678	0.801	0.947
B. subtilis	0.560	0.603	0.687	0.700	0.778
E. coli	0.110	0.605	0.503	0.660	0.620
S. enterica	0.213	0.281	0.378	0.403	0.523
A. brasiliensis	0.245	0.324	0.319	0.502	0.623
SR3	PC	2227.12 μM	1113.56 μM	556.78 μM	222.71 μM
S. epidermidis	0.489	0.502	0.589	0.663	0.786
B. subtilis	0.560	0.562	0.627	0.673	0.756
E. coli	0.110	0.100	0.111	0.235	0.407
S. enterica	0.213	0.167	0.234	0.312	0.468
A. brasiliensis	0.245	0.289	0.376	0.442	0.583
SR4	PC	2468.77 μM	1234.38 μM	617.19 μM	246.87 μM
S. epidermidis	0.489	0.403	0.468	0.554	0.649
B. subtilis	0.560	0.529	0.577	0.656	0.734
E. coli	0.110	0.101	0.124	0.248	0.323
S. enterica	0.213	0.167	0.220	0.334	0.488
A. brasiliensis	0.245	0.236	0.420	0.553	0.761
SR5	PC	2386.17 μM	1193.08 μM	596.54 μM	238.61 μM
S. epidermidis	0.489	0.122	0.349	0.468	0.629
B. subtilis	0.560	0.234	0.408	0.554	0.723
E. coli	0.110	0.092	0.127	0.141	0.392
S. enterica	0.213	0.201	0.370	0.417	0.415
A. brasiliensis	0.245	0.207	0.262	0.413	0.602
SR6	PC	2694.69 μM	1347.34 μM	673.67 μM	269.46 μM
S. epidermidis	0.489	0.475	0.544	0.613	0.681
B. subtilis	0.560	0.569	0.664	0.723	0.812
E. coli	0.110	0.068	0.092	0.178	0.297
S. enterica	0.213	0.342	0.477	0.556	0.680
A. brasiliensis	0.245	1.889	1.363	2.149	0.689
SR7	PC	2403.32 μM	1201.66 μM	600.83 μM	240.33 μM
S. epidermidis	0.489	0.378	0.402	0.512	0.677
B. subtilis	0.560	0.479	0.526	0.578	0.892
E. coli	0.110	0.060	0.111	0.201	0.198
S. enterica	0.213	0.278	0.370	0.417	0.415
A. brasiliensis	0.245	0.291	0.306	0.427	0.676
SR8	PC	2386.17 μM	1193.08 μM	596.54 μM	238.61 μM
S. epidermidis	0.489	0.425	0.503	0.612	0.618
B. subtilis	0.560	0.577	0.631	0.656	0.803
E. coli	0.110	0.074	0.075	0.126	0.229
S. enterica	0.213	0.092	0.098	0.165	0.118
A. brasiliensis	0.245	0.417	0.527	0.632	0.712
SR9	PC	2456.51 μM	1228.25 μM	614.12 μM	245.65 μM
S. epidermidis	0.489	0.300	0.389	0.487	0.524
B. subtilis	0.560	0.127	0.258	0.532	0.678
E. coli	0.110	0.111	0.073	0.122	0.128
S. enterica	0.213	0.199	0.206	0.289	0.489
A. brasiliensis	0.245	0.250	0.364	0.320	0.499
SR10	PC	2456.51 μM	1228.25 μM	614.12 μM	245.65 μM
S. epidermidis	0.489	0.356	0.436	0.499	0.677
B. subtilis	0.560	0.274	0.381	0.506	0.652
E. coli	0.110	0.032	0.087	0.137	0.277
S. enterica	0.213	0.200	0.245	0.377	0.447
A. brasiliensis	0.245	0.209	0.287	0.345	0.434
SR11	PC	2596.59 μM	1298.29 μM	649.14 μM	259.65 μM
S. epidermidis	0.489	0.382	0.452	0.549	0.678
B. subtilis	0.560	0.377	0.486	0.567	0.681
E. coli	0.110	0.244	0.539	0.435	0.612
S. enterica	0.213	0.174	0.207	0.464	0.588
A. brasiliensis	0.245	0.232	0.317	0.440	0.589

SR12	PC	2374.62 μM	1187.31 μM	593.65 μM	237.46 μM
S. epidermidis	0.489	0.451	0.509	0.576	0.646
B. subtilis	0.560	0.442	0.548	0.613	0.682
E. coli	0.110	0.097	0.122	0.204	0.344
S. enterica	0.213	0.151	0.227	0.405	0.489
A. brasiliensis	0.245	0.301	0.412	0.478	0.541
SR13	PC	2686.72 μM	1343.36 μM	671.68 μM	268.67 μM
S. epidermidis	0.489	0.458	0.524	0.586	0.745
B. subtilis	0.560	0.567	0.641	0.703	0.776
E. coli	0.110	0.073	0.118	0.210	0.248
S. enterica	0.213	0.165	0.224	0.321	0.486
A. brasiliensis	0.245	0.391	0.354	0.415	0.548
SR14	PC	2589.93 μM	1294.96 μM	647.48 μM	258.99 μM
S. epidermidis	0.489	0.434	0.467	0.512	0.638
B. subtilis	0.560	0.489	0.556	0.614	0.676
E. coli	0.110	0.083	0.124	0.162	0.291
S. enterica	0.213	0.177	0.234	0.250	0.378
A. brasiliensis	0.245	0.256	0.389	0.472	0.583
SR15	PC	2408.88 μM	1204.44 μM	602.22 μM	240.88 μM
S. epidermidis	0.489	0.554	0.569	0.665	0.748
B. subtilis	0.560	0.560	0.660	0.792	0.843
E. coli	0.110	0.115	0.224	0.363	0.415
S. enterica	0.213	0.232	0.362	0.467	0.488
A. brasiliensis	0.245	0.229	0.229	0.391	0.497
SR16	PC	2374.73 μM	1187.36 μM	593.68 μM	237.47 μM
S. epidermidis	0.489	0.468	0.413	0.563	0.712
B. subtilis	0.560	0.406	0.503	0.605	0.620
E. coli	0.110	0.081	0.075	0.102	0.321
S. enterica	0.213	0.188	0.200	0.321	0.468
A. brasiliensis	0.245	0.210	0.338	0.529	0.612

[a] Streptomycin, Chloramphenicol and Nystatin acts as positive control (PC). MIC (μM) value of drugs at different dilution (2694.69–222.71 μM) against two Gram-positive bacteria *Staphylococcus epidermidis, Bacillus subtilis*; two Gram-negative bacteria *E. coli, Salmonella enterica*; and one Fungi *Aspergillus brasiliensis* has been obtained.

between alkyne (**5**) and azide (**2**) and the resulting solution was further reacted with amine (**8f**) for 6 h lead to the white solid; Yield: 78%; M.P.: 235 °C; **FT-IR** (KBr), cm^{-1}: 3356.35 (NH), 3092.12 (Ar-H), 2954.04 (C—H), 1679.98 (C = O), 1512.24 (C = C-Ar), 1352.50 (NO_2), 1287.46 (F-Ar), 1058.38 (C—O).; **^{1}H NMR** (400 MHz, DMSO-d^6) δ 10.74 s (1H, NH), 8.46 s (1H, H_{arom}), 8.20–8.19 d (1H_{arom}, *J* = 8.5 Hz), 7.66 s (1H, H_{arom}), 7.51–7.50 d (1H_{arom}, *J* = 9.5 Hz), 7.37–7.36 d (2H_{arom}, *J* = 7.5 Hz), 7.20–7.18 t (2H_{arom}, *J* = 6.5 Hz), 6.93–6.91 t (1H_{arom}, *J* = 5.5 Hz), 5.46 s (2H, CH_2), 5.39 s (2H, CH_2).; **^{13}C NMR** (101 MHz, DMSO-d^6): 164.312, 151.872, 151.612, 149.143, 141.070, 140.362, 137.451, 133.189, 130.489, 127.018, 121.292, 119.191, 114.623, 112.181, 111.952, 62.524, 52.153.; **Mass**: Calculated: 371.10, Found: 371.5; **Elemental Analysis:** Calculated for $C_{17}H_{14}FN_5O_4$: C-54.99, H-3.80, N-18.86 Found: C-54.97, H-3.78, N-18.84%

2.2.7. 2-(4-((2-fluoro-4-nitrophenoxy)methyl)−1H-1,2,3-triazol-1-yl)-N-(4-nitrophenyl)acetamide (SR7)

Compound **SR7** was obtained via 1,3-dipolar cycloaddition reaction between alkyne (**5**) and azide (**2**) and the resulting solution was further reacted with amine (**8g**) for 6 h lead to the yellow solid; Yield: 72%; M.P.: 268 °C; **FT-IR** (KBr), cm^{-1}: 3525.99 (NH), 3093.92 (Ar-H), 2947.33 (C—H), 1658.84 (C = O), 1504.53 (C = C-Ar), 1342.50 (NO_2), 1288.49 (F-Ar), 1064.74 (C—O).; **^{1}H NMR** (400 MHz, DMSO-d^6) δ 10.43 s (1H, NH), 8.19–8.16 m (2H, H_{arom}), 8.14 s (1H, H_{arom}) 7.95–7.93 d (1H_{arom}, *J* = 7.5 Hz), 7.69–7.64 m (1H, H_{arom}), 6.73 s (1H, H_{arom}), 6.60–6.58 d (1H_{arom}, *J* = 8.5 Hz), 5.47 s (2H, CH_2), 5.43 s (2H, CH_2).; **^{13}C NMR** (101 MHz, DMSO-d^6): 165.393, 155.677, 151.879, 151.599, 149.130, 140.862, 140.326, 135.559, 126.973, 126.365, 121.313, 114.599, 112.324, 112.184, 111.955, 62.552, 50.766.; **Mass**: Calculated: 416.09, Found: 416.5; **Elemental Analysis:** Calculated for $C_{17}H_{13}FN_6O_6$: C-49.04, H-3.15, N-20.19 Found: C-49.01, H-3.12, N-20.16%

2.2.8. N-(4-chloro-3-methylphenyl)−2-(4-((2-fluoro-4-nitrophenoxy)methyl)−1H-1,2,3-triazol-1-yl)acetamide (SR8)

Compound **SR8** was obtained via 1,3-dipolar cycloaddition reaction between alkyne (**5**) and azide (**2**) and the resulting solution was further reacted with amine (**8h**) for 5 h lead to the pale yellow solid; Yield: 83%; M.P.: 272 °C; **FT-IR** (KBr), cm^{-1}: 3348.54 (NH), 3101.64 (Ar-H), 2955.04 (C—H), 1689.70 (C = O), 1512.24 (C = C-Ar), 1342.50 (NO_2), 1219.05 (F-Ar), 1064.74 (C—O).; **^{1}H NMR** (400 MHz, DMSO-d^6) δ 10.61 s (1H, NH), 8.35 s (1H, H_{arom}), 8.19–8.15 d (2H_{arom}, *J* = 6.5 Hz), 7.76 s (1H, H_{arom}), 7.67 s (1H, H_{arom}), 7.31–7.29 d (2H_{arom}, *J* = 3.5 Hz), 5.46 s (2H, CH_2), 5.38 s (2H, CH_2), 2.27 s (3H, CH_3).; **^{13}C NMR** (101 MHz, DMSO-d^6): 164.310, 151.858, 149.137, 141.059, 140.360, 137.437, 133.076, 131.362, 130.485, 127.007, 121.330, 119.184, 117.828, 114.615, 111.975, 62.506, 52.175, 18.921.; **Mass**: Calculated: 419.08, Found: 419.1; **Elemental Analysis:** Calculated for $C_{18}H_{15}ClFN_5O_4$: C-51.50, H-3.60, N-16.68 Found: C-51.48, H-3.58, N-16.66%

2.2.9. N-(2,4-difluorophenyl)−2-(4-((2-fluoro-4-nitrophenoxy)methyl)−1H-1,2,3-triazol-1-yl)acetamide (SR9)

Compound **SR9** was obtained via 1,3-dipolar cycloaddition reaction between alkyne (**5**) and azide (**2**) and the resulting solution was further reacted with amine (**8i**) for 6 h lead to the white solid; Yield: 80%; M.P.: 258 °C; **FT-IR** (KBr), cm^{-1}: 3350.62 (NH), 3110.52 (Ar-H), 2964.12 (C—H), 1689.70 (C = O), 1521.27 (C = C-Ar), 1349.58 (NO_2), 1220.51 (F-Ar), 1092.85 (C—O).; **^{1}H NMR** (400 MHz, DMSO-d^6) δ 10.78 s (1H, NH), 8.89 s (1H, H_{arom}), 8.79 s (1H, H_{arom}), 8.32–8.29 d (2H_{arom}, *J* = 9.5 Hz), 7.65 s (1H, H_{arom}), 7.58–7.56 d (1H_{arom}, *J* = 7.5 Hz), 7.38–7.36 d (1H_{arom}, *J* = 2.5 Hz), 5.46 s (2H, CH_2), 5.38 s (2H, CH_2).; **^{13}C NMR** (101 MHz, DMSO-d^6): 164.321, 151.874, 149.145, 141.094, 140.385, 137.456, 133.158, 131.456, 130.758, 127.254, 121.540, 119.245, 117.912, 114.541, 111.955, 62.405, 52.256.; **Mass**: Calculated: 407.08, Found: 407.3; **Elemental Analysis:** Calculated for $C_{17}H_{12}F_3N_5O_4$: C-

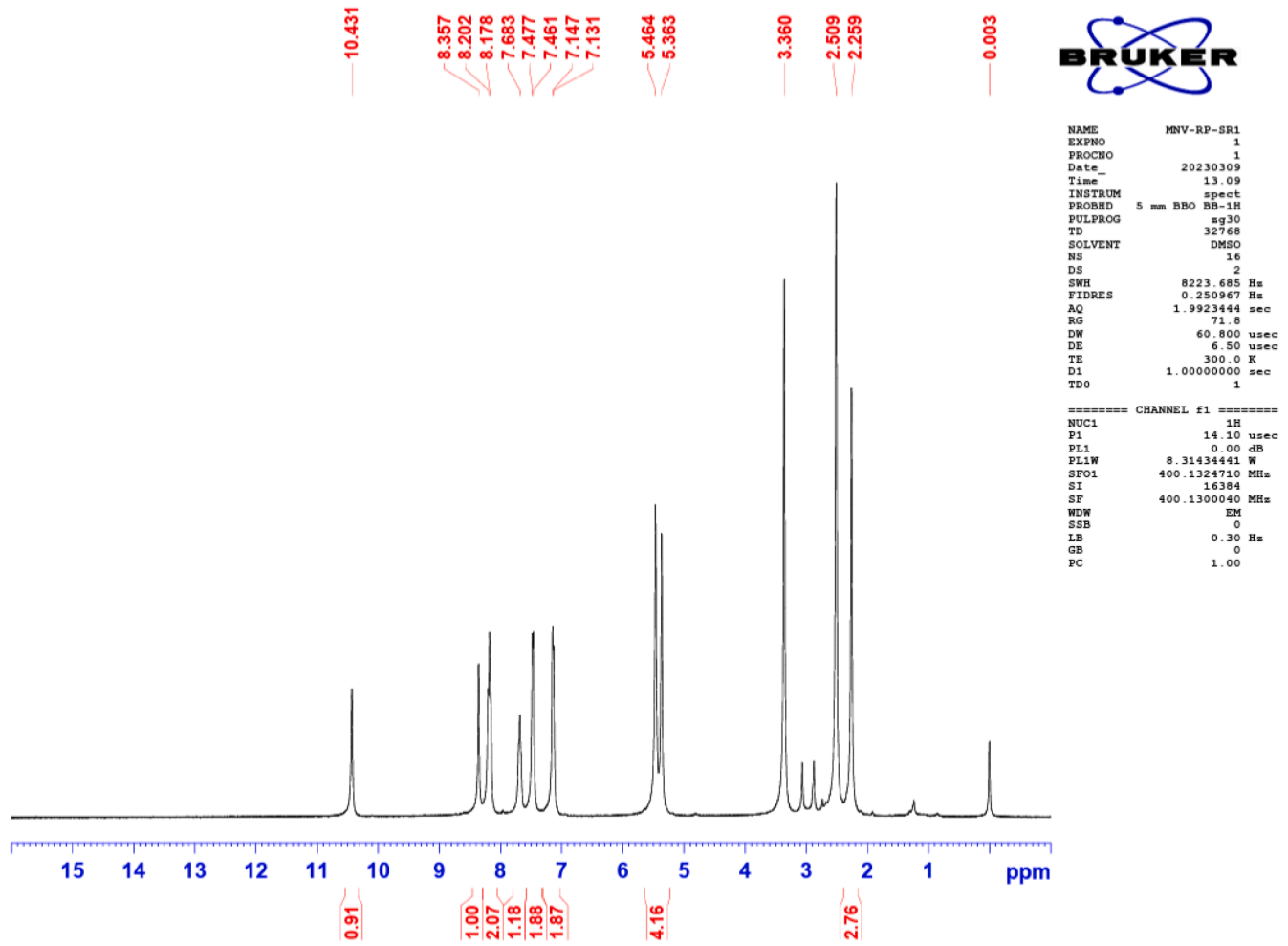

Fig. 4. ^{1}H NMR spectrum of compound SR1.

50.13, H-2.97, N-17.19 Found: C-50.10, H-2.94, N-17.16%

2.2.10. N-(2,6-difluorophenyl)−2-(4-((2-fluoro-4-nitrophenoxy) methyl)−1H-1,2,3-triazol-1-yl)acetamide (SR10)

Compound **SR10** was obtained via 1,3-dipolar cycloaddition reaction between alkyne (**5**) and azide (**2**) and the resulting solution was further reacted with amine (**8j**) for 6 h lead to the white solid; Yield: 73%; M.P.: 267 °C; **FT-IR** (KBr), cm^{-1}: 3286.81 (NH), 3093.92 (Ar-H), 2947.33 (C—H), 1658.84 (C = O), 1512.24 (C = C-Ar), 1342.50 (NO_2), 1288.49 (F-Ar), 1072.46 (C—O).; **^{1}H NMR** (400 MHz, DMSO-d^{6}) δ 10.42 s (1H, -NH), 8.33 s (1H, H_{arom}), 8.20–8.15 m (4H, H_{arom}), 7.96 s (1H, H_{arom}), 7.70–7.66 t (1H_{arom}, *J* = 6.5 Hz), 5.48 s (2H, CH_2), 5.44 s (2H, CH_2). **^{13}C NMR** (101 MHz, DMSO-d^{6}): 167.656, 165.398, 151.887, 151.611, 149.140, 141.322, 140.866, 140.337, 140.262, 126.975, 126.700, 121.322, 114.634, 112.198, 111.968, 62.559, 52.544.; **Mass**: Calculated: 407.08, Found: 407.8; **Elemental Analysis:** Calculated for $C_{17}H_{12}F_3N_5O_4$: C-50.13, H-2.97, N-17.19 Found: C-50.15, H-2.99, N-17.21%

2.2.11. 2-(4-((2-fluoro-4-nitrophenoxy)methyl)−1H-1,2,3-triazol-1-yl)-N-(o-tolyl)acetamide (SR11)

Compound **SR11** was obtained via 1,3-dipolar cycloaddition reaction between alkyne (**5**) and azide (**2**) and the resulting solution was further reacted with amine (**8k**) for 5 h lead to the light grey solid; Yield: 85%; M.P.: 262 °C; **FT-IR** (KBr), cm^{-1}: 3263.66 (NH), 3070.78 (Ar-H), 2939.61 (C—H), 1666.55 (C = O), 1527.67 (C = C-Ar), 1350.22 (NO_2), 1219.05 (F-Ar), 1064.74 (C—O).; **^{1}H NMR** (400 MHz, DMSO-d^{6}) δ 9.82 s (1H, NH), 8.35 s (1H, H_{arom}), 8.20–8.19 d (1H_{arom}, *J* = 9.5 Hz), 8.17–8.15 d (1H_{arom}, *J* = 7.5 Hz), 7.67 s (1H, H_{arom}), 7.43–7.41 d (1H_{arom}, *J* = 5.5 Hz), 7.24–7.22 d (1H_{arom}, *J* = 6.5 Hz), 7.19–7.15 t (1H_{arom}, *J* = 6.5 Hz), 7.12–7.09 t (1H_{arom}, *J* = 2.5 Hz), 5.47–5.46 s (2H, CH_2), 5.43–5.42 s (2H, CH_2), 2.23 s (3H, CH_3).; **^{13}C NMR** (101 MHz, DMSO-d^{6}): 164.284, 151.865, 151.610, 149.140, 141.024, 140.360, 135.447, 131.552, 130.419, 126.988, 124.702, 121.329, 114.640, 112.207, 111.980, 62.519, 51.938, 17.768.; **Mass**: Calculated: 385.12, Found: 383.8; **Elemental Analysis:** Calculated for $C_{18}H_{16}FN_5O_4$: C-56.10, H-4.19, N-18.17 Found: C-56.07, H-4.16, N-18.14%

2.2.12. 2-(4-((2-fluoro-4-nitrophenoxy)methyl)−1H-1,2,3-triazol-1-yl)-N-(naphthalen-1-yl)acetamide (SR12)

Compound **SR12** was obtained via 1,3-dipolar cycloaddition reaction between alkyne (**5**) and azide (**2**) and the resulting solution was further reacted with amine (**8l**) for 6 h lead to the purple solid; Yield: 82%; M.P.: 276 °C; **FT-IR** (KBr), cm^{-1}: 3273.52 (NH), 3082.54 (Ar-H), 2985.67 (C—H), 1666.55 (C = O), 1552.25 (C = C-Ar), 1374.32 (NO_2), 1254.65 (F-Ar), 1056.82 (C—O).; **^{1}H NMR** (400 MHz, DMSO-d^{6}) δ 10.74 s (1H, -NH), 8.89 s (1H, H_{arom}), 8.70–8.68 d (1H_{arom}, *J* = 7.5 Hz), 8.56–8.52 d (2H_{arom}, *J* = 6.5 Hz), 7.66 s (1H, H_{arom}), 7.57–7.54 d (1H_{arom}, *J* = 8.5 Hz), 7.23–7.22 d (1H_{arom}, *J* = 9.5 Hz), 7.43–7.41 d (1H_{arom}, *J* = 7.5 Hz), 7.30–7.26 t (2H_{arom}, *J* = 4.5 Hz), 7.19–7.16 t (1H_{arom}, *J* = 3.5 Hz), 5.49–5.48 s (2H, CH_2), 5.47–5.45 s (2H, CH_2).; **^{13}C NMR** (101 MHz, DMSO-d^{6}): 165.252, 151.732, 151.615, 149.235, 141.125, 140.153, 135.457, 131.574, 130.256, 128.236, 126.876, 126.576, 125.754, 124.546, 121.452, 121.215, 114.541, 112.567,

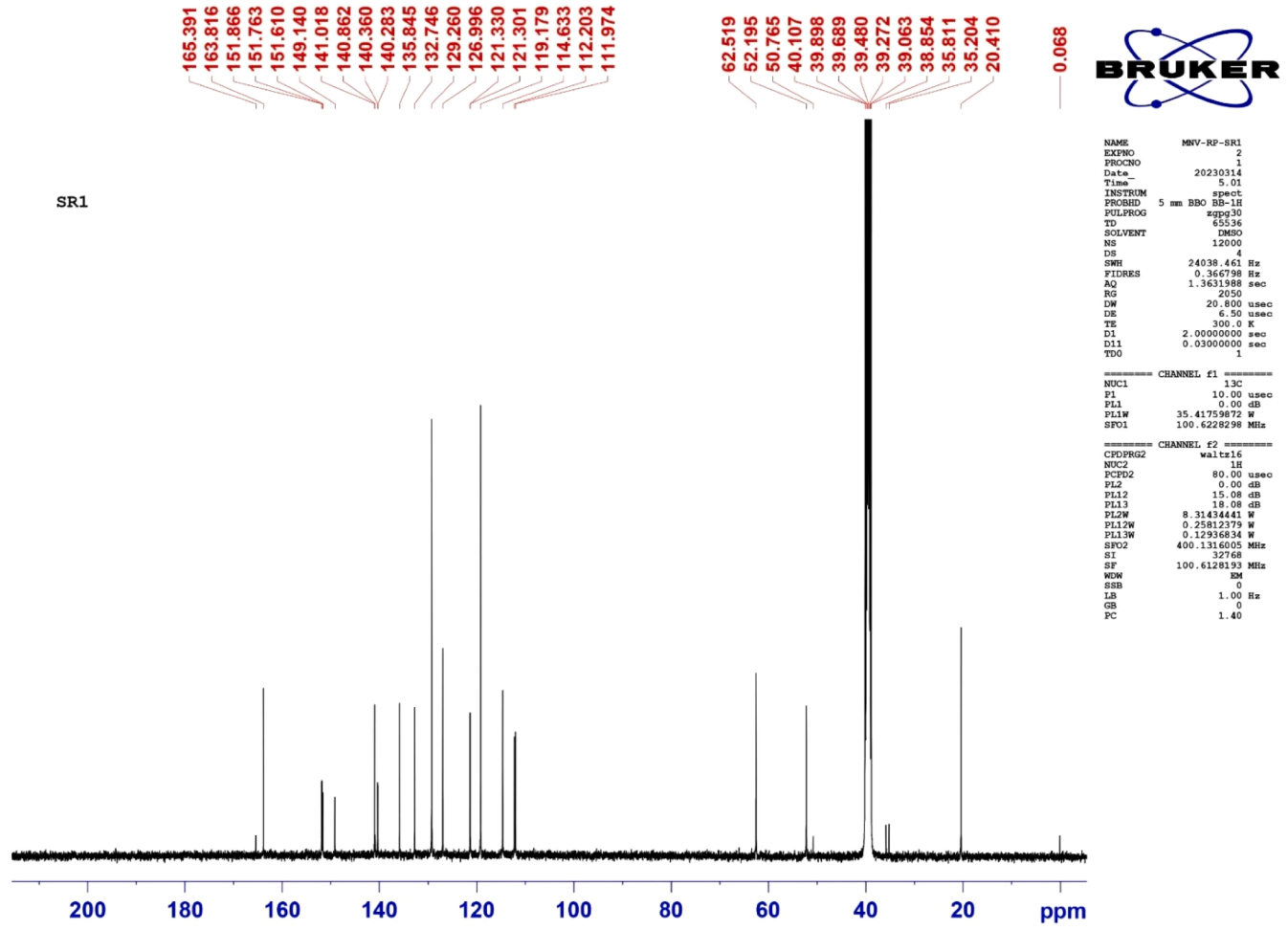

Fig. 5. ^{13}C NMR spectrum of compound SR1.

111.547, 62.657, 51.854.; **Mass**: Calculated: 421.12, Found: 421.8; **Elemental Analysis:** Calculated for $C_{21}H_{16}FN_5O_4$: C-59.86, H-3.83, N-16.62 Found: C-59.84, H-3.81, N-16.60%

2.2.13. 2-(4-((2-fluoro-4-nitrophenoxy)methyl)−1H-1,2,3-triazol-1-yl)-N-(pyridin-3-yl)acetamide (SR13)

Compound **SR13** was obtained via 1,3-dipolar cycloaddition reaction between alkyne (**5**) and azide (**2**) and the resulting solution was further reacted with amine (**8m**) for 6 h lead to the off-white solid; Yield: 78%; M.P.: 288 °C; **FT-IR** (KBr), cm^{-1}: 3271.38 (NH), 3101.64 (Ar-H), 2947.33 (C—H), 1658.84 (C = O), 1512.24 (C = C-Ar), 1350.22 (NO_2), 1219.05 (F-Ar), 1064.74 (C—O).; **^{1}H NMR** (400 MHz, DMSO-d^6) δ 10.74 s (1H, -NH), 8.75 s (1H, H_{arom}), 8.37 s (1H, H_{arom}), 8.20–8.15 m (3H, H_{arom}), 8.02–8.00 d (1H_{arom}, *J* = 8.5 Hz), 7.70–7.67 m (1H, H_{arom}), 7.40–7.37 m (1H, H_{arom}), 5.48 s (2H, CH_2), 5.44 s (2H, CH_2). **^{13}C NMR** (101 MHz, DMSO-d^6): 165.391, 151.879, 151.608, 149.137, 144.756, 140.860, 140.776, 140.263, 126.966, 126.250, 121.323, 114.624, 112.203, 111.975, 62.556, 50.761.; **Mass**: Calculated:372.20, Found: 372.7.; **Elemental Analysis:** Calculated for $C_{16}H_{13}FN_6O_4$: C-51.62, H-3.52, N-22.57 Found: C-51.60, H-3.50, N-22.55%

2.2.14. 2-(4-((2-fluoro-4-nitrophenoxy)methyl)−1H-1,2,3-triazol-1-yl)-N-(5-methylpyridin-2-yl)acetamide (SR14)

Compound **SR14** was obtained via 1,3-dipolar cycloaddition reaction between alkyne (**5**) and azide (**2**) and the resulting solution was further reacted with amine (**8n**) for 6 h lead to the white solid; Yield: 76%; M.P.: 267 °C; **FT-IR** (KBr), cm^{-1}: 3267.25 (NH), 3125.64 (Ar-H), 2957.33 (C—H), 1658.84 (C = O), 1512.24 (C = C-Ar), 1256.22 (NO_2), 1219.35 (F-Ar), 1084.74 (C—O).; **^{1}H NMR** (400 MHz, DMSO-d^6) δ 10.42 s (1H, NH), 8.62 s (1H, H_{arom}), 8.47–8.45 d (1H_{arom}, *J* = 7.5 Hz), 7.74–7.73 d (2H_{arom}, *J* = 9.5 Hz), 7.66 s (1H, H_{arom}), 7.44–7.42 d (1H_{arom}, *J* = 6.5 Hz), 7.28–7.25 d (1H_{arom}, *J* = 4.5 Hz), 5.49–5.48 s (2H, CH_2), 5.45–5.43 s (2H, CH_2), 2.40 s (3H, CH_3).; **^{13}C NMR** (101 MHz, DMSO-d^6): 165.425, 151.458, 151.754, 149.456, 144.457, 140.765, 140.485, 140.274, 126.256, 126.126, 121.674, 114.264, 112.502, 111.023, 62.574, 50.572, 17.285.; **Mass**: Calculated:386.11, Found: 386.7.; **Elemental Analysis:** Calculated for $C_{17}H_{15}FN_6O_4$: C-52.85, H-3.91, N-21.75 Found: C-52.87, H-3.93, N-21.77%

2.2.15. 2-(4-((2-fluoro-4-nitrophenoxy)methyl)−1H-1,2,3-triazol-1-yl)-N-(4-methoxybenzyl)acetamide (SR15)

Compound **SR15** was obtained via 1,3-dipolar cycloaddition reaction between alkyne (**5**) and azide (**2**) and the resulting solution was further reacted with amine (**8o**) for 5 h lead to the white solid; Yield: 81%; M.P.: 267 °C; **FT-IR** (KBr), cm^{-1}: 3286.81 (NH), 3093.92 (Ar-H), 2939.61 (C—H), 1658.84 (C = O), 1519.96 (C = C-Ar), 1350.22 (NO_2), 1288.49 (F-Ar), 1033.88 (C—O).; **^{1}H NMR** (400 MHz, DMSO-d^6) δ 8.78–8.80 t (1H, NH, *J* = 2.5 Hz), 8.29 s (1H, H_{arom}), 8.20–8.19 d (1H_{arom}, *J* = 9.5 Hz), 8.17–8.14 d (1H_{arom}, *J* = 3.5 Hz), 7.67 s (1H, H_{arom}), 7.22–7.20 d (2H_{arom}, *J* = 7.5 Hz), 6.90–6.88 d (2H_{arom}, *J* = 4.5 Hz), 5.44 s (2H, CH_2), 5.18 s (2H, CH_2), 4.25–4.24 d (2H, CH_2, *J* = 1.5 Hz), 3.73 s (3H, CH_3).; **^{13}C NMR** (101 MHz, DMSO-d^6): 165.136, 158.349, 151.864, 151.603, 149.135, 140.940, 140.353, 130.566, 128.786, 126.879, 121.326, 114.626, 113.732, 112.201, 111.974, 62.508, 55.051, 51.608, 41.838.; **Mass**: Calculated: 415.13, Found: 415.5.; **Elemental Analysis:** Calculated for $C_{19}H_{18}FN_5O_5$: C-54.94, H-

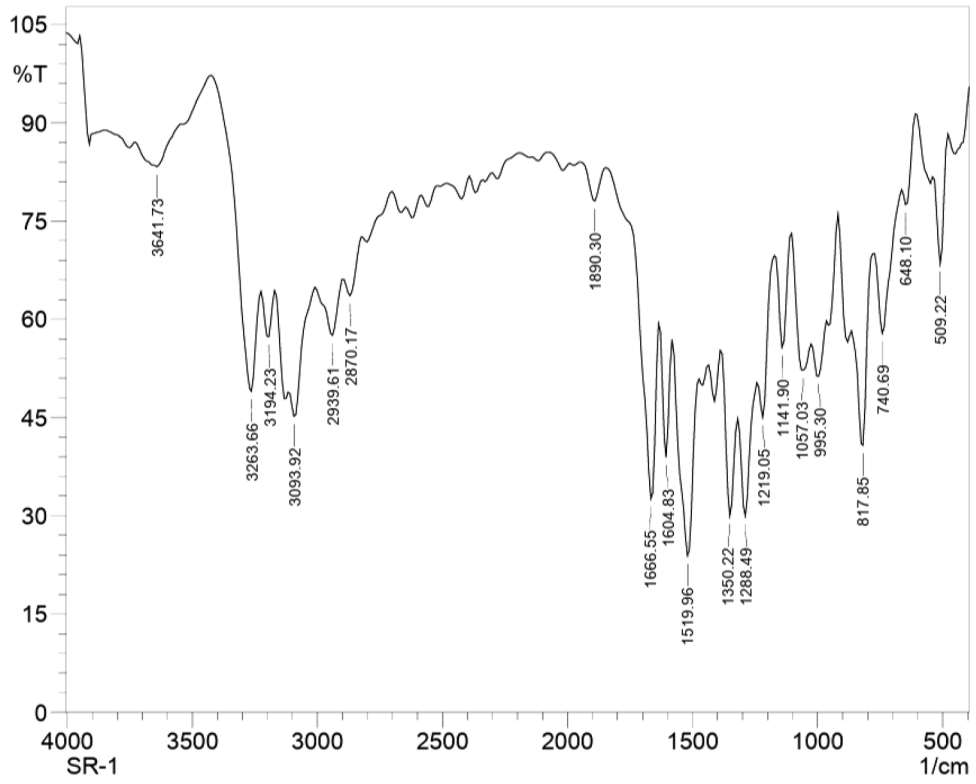

Fig. 6. IR spectrum of compound SR1.

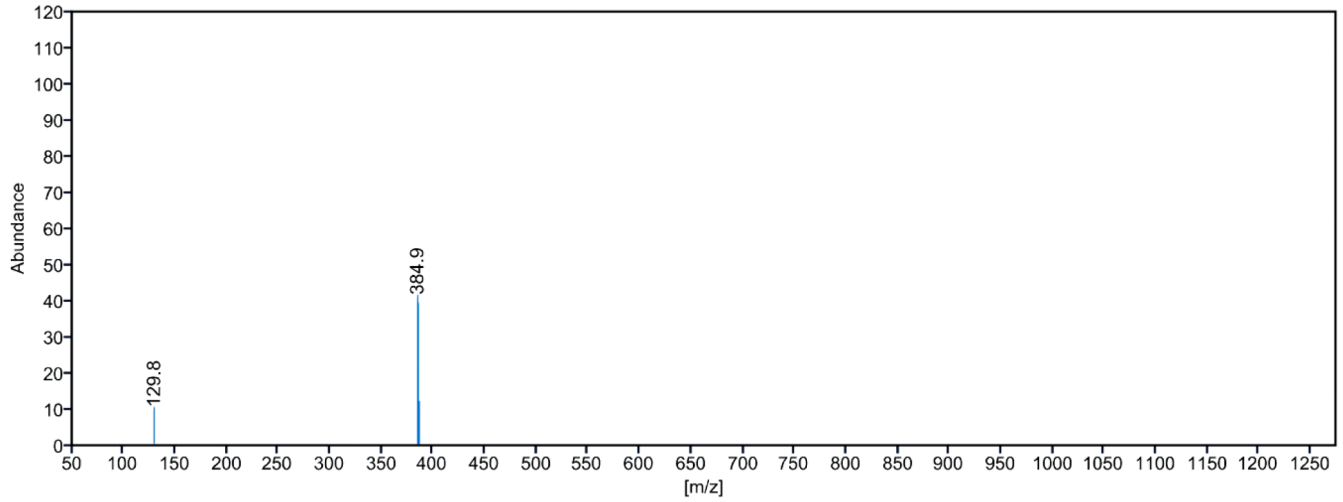

Fig. 7. Mass spectrum of compound SR1.

4.37, N-16.86 Found: C-54.90, H-4.33, N-16.83%

2.2.16. N-(2,4-difluorobenzyl)−2-(4-((2-fluoro-4-nitrophenoxy)methyl)−1H-1,2,3-triazol-1-yl)acetamide (SR16)

Compound **SR16** was obtained via 1,3-dipolar cycloaddition reaction between alkyne (**5**) and azide (**2**) and the resulting solution was further reacted with amine (**8p**) for 6 h lead to the yellowish white solid; Yield: 79%; M.P.: 239 °C; FT-IR (KBr), cm^{-1}: 3286.81 (NH), 3086.21 (Ar-H), 2939.61 (C—H), 1666.55 (C = O), 1519.96 (C = C-Ar), 1350.22 (NO_2), 1288.49 (F-Ar), 1041.60 (C—O).; **^{1}H NMR** (400 MHz, DMSO-d^6) δ 8.87–8.90 t (1H, NH, J = 2.5 Hz), 8.28 s (1H, H_{arom}), 8.20–8.19 d (1H_{arom}, J = 9.5 Hz), 8.16–8.13 m (1H, H_{arom}), 7.68–7.64 m (1H, H_{arom}), 7.44–7.38 m (1H, H_{arom}), 7.27–7.21 m (1H, H_{arom}), 7.10–7.05 m (1H, H_{arom}), 5.43 s (2H, CH_2), 5.20 s (2H, CH_2), 4.33–4.31 d (2H, CH_2, J = 3.5 Hz).; **^{13}C NMR** (101 MHz, DMSO-d^6): 165.464, 151.856, 149.128, 140.957, 140.351, 131.194, 126.894, 121.790, 121.324, 114.622, 112.201, 111.973, 103.992, 103.736, 103.480, 62.494, 51.488, 35.924.; **Mass**: Calculated: 421.10, Found: 421.6; **Elemental Analysis:** Calculated for $C_{18}H_{14}F_3N_5O_4$: C-51.31, H-3.35, N-16.62 Found: C-51.30, H-3.34, N-16.61%

2.3. Pharmacology

2.3.1. Molecular docking studies

Molecular docking was carried out using PyRx 0.8, a software utilizing Autodock Vina for docking analysis [21]. The primary objective of this study is to explore the binding interactions between the designated protein (3QGT) and a set of ligands. This set included the established

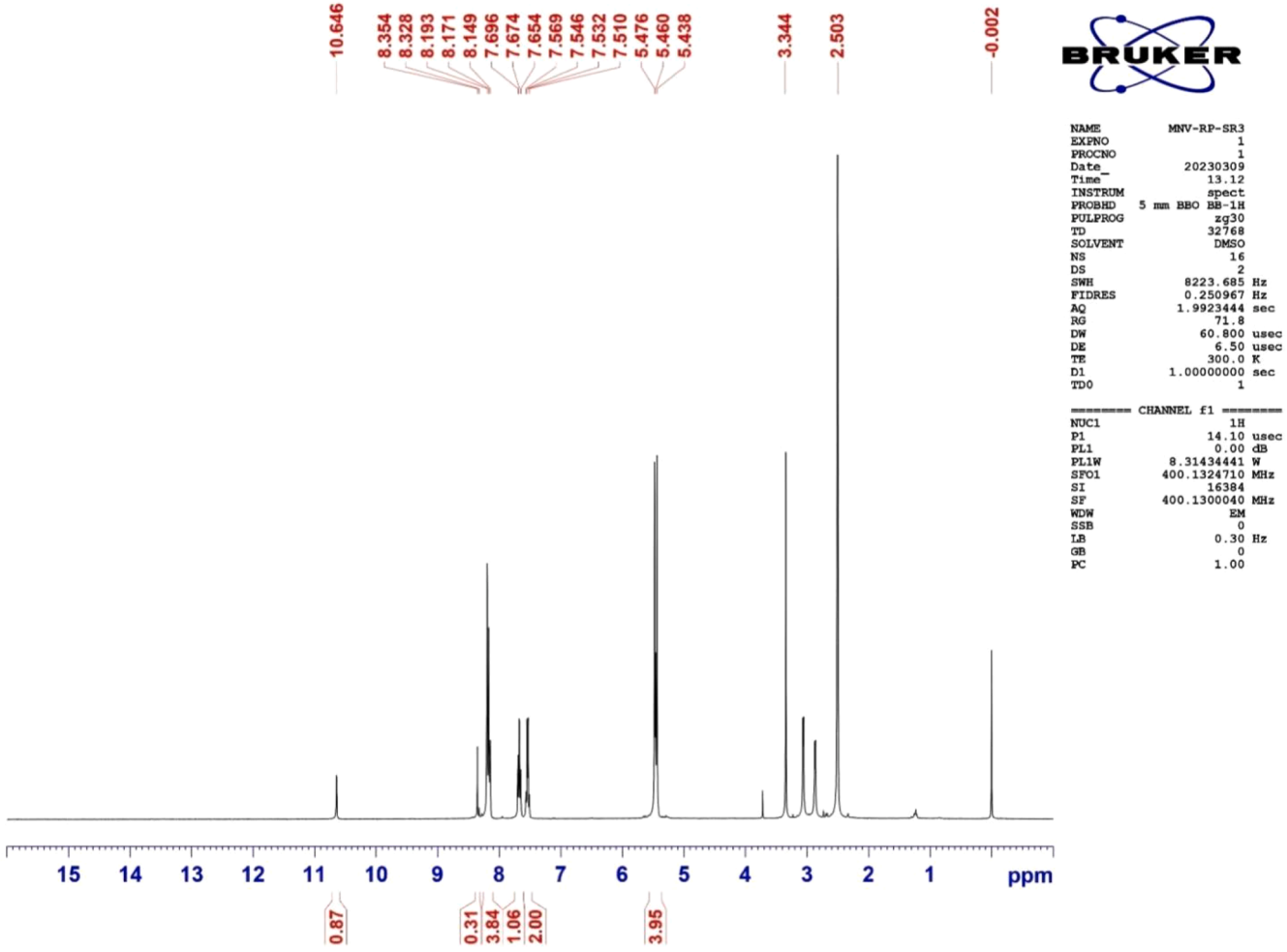

Fig. 8. ^{1}H NMR spectrum of compound SR3.

drug chloroquine and 16 synthesized compounds (**SR1** to **SR16**), with the purpose of evaluating their potential as inhibitors.

2.3.1.1. Target protein. The structural data for the target protein, 3QGT, was sourced from the Protein Data Bank (PDB) [25]. To prepare the protein structure; water molecules and co-crystallized ligands were removed. Subsequently, hydrogen atoms were added, and charges were assigned using the Amber force field.

2.3.1.2. Ligands. The ligands utilized in this study comprised both commercially obtained chloroquine and 16 synthesized compounds (**SR1** to **SR16**). The synthesis of the compounds followed established laboratory protocols. To ensure accurate representation, the structures of these ligands were optimized for geometry and charges. This optimization was carried out using Open Babel software with the Universal Force Field (UFF), as described by O'Boyle et al. (2011) [26].

2.3.1.3. Docking setup. The docking grid was established based on the presumed binding site of the target protein (PDB ID 3QGT), as determined through a comprehensive analysis of the protein structure and relevant literature sources [25]. To allow potential ligand flexibility and various conformations during the docking process, the grid parameters were meticulously set. The center coordinates of the grid were defined as 35.871, 11.16, 38.03, with a grid size of 58.39, 84.81, and 85.47. Furthermore, exhaustiveness and other pertinent parameters were configured to their default values, following the recommendations outlined in the Autodock Vina guidelines [22]. This approach ensured a thorough and reliable exploration of the ligand-protein binding interactions within the specified binding site.

2.3.1.4. Docking analysis. The ligands, encompassing chloroquine and the synthesized compounds (**SR1** to **SR16**), were subjected to molecular docking within the active site of the target protein (3QGT) using Autodock Vina in PyRx. Multiple docking runs were executed, and the resulting poses were systematically ranked according to their respective binding energies. To gain insights into the ligand-protein interactions, including hydrogen bonding and hydrophobic interactions, the docking results were meticulously analyzed using Discovery Studio Visualizer. This comprehensive analysis facilitated a detailed examination of the molecular interactions within the binding site, providing valuable information for the evaluation of ligand binding and potential inhibitory activity.

2.3.2. in vitro antimalarial activity

2.3.2.1. Chemicals

RPMI-1640 medium and cell culture grade (AlbuMAX II) were procured from HiMedia, Maharashtra, India and cell culture grade (Gentamycin Sulfate) was purchased from Sigma Aldrich, St. Louis, MO, USA. All remaining chemicals were used as analytical reagents grade.

2.3.2.2. In vitro culture of plasmodium falciparum

P. falciparum CQ-resistant strain RKL-9 obtained from National Institute of Malaria Research (NIMR), New Delhi, was maintained in

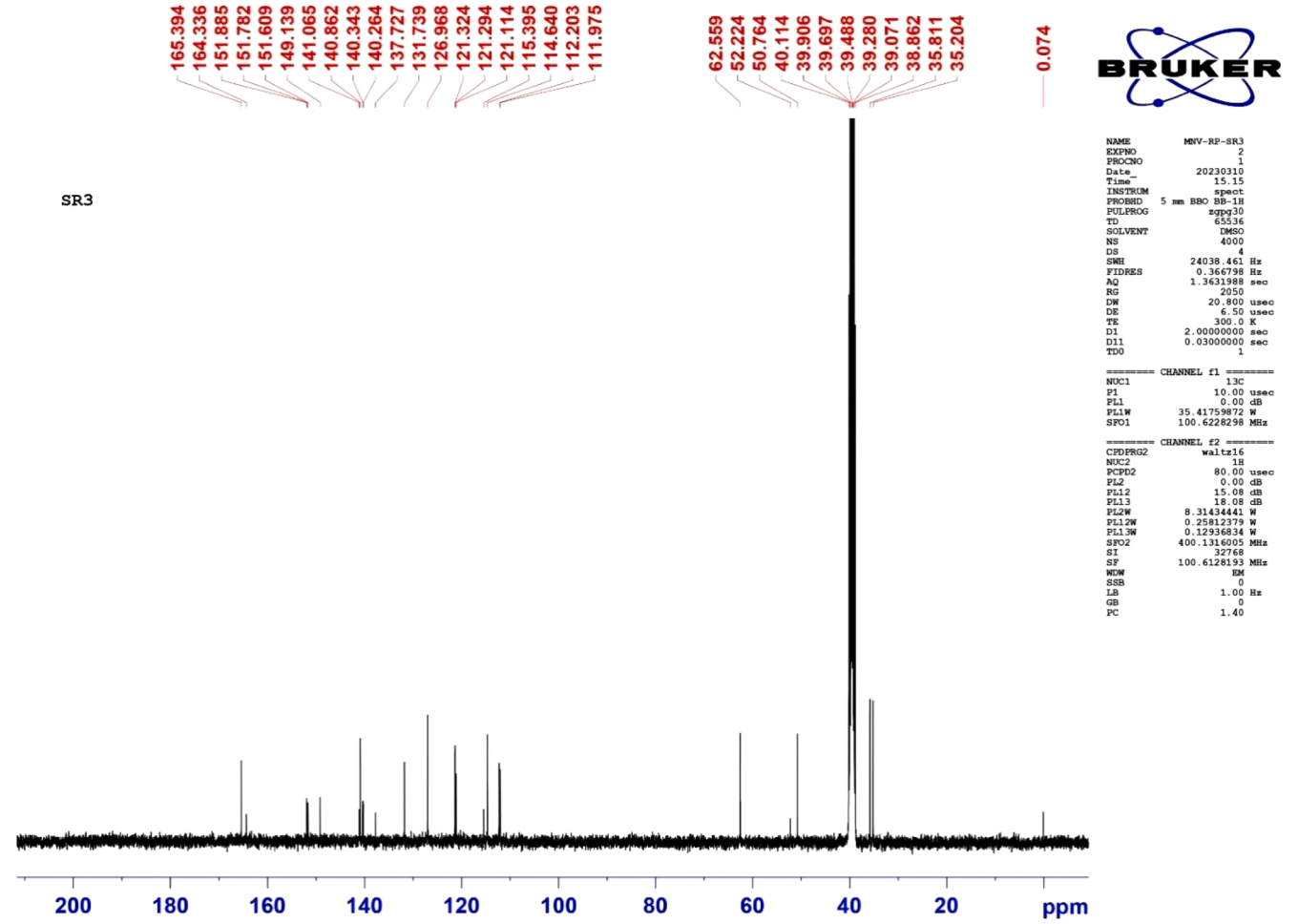

Fig. 9. ^{13}C NMR spectrum of compound SR3.

RPMI-1640 medium with HEPES and L-glutamine, supplemented with 25 Mm HEPES, 50 μg/L gentamicin sulphate and 0.2% sodium bicarbonate. At 37 °C *P. falciparum* cultures were incubated under an atmosphere of mixed gasses such as 5% CO_2, 5% O_2 and 90% N_2. 10% O^{+ve} blood was used as a basis of host erythrocytes at 5% hematocrit. The erythrocytes were collected from whole blood under sterile situations by elimination of the Peripheral Blood Mononuclear Cells (PBMCs) and plasma using a Histopaque 1077 gradient solution. Parasitemia was identified by Giemsa examination of TBS (Thin Blood Smears).

2.3.2.3. Drug dilutions

Chloroquine and stock solutions of synthesized phenoxy methyl-1,2,3-triazoles (**SR1** to **SR16**) were prepared by dissolving in DMSO, methanol and double distilled water, respectively and stored at −20 °C. Working solutions were prepared fresh in an incomplete media, and drug dilutions (two-fold in triplicates) were prepared in 96 well microtiter plates (final solvent concentration <1.0%) and plated at 5% hematocrit and 2% mixed stage parasitemia.

2.3.2.4. In vitro antimalarial activity

In vitro % inhibition of entry of parasites calculation was determined by Linz-Buoy G et al. with few modifications [27]. Normal erythrocytic were treated with the newly synthesized compounds (two-fold serial dilutions of each compound) for 24 h and showing to infected erythrocytic with 2% parasitemia with early ring stages. For positive control, we used normal erythrocytic without treatment with newly synthesized compounds. For 20–24 h, the plates were incubated at 37 °C, after confirming the presence of mature schizonts in control wells, without drug. The blood from every well was collected and a thin film was prepared, subsequently the films were static with methanol and stained with malarial parasite stain (JSB I and JSB II). Many schizonts of the control and tested samples were counted to study the effect of the newly synthesized derivatives. Growth inhibition was denoted as the percentage number of schizonts for every concentration, compared with untested controls. Mean IC_{50} results were calculated from dose-response curves (logarithm of drug concentration vs. percentage of schizonts). All these results are expressed as % inhibition of entry of parasites.

2.3.3. In vitro antimicrobial activity

The *in vitro* antimicrobial activity was examined using standard turbidimetric method as per National Committee for Clinical Laboratory Standard (NCCLS) [28]. Two-gram positive bacteria, *Staphylococcus epidermidis* (MTCC 3615), *Bacillus subtilis* (MTCC 441); two-gram negative bacteria, *Escherichia coli* (MTCC 739), *Salmonella enterica* (MTCC 3858) & one fungi, *Aspergillus brasiliensis* (MTCC 1344) were used to test the samples. Nutrient broth was used as growth media for bacteria whereas Potato dextrose agar used to grow fungi. Streptomycin, Chloramphenicol was used as standard drug against bacteria and Nystatin for fungi. Antimicrobial activity of different compounds dissolved in DMSO at 1000 μg/mL concentration was tested against 18 h old actively grown culture bacterial and fungal culture. The bacterial culture was incubated at 37 °C and fungal culture at 28 °C. Turbidimetric analysis of the culture growth inhibition was performed after 24 h for bacterial culture and 48 h for fungal cultures. Activities of the compounds were reported on basis of the change of growth based on measured optical density of the culture.

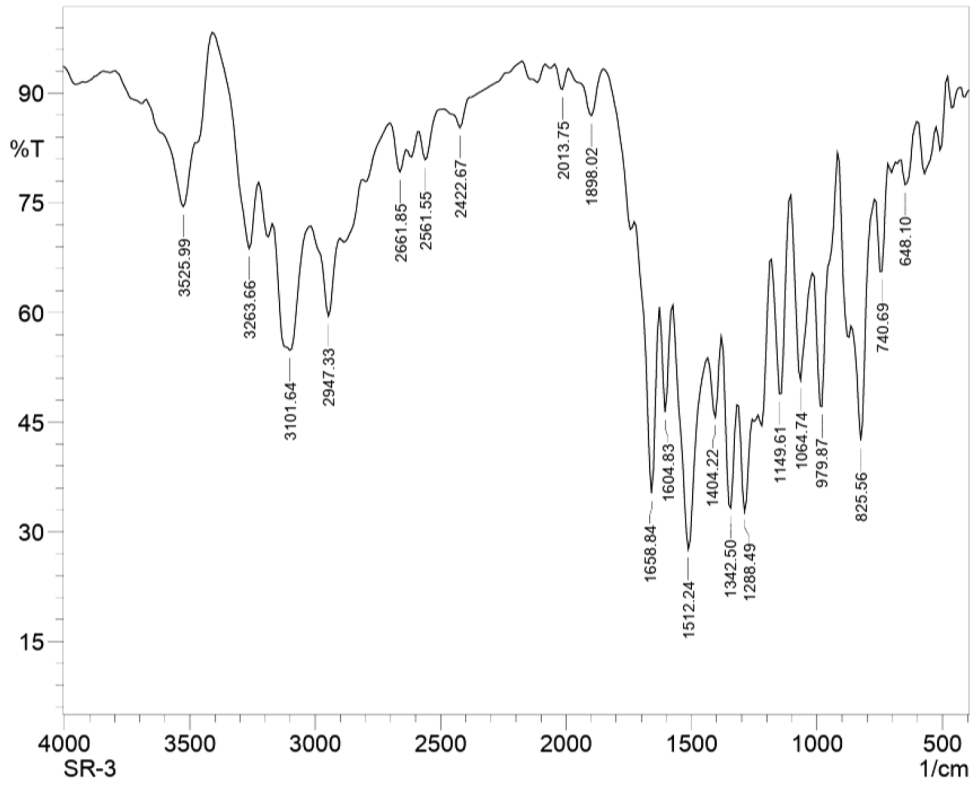

Fig. 10. IR spectrum of compound SR3.

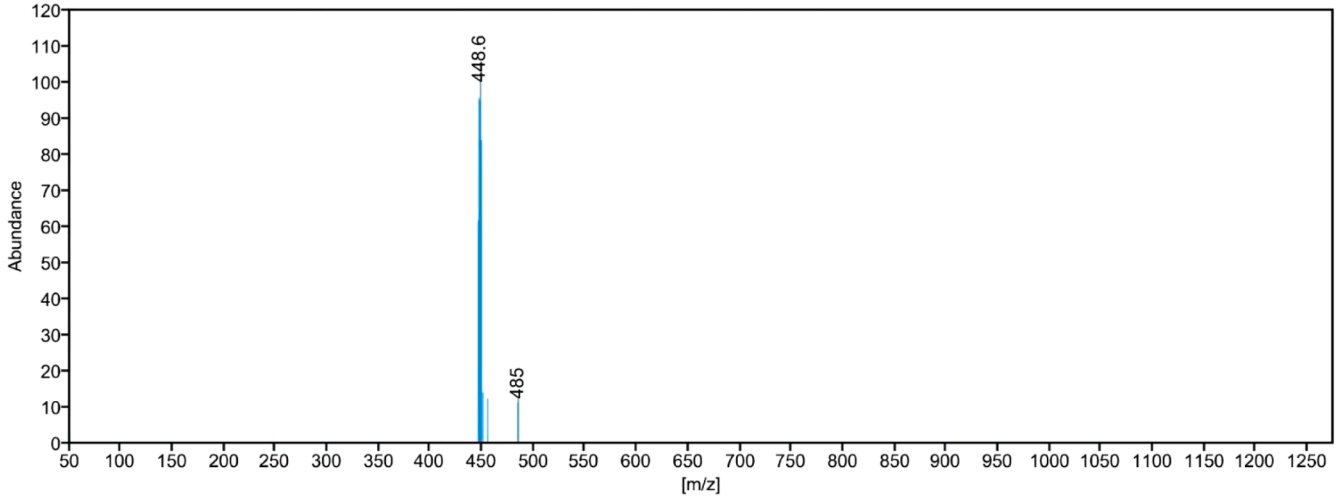

Fig. 11. Mass spectrum of compound SR3.

2.3.3.1. Minimum inhibitory concentration of compounds. MIC of each compound was tested against gram-positive, gram-negative bacteria and fungi using microtitre broth dilution method. Streptomycin, Chloramphenicol and Nystatin were used as standard drug. All the samples were diluted in DMSO in the range of 222.71–2694.69 μM. Compounds in DMSO solution are considered as negative control whereas microorganisms without drug act as positive control. Actively grown test microbial strains were grown in the nutrient broth medium. Bacterial strain was incubated at 37 °C whereas 28 °C was provided for fungi. Absorbance was measured at 600 nm after 24 h for bacterial cultures and after 48 h for fungi using microplate reader.

3. Results and discussion

3.1. Chemistry

Series of reports available on the synthesis of 1,4-disubstituted 1,2,3-triazole compounds bearing amide functionality and displaying various notable biological activities [29]. Recently, Ferroni et al. developed triazoles as non-steroidal anti-androgens for prostate cancer treatment [30]. On basis of these findings, we designed and synthesized 1,2,3-triazoles with amide linkage in their structures. Initially, the starting materials, i.e., ethyl 2-azidoacetate (**2**) were prepared by azidation of ethyl 2-bromoacetate (**1**) in the presence of sodium azide in water/acetone mixture at room temperature with 83% yield after 24 h. Simultaneously,

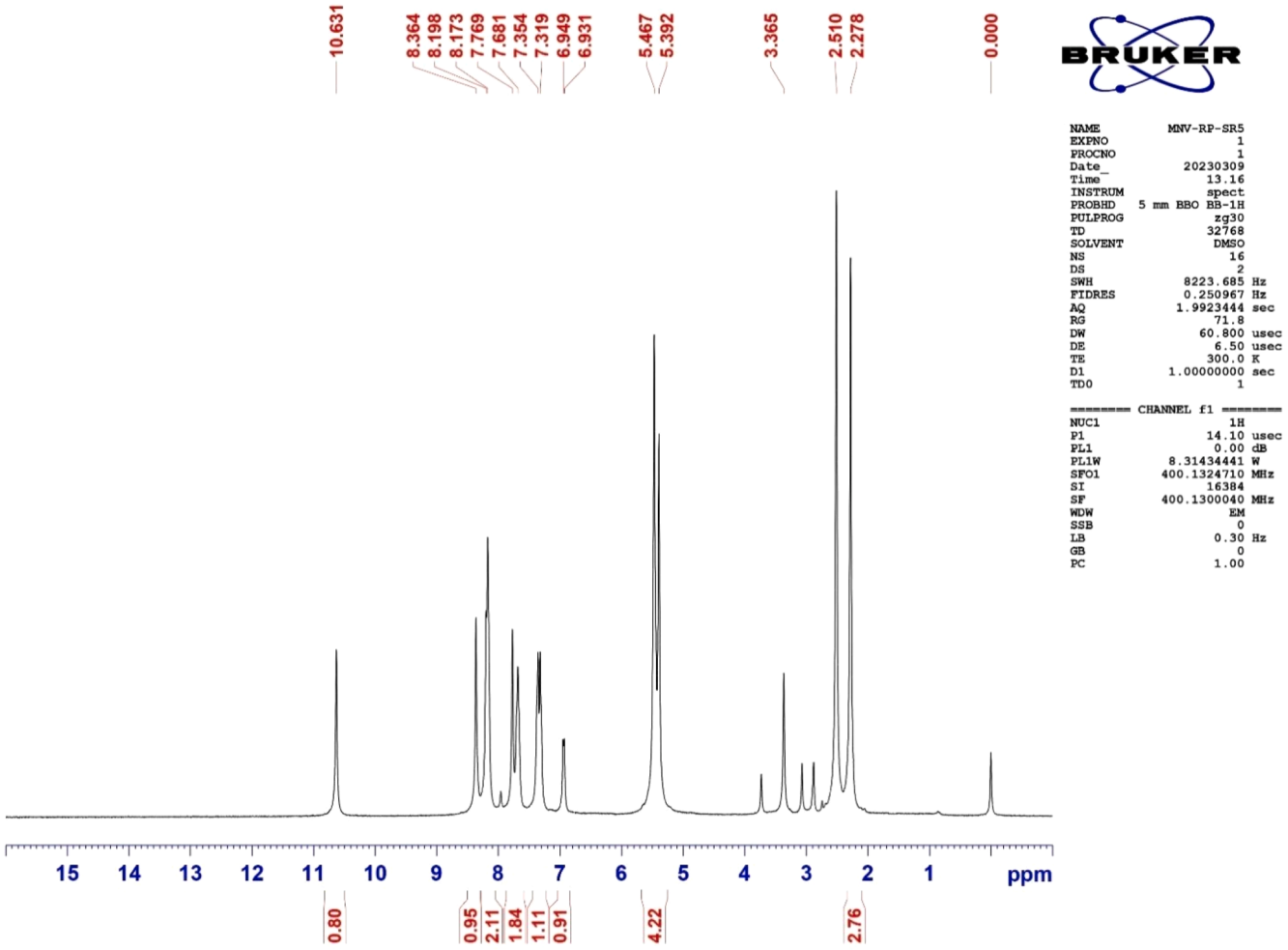

Fig. 12. ^{1}H NMR spectrum of compound SR5.

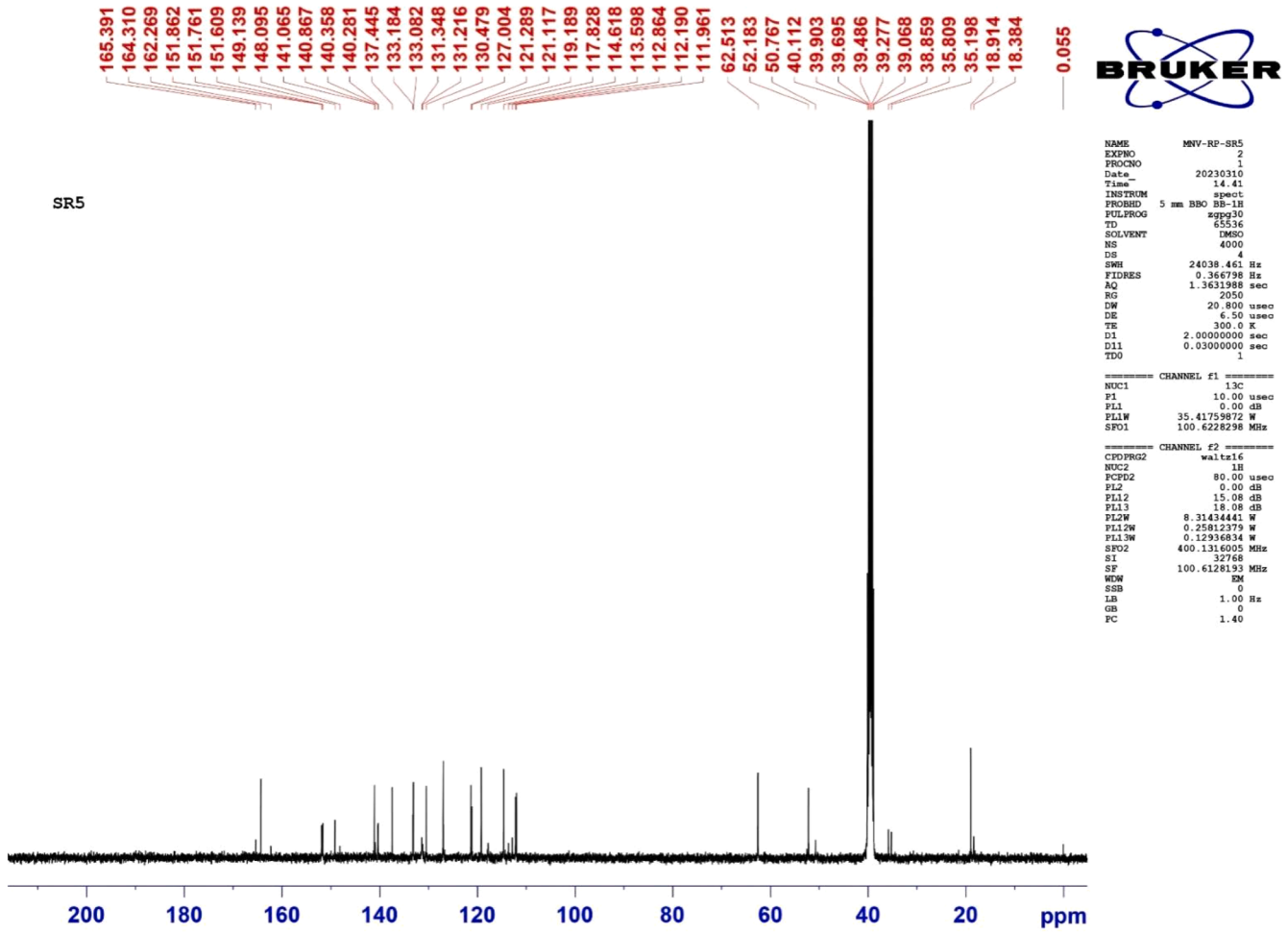

Fig. 13. ^{13}C NMR spectrum of compound SR5.

the terminal alkynes (**5**) were synthesized by the propargylation of 1, 2-difluoro-4-nitrobenzene (**3**) in the presence of propargyl alcohol in K_2CO_3 as a base in *N,N*-dimethylformamide (DMF) at 50 °C with 88% yield after 12 h.

However, at high temperature, the 1,2,3-triazole forming 1,3-dipolar cycloaddition (for long duration) in between azide and alkyne generally gives the mixture of two isomers. i.e., 1,4 and 1,5-disubstituted 1,2,3-triazoles. If the reaction is taking place in the presence of Cu(I) catalyst the reaction is regioselective because Cu(I) catalyst is highly activating the terminal acetylenes towards 1,3-dipolar cycloadditions reaction with azide to obtained 1,4-disubstituted 1,2,3-triazoles. With the optimized condition in hand, from derivative (**05**) by using $CuSO_4{\cdot}5H_2O$, triazole acetate derivative (**06**) was synthesized in presence of ascorbate sodium, at room temperature for 12 h in aqueous methanol and H_2O (4:1) with 84% yield. Subsequently, the triazole acid derivative (**07**) were prepared by the hydrolysis of triazole acetate derivative (**06**) in the presence of Lithium hydroxide dihydrate ($LiOH{\cdot}2H_2O$) in methanol and water (3:1) at room temperature with 88% yield after 2 h.

We accept the coupling of triazole acid derivative (**07**) with different amines (**8a-p**) to synthesize our final products **SR1**–**SR16**. The widely used coupling reagents are HBTU (N-1H-1,2,3-triazo[4,5-b]pyridine-1-ylmethylene]-N-methylmethanaminium Hexafluorophos-phate-N-oxide) carbodiimides, HATU (1-[Bis(dimethylamino)methylene]−1H-1,2,3-triazolo[4,5-b]pyridinium 3-oxid hexafluorophosphate) and propane phosphonic cyclic anhydride (T3P). Among these most characteristically utilized guanidinium reagent are HATU. Advanced condition for the amide coupling were attained using HATU in dimethylformamide (DMF) at room temperature. The synthesis of amides achieved from **(7)** with poles apart different amines to obtain the final products **SR1**–**SR16** by using HATU, *N,N*-Diisopropylethylamine (DIPEA) in dimethylformamide (DMF) at room temperature for 5–6 h as shown in Scheme 1. HATU used as coupling agent in addition to as solvent DMF is used in view of the reaction occurs, most important in the polar aprotic solvents as well as DIPEA is used as a base to deprotonate the triazole acid derivatives. Found yield is 72–85%. This pattern was specifically designed by introducing a previously unexplored atomic configuration. It has significant potential for new chemical reactions, materials, and pharmaceuticals. This unique contribution enhances understanding of chemical behaviours and interactions.

Regioselective formation of 1,4-disubstituted 1,2,3-triazole amide derivatives **SR1**–**SR16** has been confirmed by physical data and analytical techniques such as Fourier Transform Infrared Spectroscopy (FT-IR), ^{1}H nuclear magnetic resonance (NMR), ^{13}C NMR, and mass spectra (MS). According to the FT-IR of compound **SR1**, the band observed at 3263 cm^{-1} confirmed the presence of –NH group of amide functionality, and the band observed at 1666 cm^{-1} indicate the presence of the amidic C = O stretching and the band observed at 1350 cm^{-1} indicates the presence of one nitro group. In the ^{1}H NMR spectrum of compound **SR1**, the signal at 2.76 ppm indicates the presence of one methyl group on the aromatic amide ring, and signals at 5.36 and 5.46

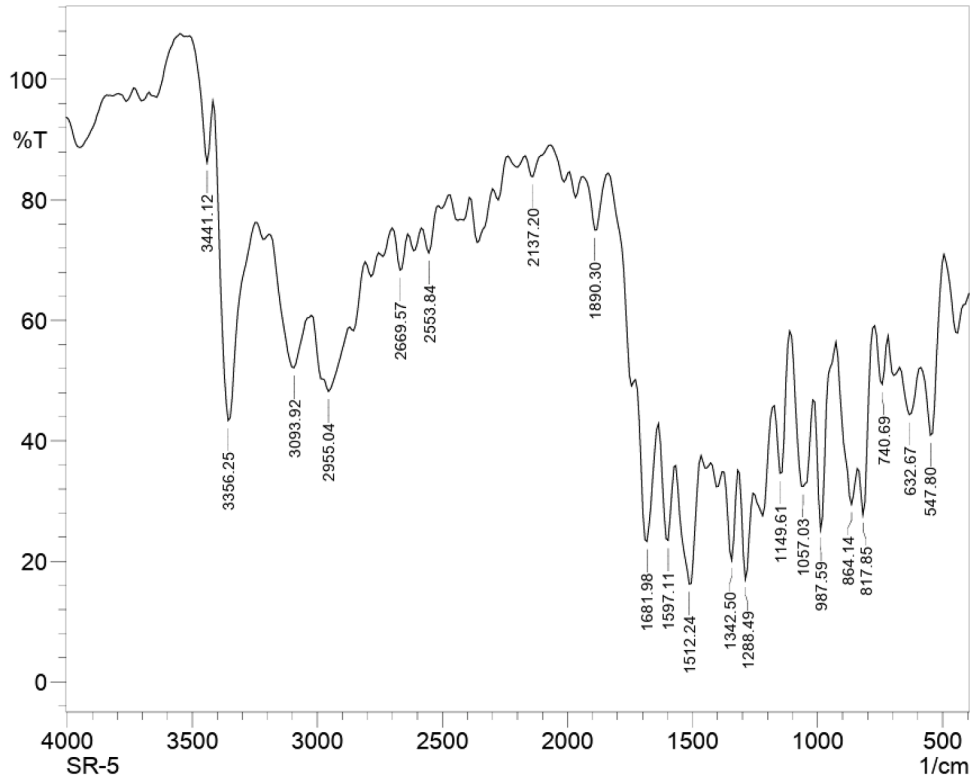

Fig. 14. IR spectrum of compound SR5.

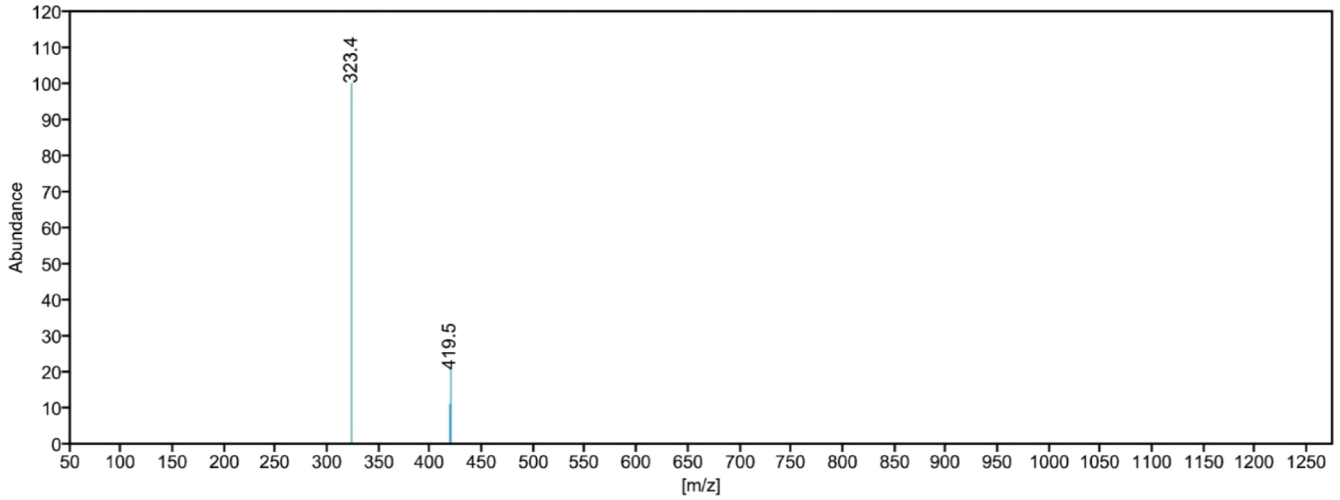

Fig. 15. Mass spectrum of compound SR5.

ppm indicate the presence of two methylene groups attached with triazole ring (1,4-disubstituted). In addition to this, the signal exhibiting at 8.35 ppm for one proton clearly indicates the formation of the 1,4-disubstituted 1,2,3-triazole ring. In the ^{13}C NMR spectrum of compound **SR1**, the signal at 20.41 ppm indicates the presence of methyl carbon on the aromatic amide ring, and the signals at 52.19 and 62.51 ppm indicate the presence of two methylene groups attached to the triazole ring. Furthermore, the signal observed at 163.81 ppm indicates the presence of amide carbonyl carbon. The formation of compound **SR1** has been further confirmed by mass spectrometry. The calculated [$M + 1$] for compound **SR1** is at 385.12 and observed [$M + 1$] is at 384.9. Similarly, compounds **SR2**–**SR16** were characterized by spectral analysis. The structures of synthesized 1,4-disubstituted 1,2,3-triazole amide derivatives are represented in Fig. 2.

3.2. Pharmacology

3.2.1. Molecular docking studies

The docking simulations were performed using PyRx 0.8 software to study the interactions between chloroquine and ligands **SR1**-**SR16** with a chain of PfDHFR (PDB ID- 3QGT). The binding affinity values for the docked complexes are listed in the table provided (Table: 1). The PfDHFR enzyme (Plasmodium falciparum dihydrofolate reductase) is a critical target in antimalarial drug development due to its essential role in the parasite's folate pathway, necessary for DNA synthesis and cell replication [25]. Inhibitors like pyrimethamine and proguanil have historically targeted PfDHFR, but drug resistance has spurred the search for new inhibitors [31]. The synthesized substances in this study are designed to interact with the active site of PfDHFR, suggesting their

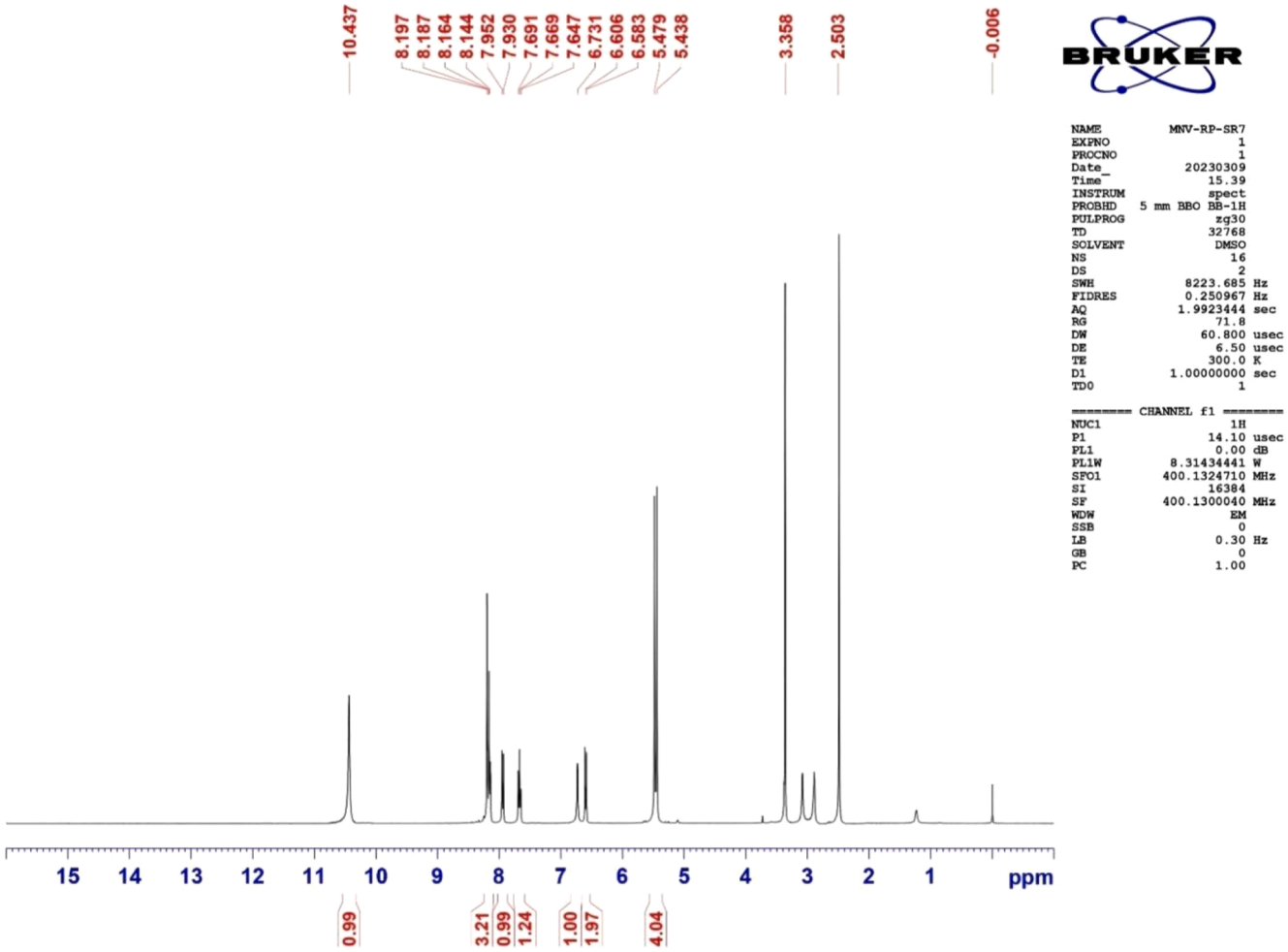

Fig. 16. ^{1}H NMR spectrum of compound SR7.

potential effectiveness as antimalarial agents [25].

From the outcomes, it is evident that chloroquine exhibited a binding affinity of −7.1 kcal/mol, indicating a moderate binding interaction with the PfDHFR receptor (Fig. 3). Among the ligands, **SR12** demonstrated the highest binding affinity with a value of −10.7 kcal/mol, indicating that it forms a strong and stable complex with the PfDHFR receptor. On the other hand, ligands **SR8** and **SR16** also showed relatively high binding affinities, with values of −8.9 kcal/mol and −9.7 kcal/mol, respectively. Suggesting that these compounds could be potential candidates for further optimization and development as antimalarial agents.

3.2.2. *Pharmacokinetics*

The ADME prediction was done by the SwissADME web server [24] for the synthesized compounds **SR1**–**SR16** and are tabulated in Table 2. The octanol/water partition coefficient (Log $P_{w/o}$) values were predicted in the range of 0.99–2.64, and as per the essential condition of Lipinsk's rule of five [32]. The molecular weights of compounds **SR1**–**SR16** were in the range of 371.32–450.22 g/mol. As molecular weights are ≤ 500 g/mol, they can be easily transported, absorbed and diffused after administered into the body [33]. The predicted rotatable bonds were in the range of 8–10, H-bond acceptors were ≤10, and H-bond donors are ≤ 5. The Topological Polar Surface Area (TPSA) of compounds were in the range of 114.86–127.75; these lower TPSA values indicate the good oral bioavailability excluding **SR7** having higher TPSA value 160.68. All compounds had zero violations of Lipinski's rule, except for **SR7**, which exhibited one Lipinski violation. The synthetic accessibility score of all compounds was found to be ≤ 10, it confirms that they can be synthesized easily [34]. The pharmacokinetic evaluation reveals that all molecules have favorable drug-likeness properties and could be considered as therapeutic agents.

3.2.3. *in vitro antimalarial activity*

All the novel synthesized phenoxy methyl-1,2,3-triazoles (**SR1** to **SR16**) have been tested for their potential antimalarial analysis against *P. falciparum* (CQ-resistant strain RKL-9) with few modifications [27]. In general, erythrocytes infected by *P. falciparum* at 2% parasitemia and 5% hematocrit were incubated with various concentrations of compounds for 48 h at 37 °C and its higher levels were used to determine the IC_{50} values which are given in Table 3 and for positive control, we've utilized chloroquine (CQ). From the table, it is found that all newly synthesized phenoxy methyl-1,2,3-triazole derivatives (**SR1** to **SR16**) demonstrate various potency (18.60 μM to 51.26 μM) against *P. falciparum in vitro*. Majority of EWG (Electron Withdrawing Group) at position number 4 in phenyl ring attached with amide functionality could favor this activity. Excluding **SR15** having ERG (Electron Releasing Group) and naphthyl substitution could also favor this activity. Amongst all the triazoles, compound **SR12** containing naphthyl substituent is found to be most active scaffold with IC_{50} of 18.60 μM.

Synthesized triazole compounds having halogen substitution on aryl ring connecting with amide functionality, the scaffold **SR16** having 2,4-difluorobenzyl methyl substituent is found lower IC_{50} (22.15 μM). In comparison, the scaffold **SR3** having 4-bromophenyl, **SR10** having 2,2-difluorophenyl, **SR4** having 4-chlorophenyl, **SR8** having 4-chloro-3-

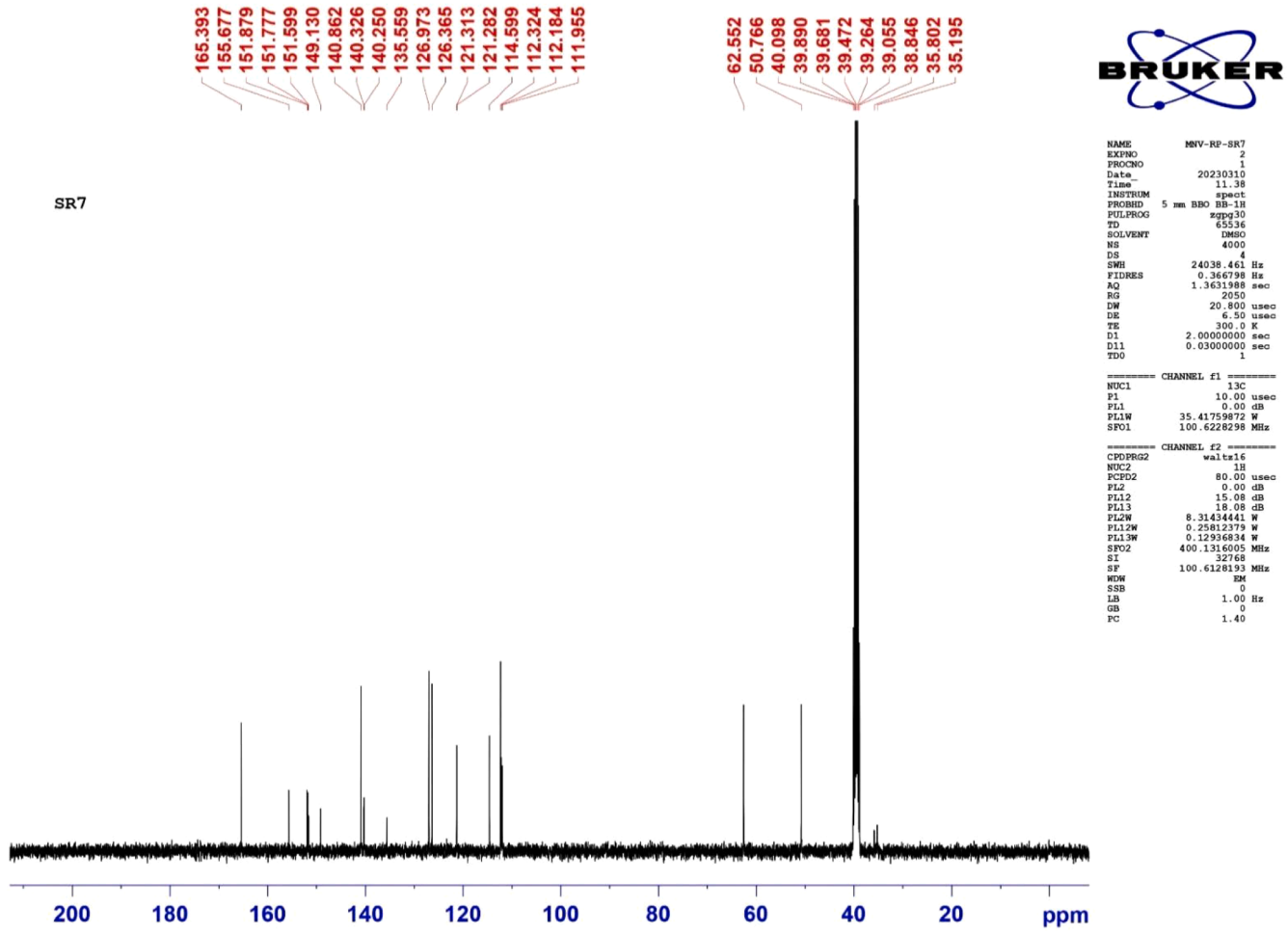

Fig. 17. ^{13}C NMR spectrum of compound SR7.

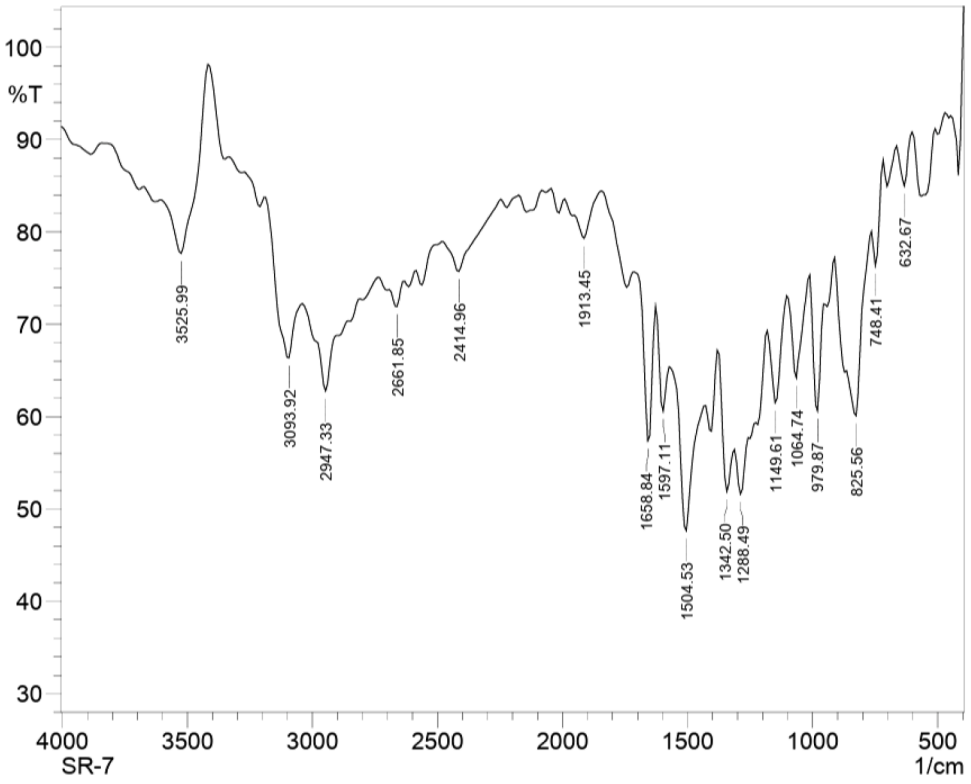

Fig. 18. IR spectrum of compound SR7.

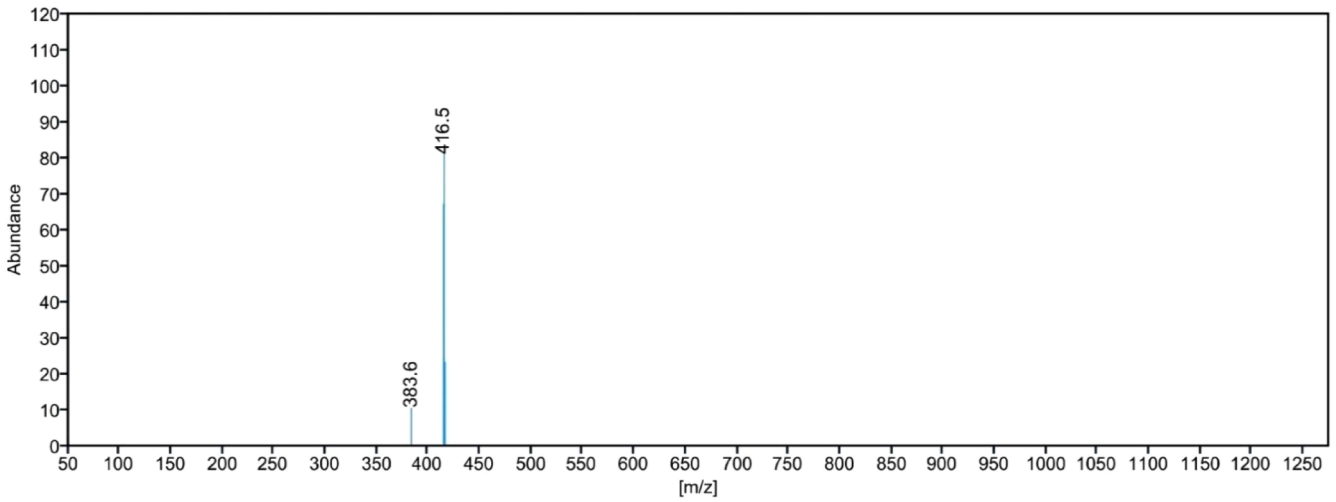

Fig. 19. Mass spectrum of compound SR7.

methylphenyl, **SR9** having 2,4-difluorophenyl, and **SR5** having 3-chloro-4-methylphenyl groups have found higher IC_{50} values such as 36.72 μM, 38.30 μM, 39.96 μM, 41.19 μM, 42.82 μM, and 43.07 μM, respectively.

1,2,3-Triazole derivatives having various electron releasing group on aryl ring connecting with amide functionality, the scaffold **SR15** having 4-methoxybenzyl substituent is found lower IC_{50} of 32.99 μM. In comparison, the scaffolds **SR11** having 2-methylphenyl, **SR2** having 4-methoxyphenyl, **SR1** having 4-methylphenyl, and **SR14** having 5-methylpyridin-2-yl groups have found higher IC_{50} values such as 41.25 μM, 42.64 μM, 45.43 μM, and 48.42 μM, respectively. The presence of a highly electro attractive nitro group at 4-position of aryl ring connecting with amide functionality, the scaffold **SR7** is found lower IC_{50} value 36.09 μM. However, other scaffolds in the prepared series such as **SR13** having pyridin-3-yl and **SR6** having phenyl ring have also found higher IC_{50} values such as 47.64 μM and 51.26 μM, respectively. Collectively, our *in vitro* experimental results suggest that the all newly synthesized phenoxy methyl-1,2,3-triazole derivatives (**SR1** to **SR16**) are found to be significantly potent against *P. falciparum*.

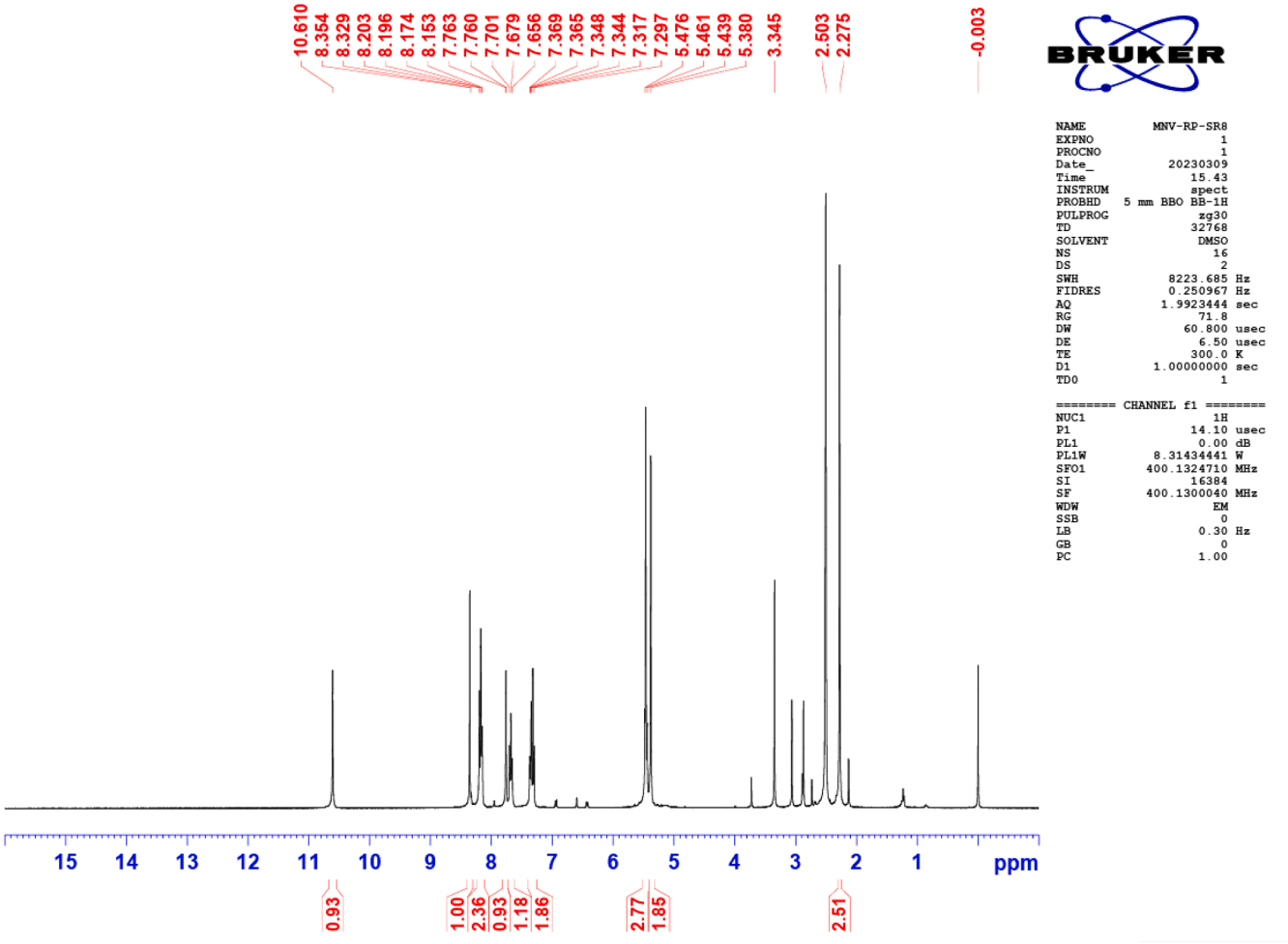

Fig. 20. ^{1}H NMR spectrum of compound SR8.

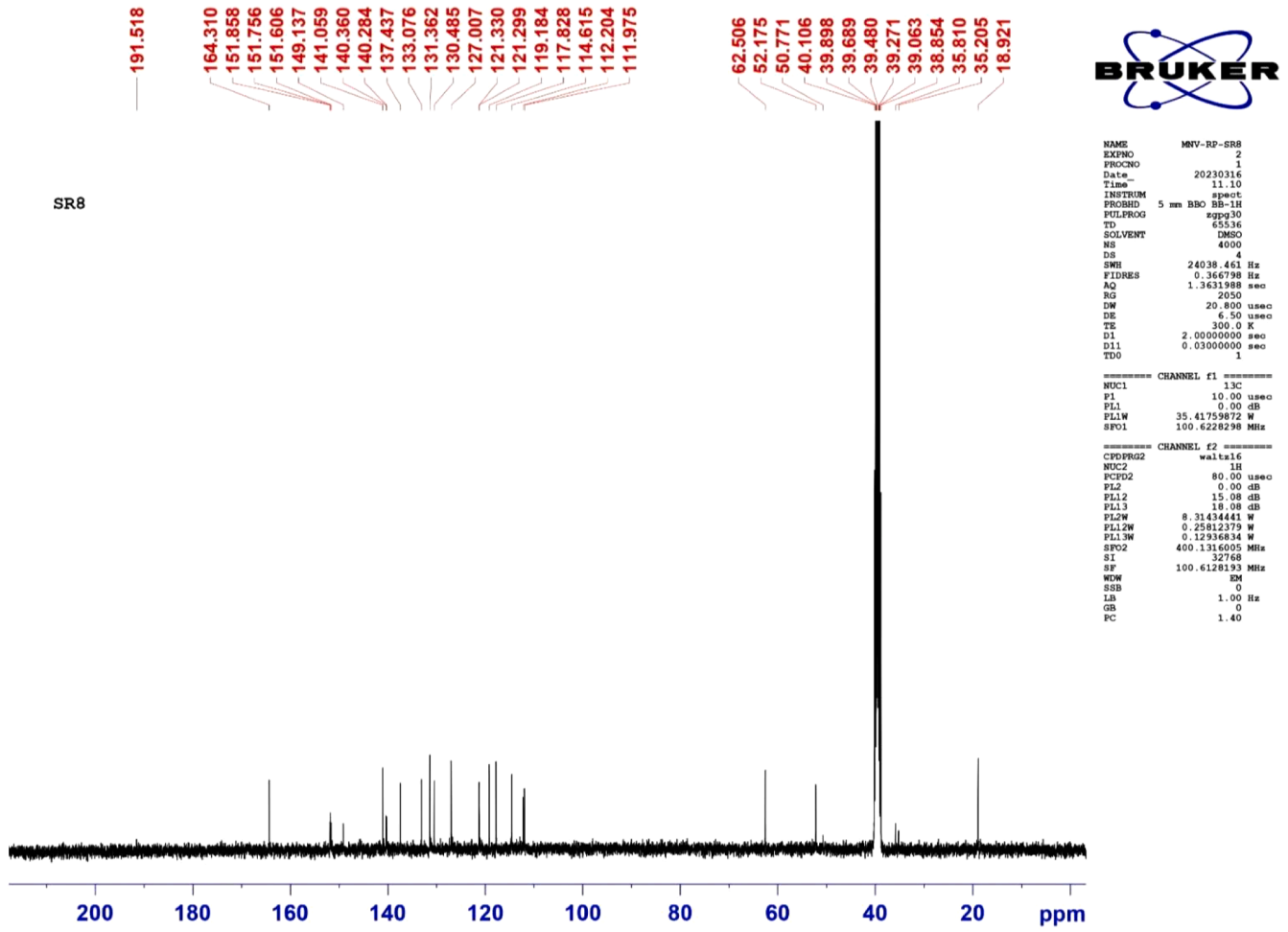

Fig. 21. ^{13}C NMR spectrum of compound SR8.

3.2.4. In vitro antimicrobial activity

Growth inhibition was observed for preliminary confirmation of the antimicrobial activity of tested compounds compression with standard antimicrobial agents against two-gram positive, two-gram negative bacteria and one fungal pathogen. The species discussed have varying clinical importance. *Staphylococcus epidermidis* is a common skin microbiota but can cause problematic infections, especially in hospital settings due to biofilm formation and antibiotic resistance [35]. *Bacillus subtilis* is generally benign but valued for its probiotic potential and industrial applications [36]. *E. coli* encompasses harmless strains as well as pathogenic types like *E. coli* O157, known for severe foodborne illnesses and urinary infections, serving as a model for bacterial genetics and resistance studies [37]. *Salmonella enterica* causes significant foodborne illnesses globally, ranging from gastroenteritis to typhoid fever, emphasizing its public health impact and vaccine research [38]. *Aspergillus brasiliensis*, while industrially useful in enzyme and acid production, poses occasional risks in immunocompromised patients, highlighting its role in opportunistic infections like invasive aspergillosis [39]. Out of 16 compounds, 9 compounds revealed the considerable antimicrobial activity (Table 4). Compounds **SR7** and **SR9** exhibited the highest antibacterial activity against bacteria at 600.83 μM and 614.12 μM concentration respectively. Although, **SR9** showed highest activity against fungus, hence considered as the most potent broad-spectrum compound at 614.12 μM concentration. Compound **SR5, SR10, SR12** and **SR14** were also observed the considerable antimicrobial potential for both bacteria and fungi. Other compounds **SR3, SR8, SR11**, and **SR16** exhibited weak antimicrobial potential whereas others observed very negligible growth inhibition effect on the tested culture.

3.2.4.1. Minimum inhibitory concentration of compounds. MIC can be determined as the lowest concentration of drug that inhibits the growth of microorganisms. Absorbance value of each drug at different dilution was compared with the negative and positive controls. The minimum dilution of antibiotic, that shows microbial growth compared to the positive control were considered as effective inhibitory concentrations as can be depicted from Table 5. Compounds **SR3, SR5, SR7, SR8, SR9, SR10, SR11, SR12, SR14** and **SR16 have** noteworthy antimicrobial potential whereas compound **SR5, SR7, SR9, SR10, SR14** and **SR14**

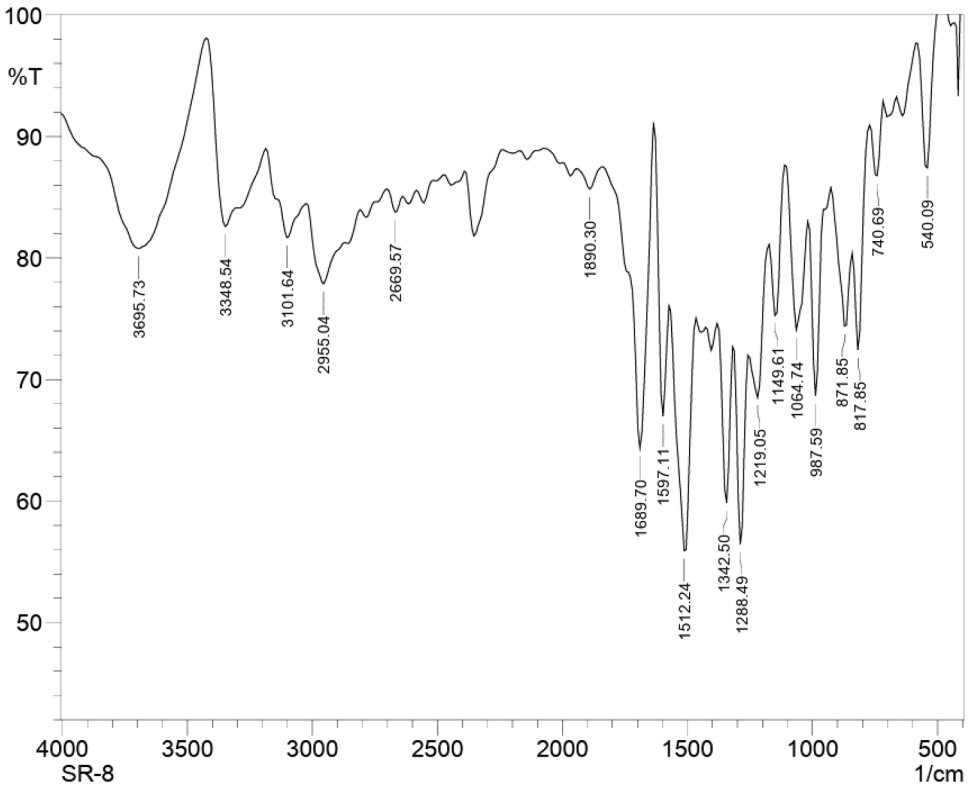

Fig. 22. IR spectrum of compound SR8.

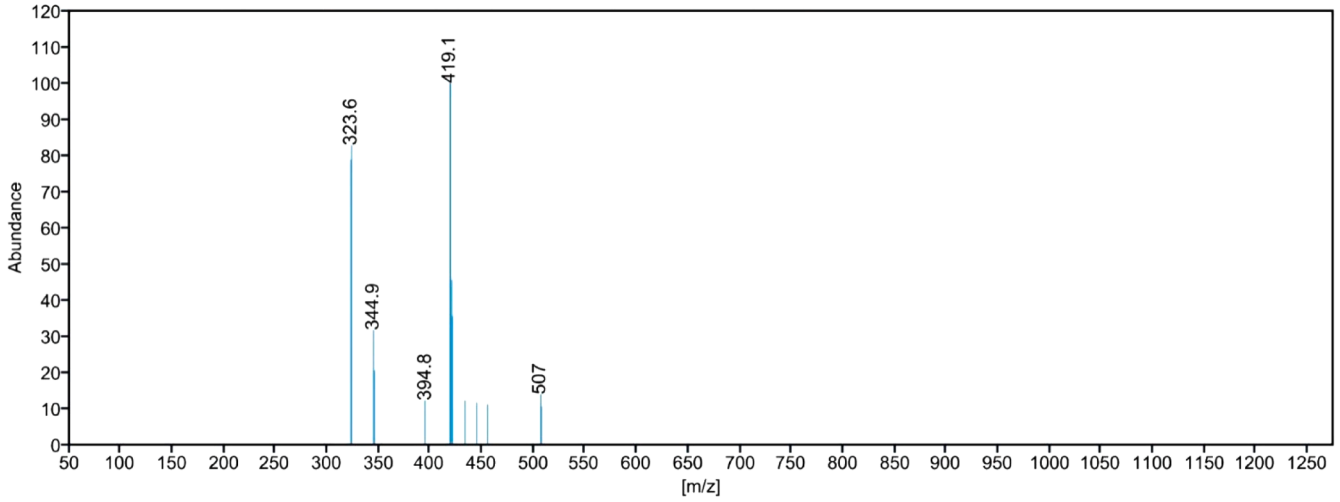

Fig. 23. Mass spectrum of compound SR8.

were found effective against tested bacterial and fungal cultures. Compound **SR9** exhibited the highest antibacterial activity against bacterial and fungal cultures (614.12 μM), whereas compound **SR7** was found effective to inhibit bacterial growth (600.83 μM). Other compounds **SR5, SR10** and **SR12** were also found effective against tested fungi. The rest of the tested compound showed weak or no antimicrobial potential against the tested cultures.

All the spectral data and antimicrobial activity bar are displayed in Figures 4–44

4. Conclusions

We synthesized novel phenoxy methyl-1,2,3-triazole derivatives (**SR1** to **SR16**) via click chemistry approach. The compounds were characterized by ^{1}H and ^{13}C NMR, FT-IR spectroscopy, mass spectrometry and elemental analysis. The docking study provides valuable computational insights into the interactions between chloroquine, 16 synthesized compounds and the PfDHFR receptor. The results highlighted potential candidates for further experimental evaluation and serve as a basis for the design and development of novel antimalarial

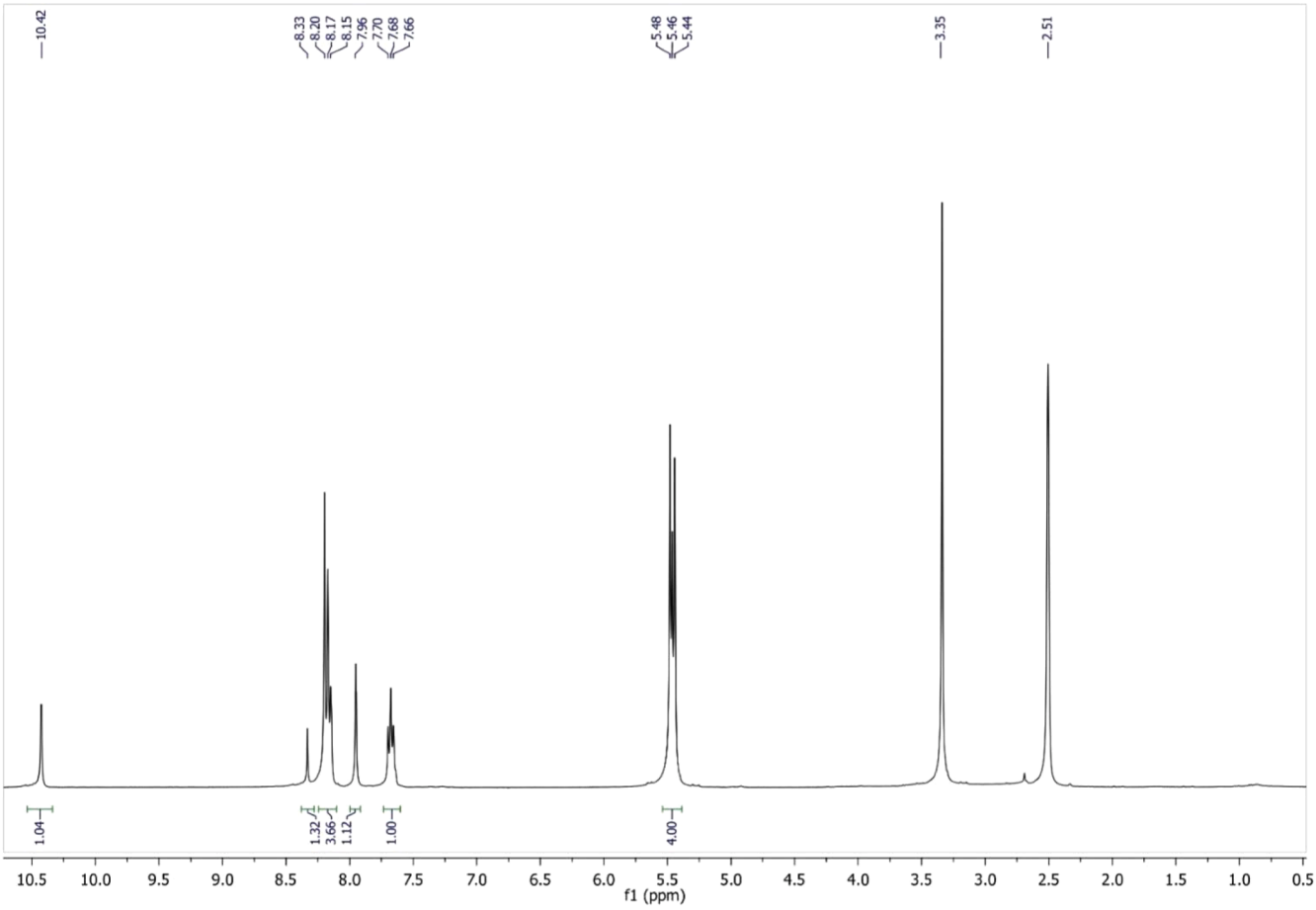

Fig. 24. ^{1}H NMR spectrum of compound SR10.

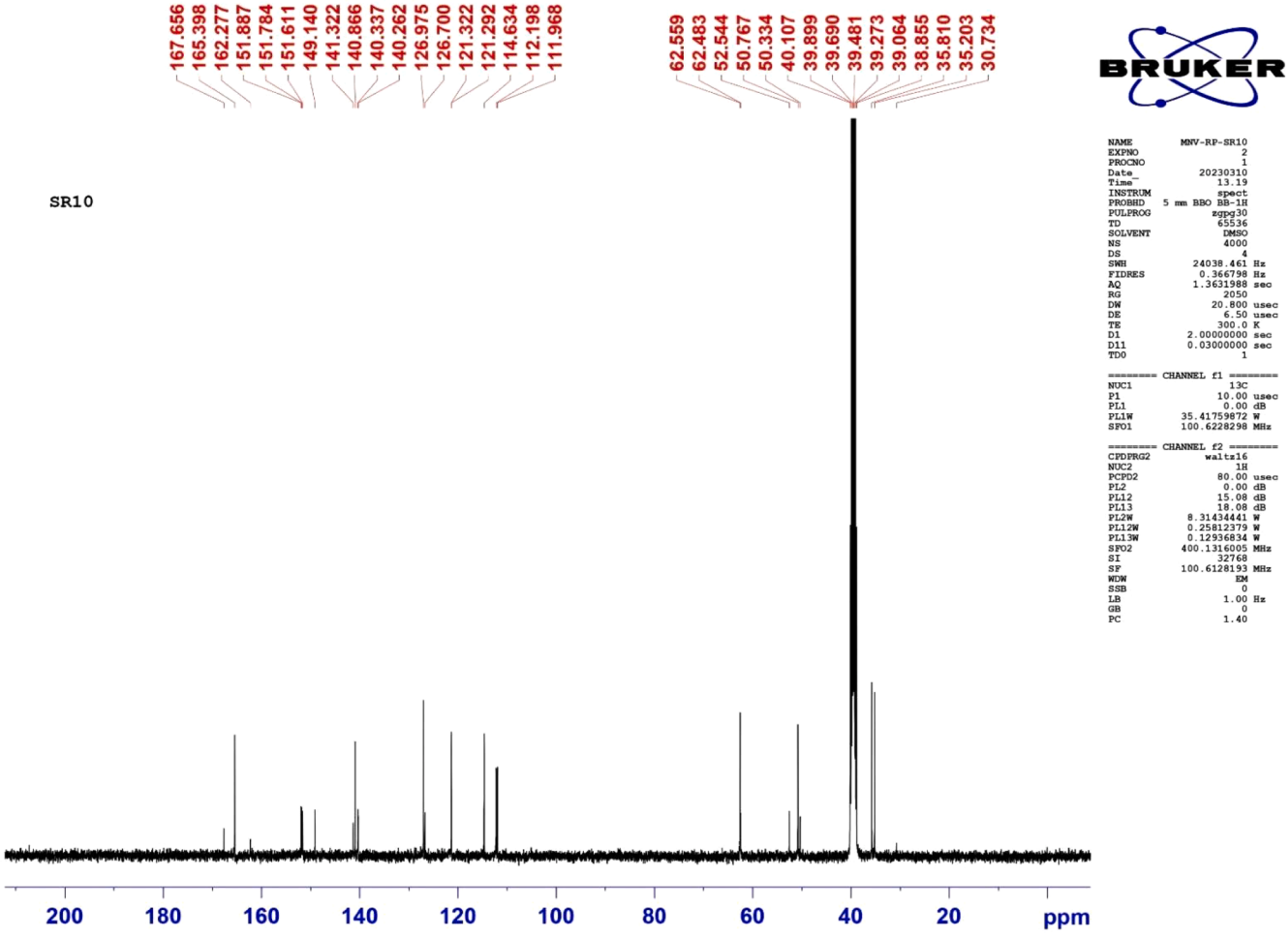

Fig. 25. ^{13}C NMR spectrum of compound SR10.

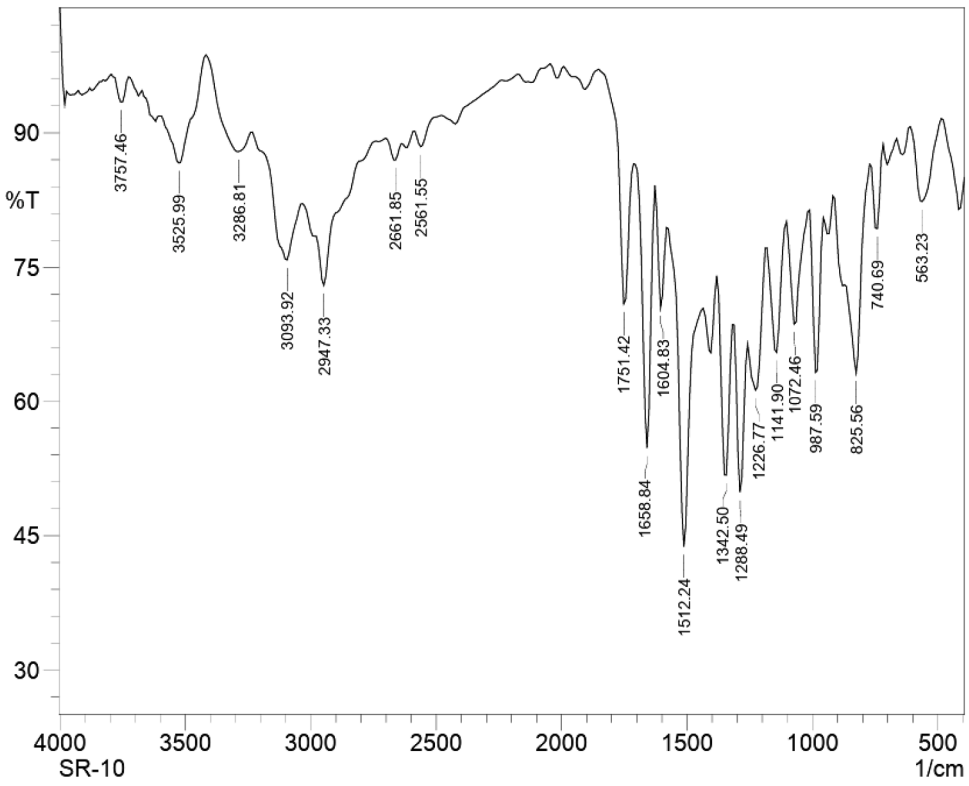

Fig. 26. IR spectrum of compound SR10.

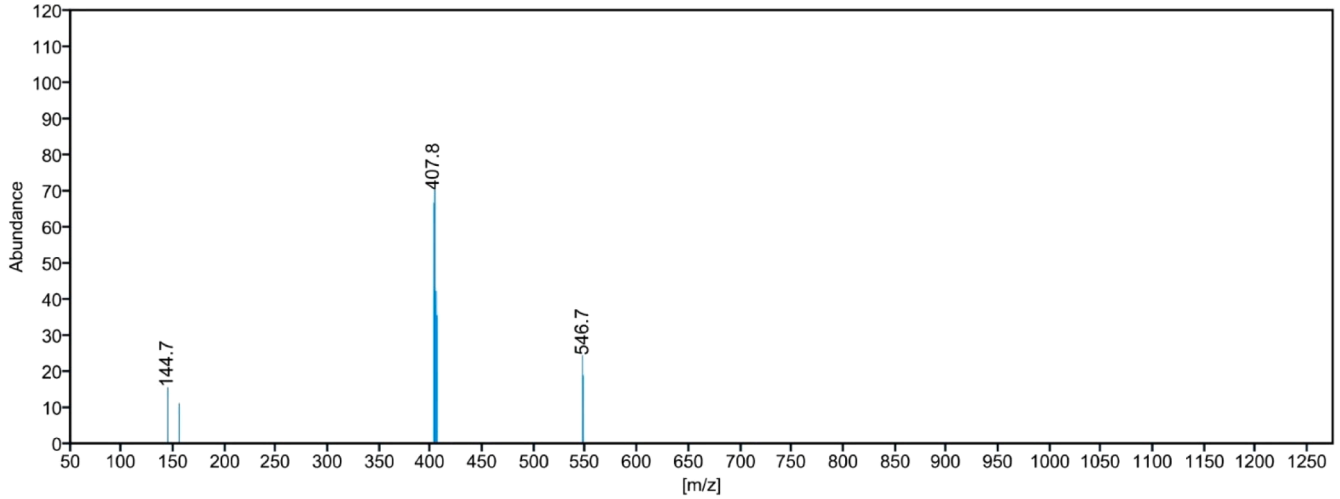

Fig. 27. Mass spectrum of compound SR10.

agents. The study of biological analysis of all the newly synthesized derivatives have found significant potency against *P. falciparum* (CQ-resistant strain RKL-9) strain *in vitro* antimalarial analysis. Amongst all derivatives; **SR12, SR15**, and **SR16** were found to be the most active compounds. Furthermore, the synthesized compounds displayed a promising antimicrobial activity as compared with the standard drugs Streptomycin, Chloramphenicol and Nystatin. Out of the sixteen tested compounds; **SR7**, and **SR9** exhibited the promising antimicrobial activity and can be considered as important lead moiety. The favourable drug-likeness properties recommend that they can be easily absorbed, distributed, metabolised, and excreted from the body. Hence, the synthesized compounds can be used in a scaffold, hoping for the design and development of potential antimalarial and antimicrobial drugs.

CRediT authorship contribution statement

Rahul V. Parmar: Writing – review & editing, Writing – original draft, Visualization, Validation, Software, Resources, Project administration, Methodology, Investigation, Funding acquisition, Data curation, Conceptualization. **Milan S. Vadodaria:** Supervision. **Seema N. Kher:** Methodology. **Nutan P. Vishwakarma:** Methodology.

Declaration of competing interest

The authors declare that they have no known competing financial interests or personal relationships that could have appeared to influence the work reported in this paper.

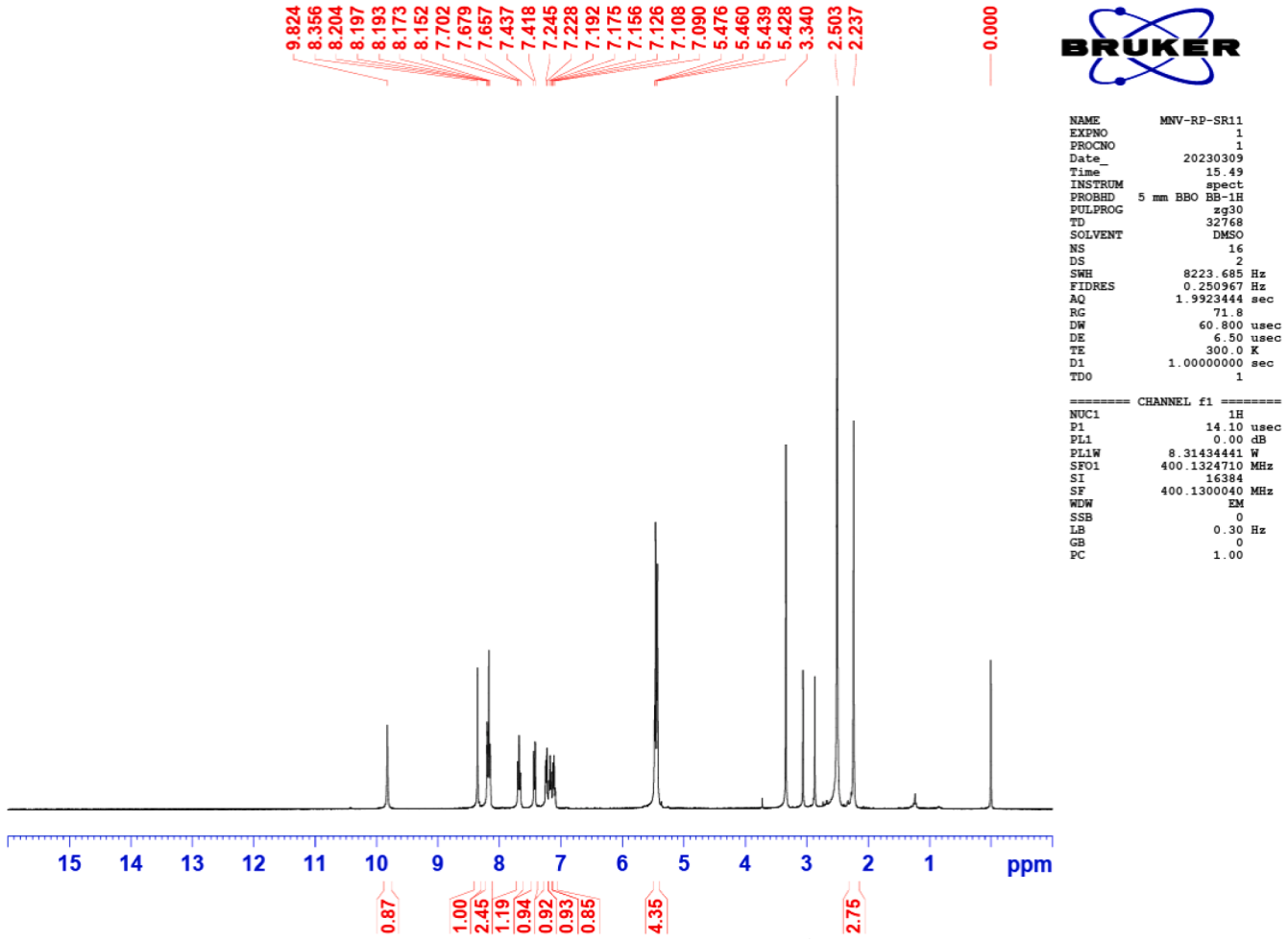

Fig. 28. ^{1}H NMR spectrum of compound SR11.

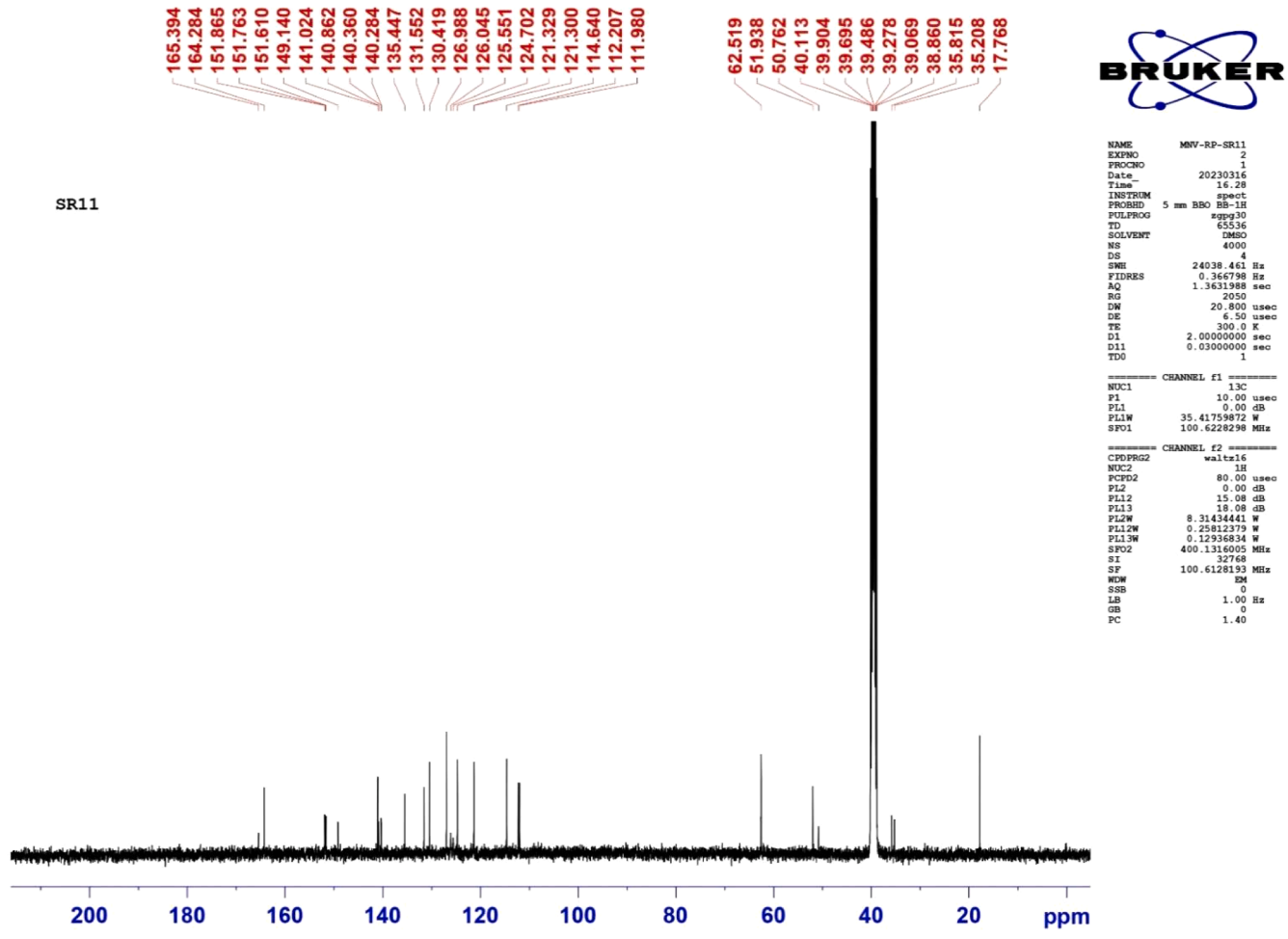

Fig. 29. ^{13}C NMR spectrum of compound SR11.

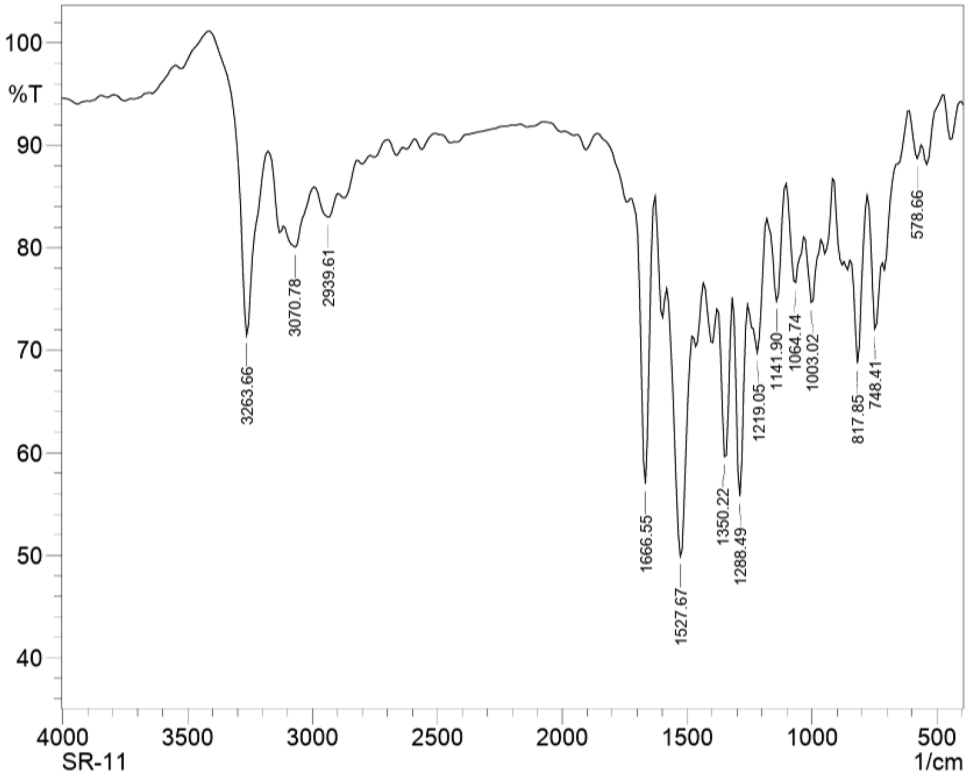

Fig. 30. IR spectrum of compound SR11.

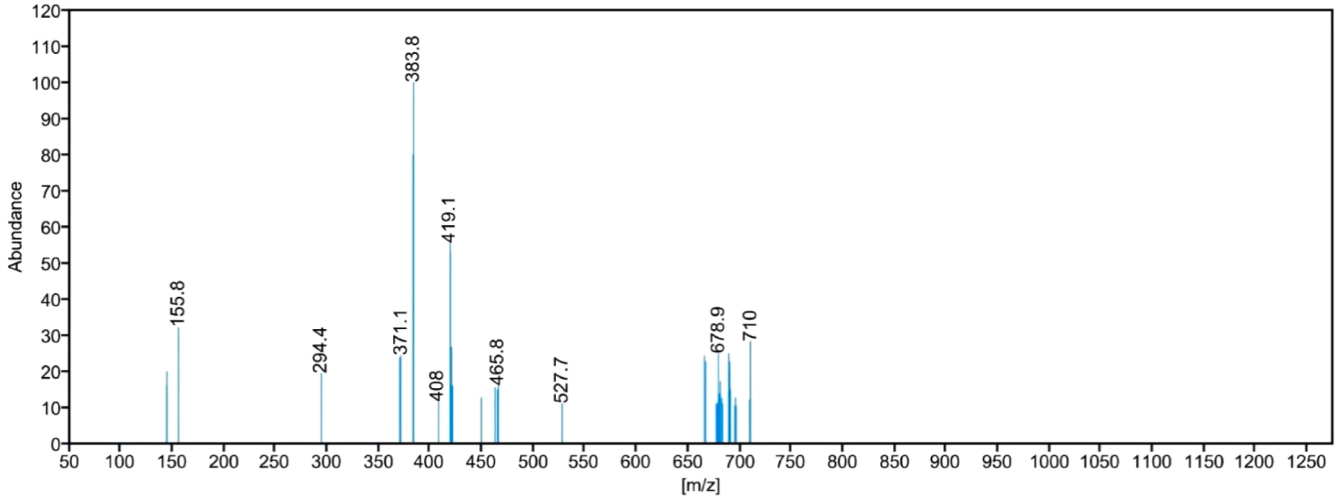

Fig. 31. Mass spectrum of compound SR11.

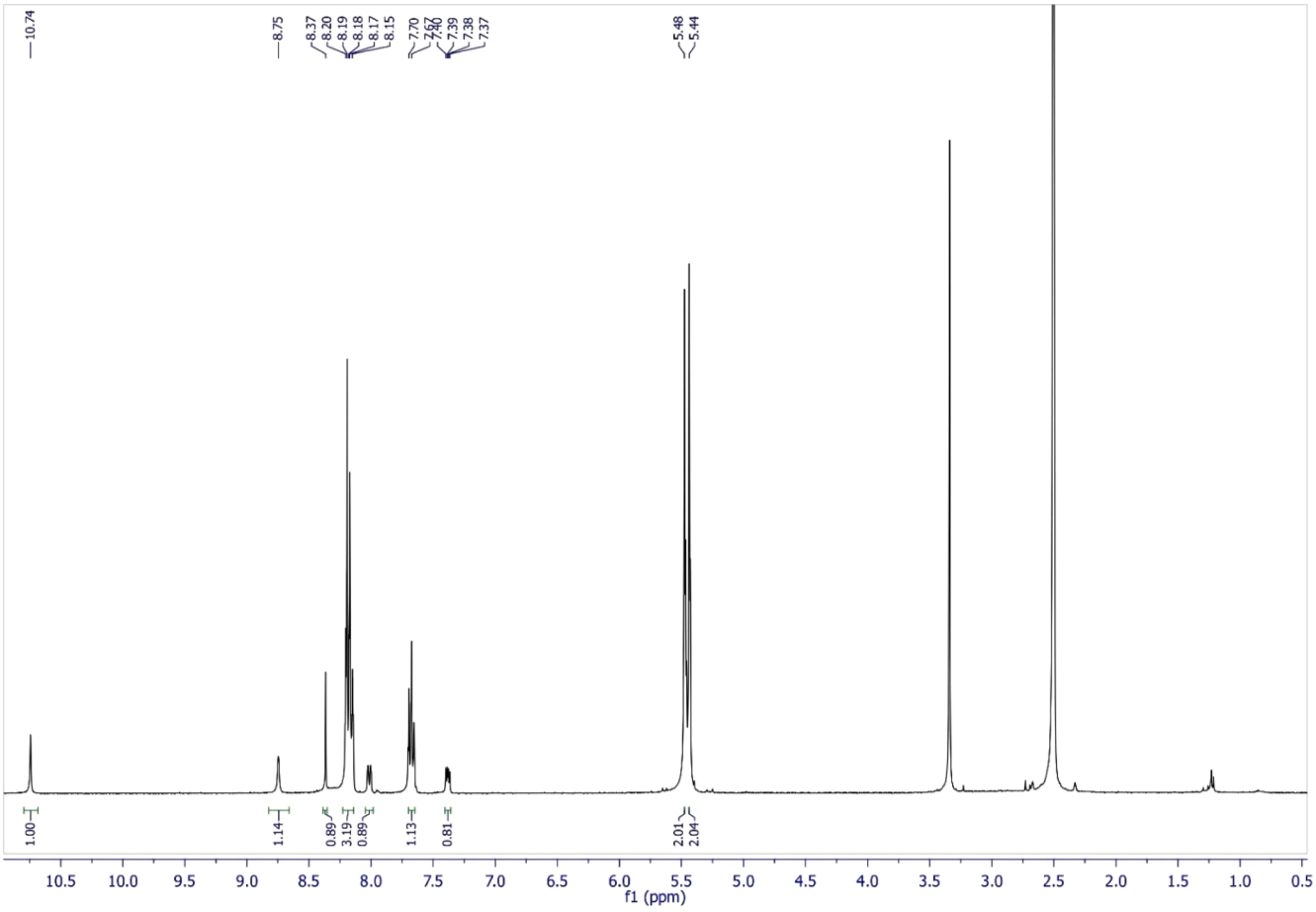

Fig. 32. ^{1}H NMR spectrum of compound SR13.

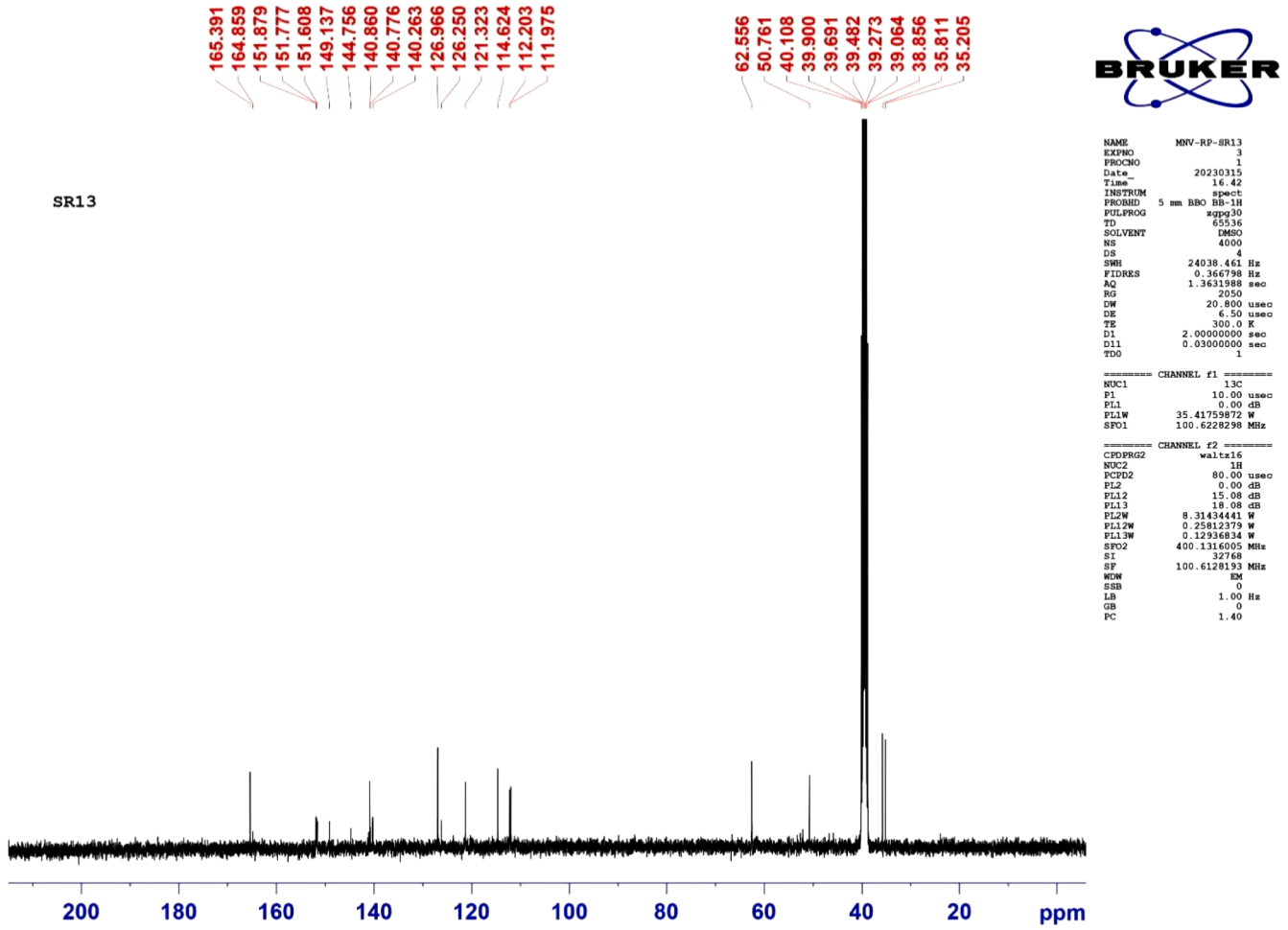

Fig. 33. ^{13}C NMR spectrum of compound SR13.

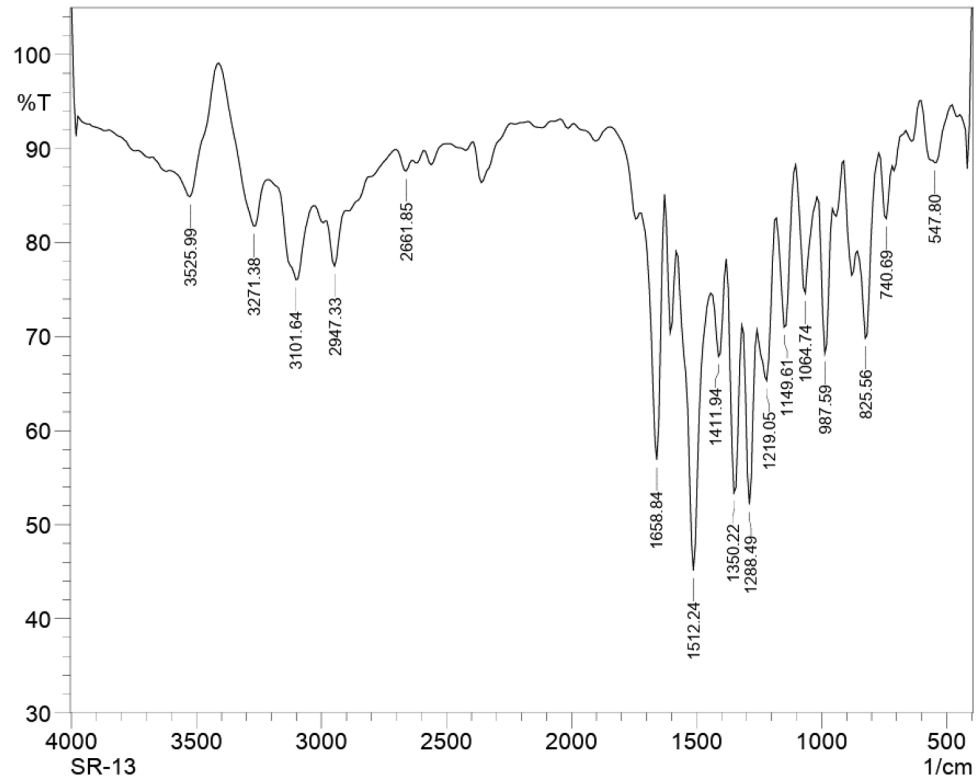

Fig. 34. IR spectrum of compound SR13.

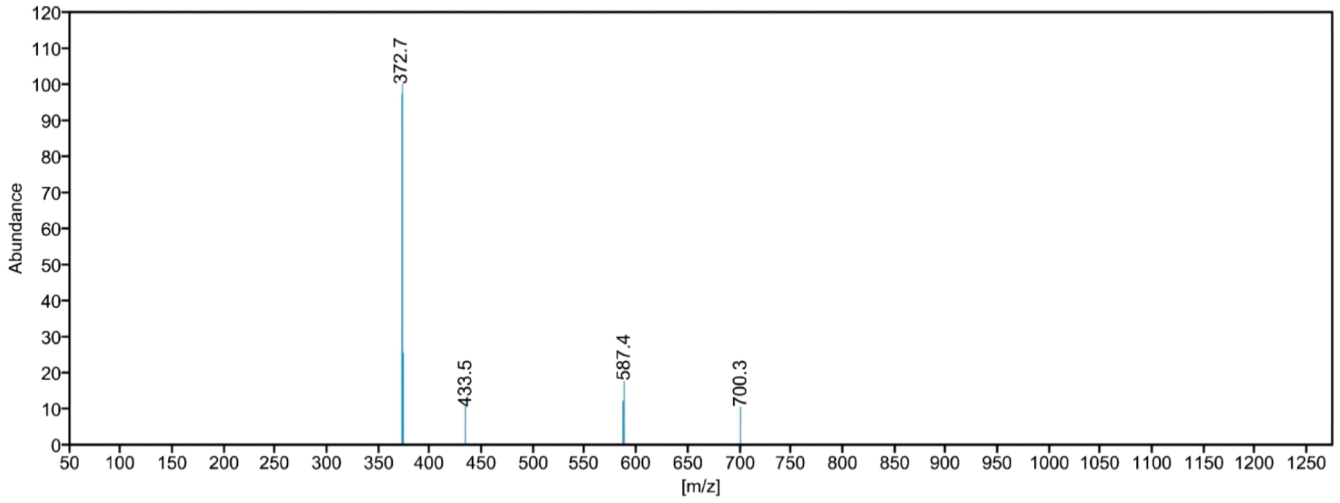

Fig. 35. Mass spectrum of compound SR13.

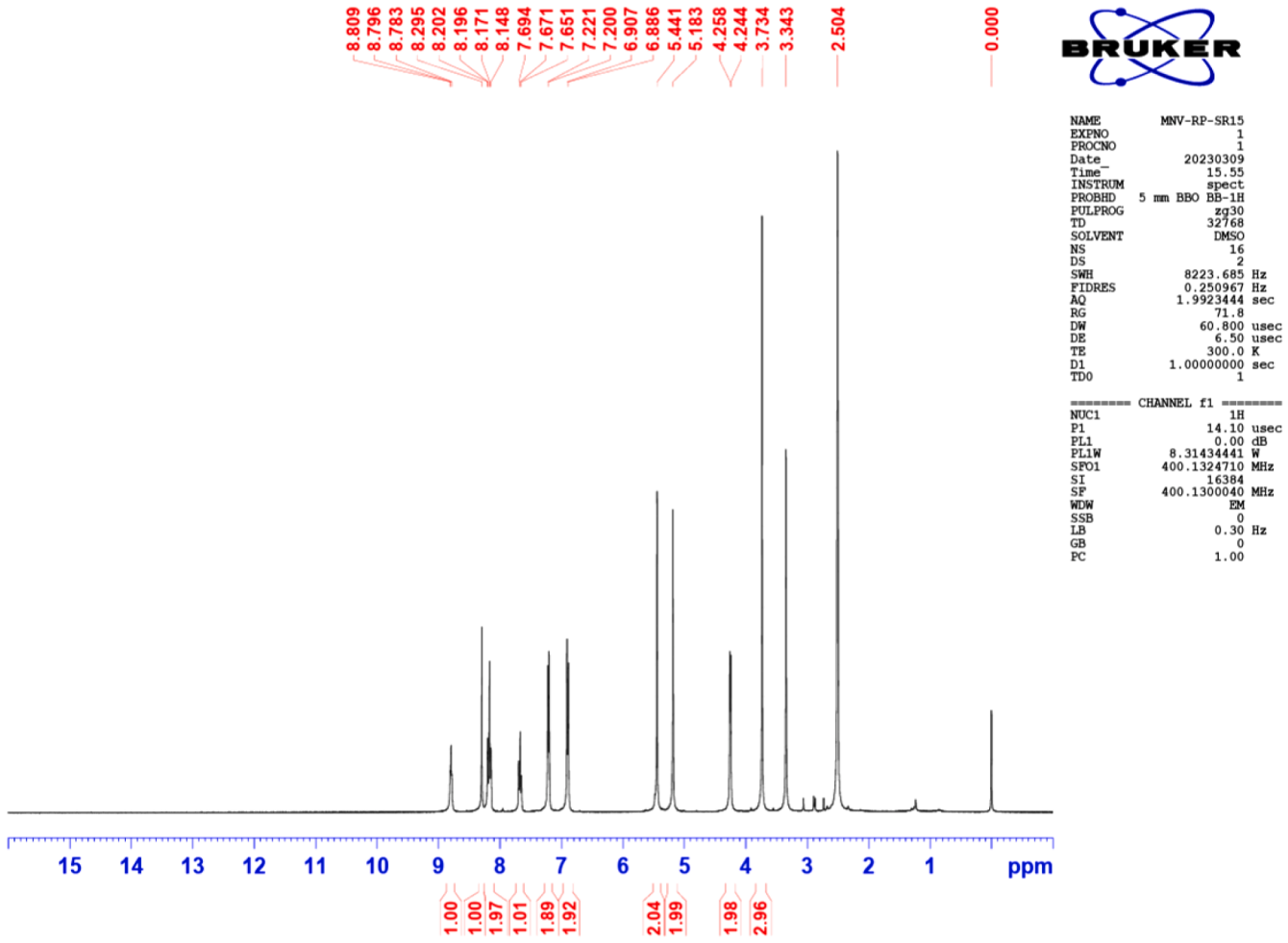

Fig. 36. ^{1}H NMR spectrum of compound SR15.

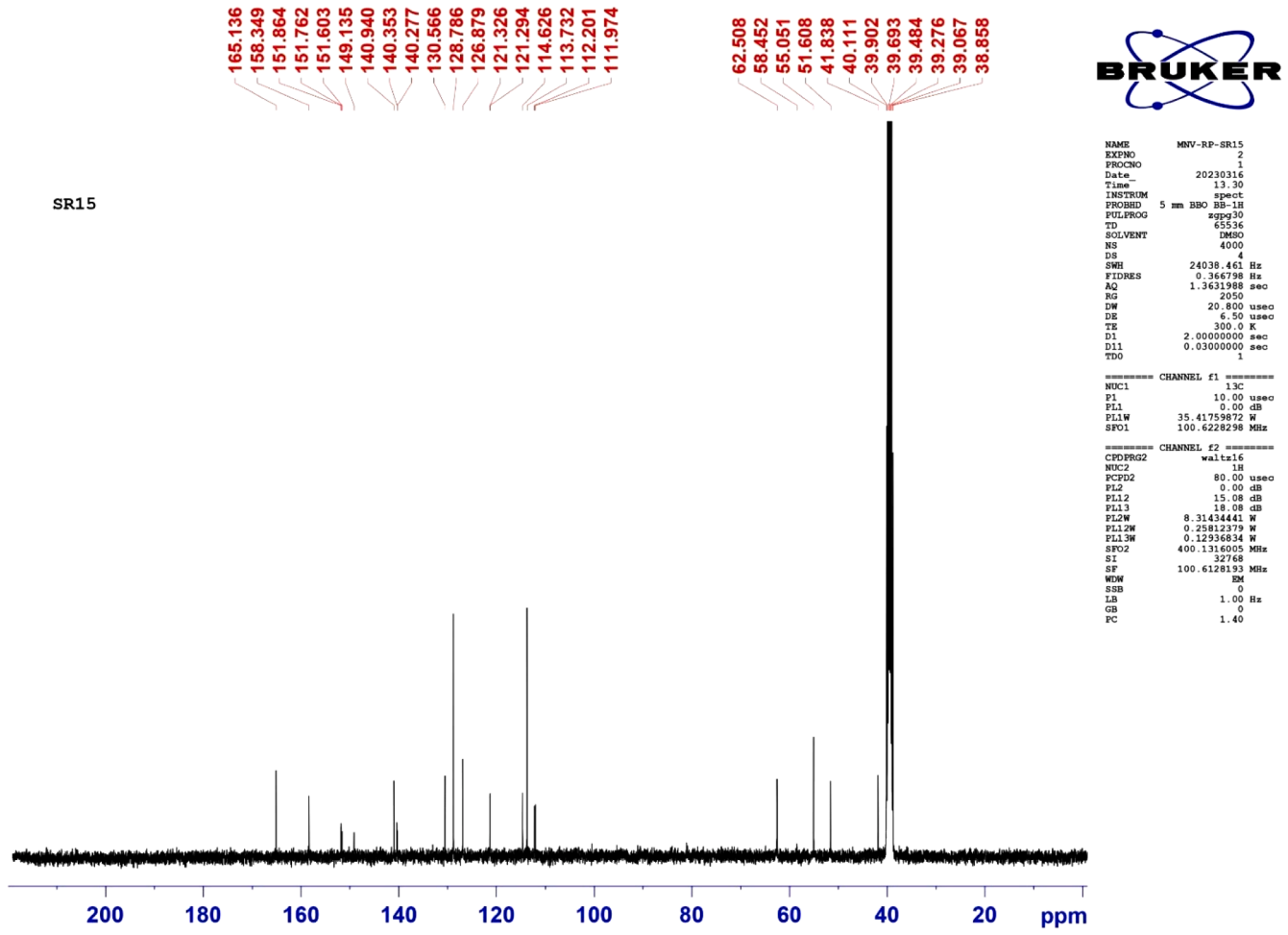

Fig. 37. ^{13}C NMR spectrum of compound SR15.

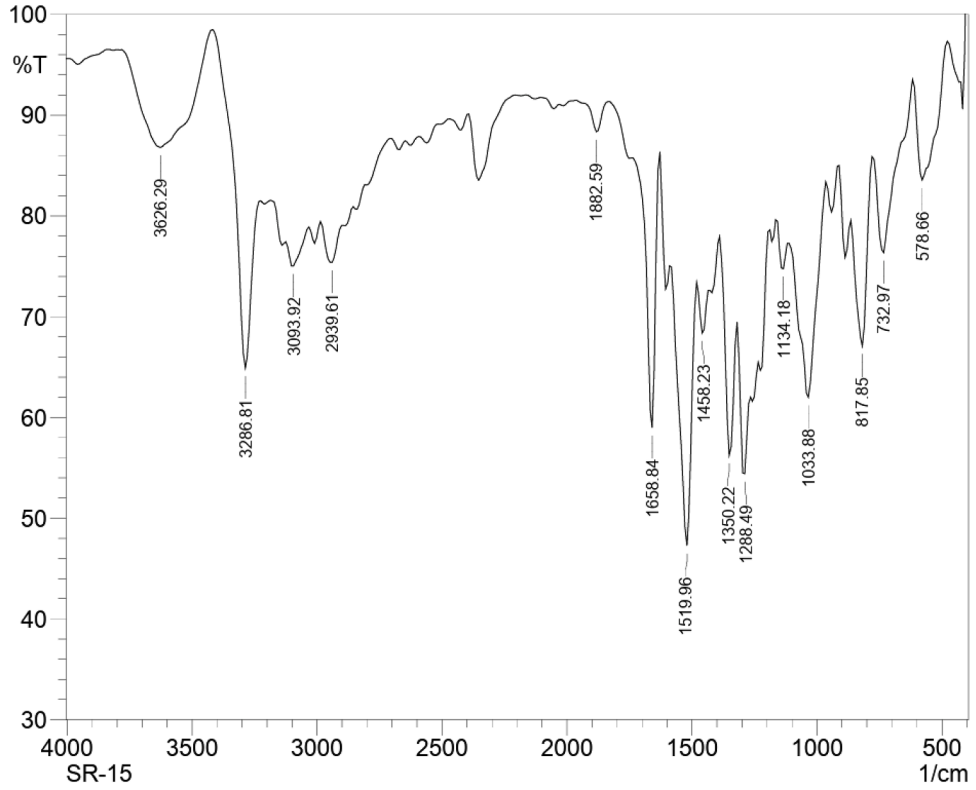

Fig. 38. IR spectrum of compound SR15.

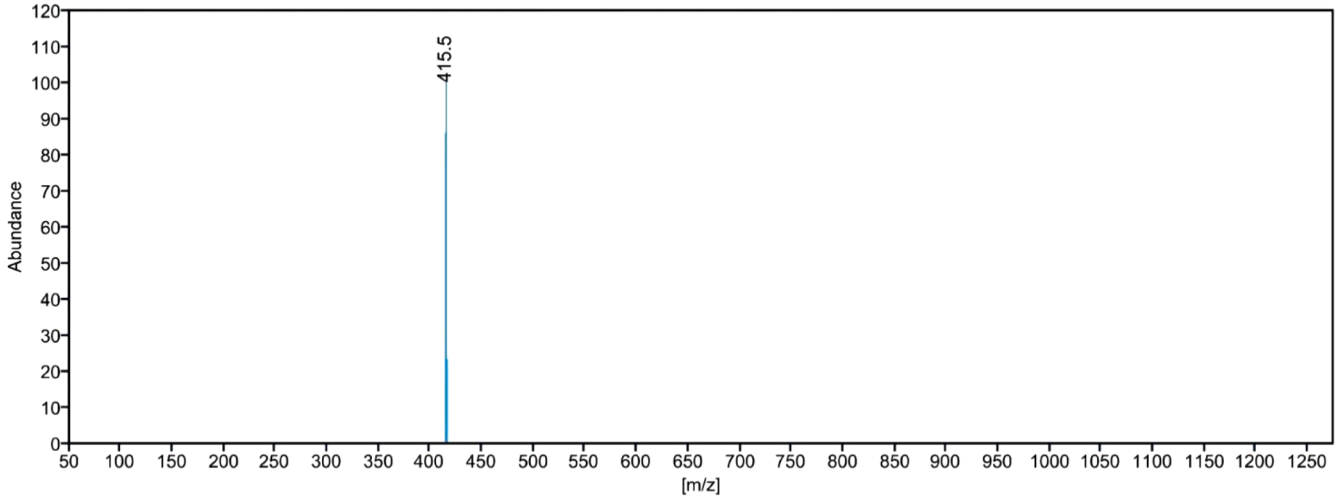

Fig. 39. Mass spectrum of compound SR15.

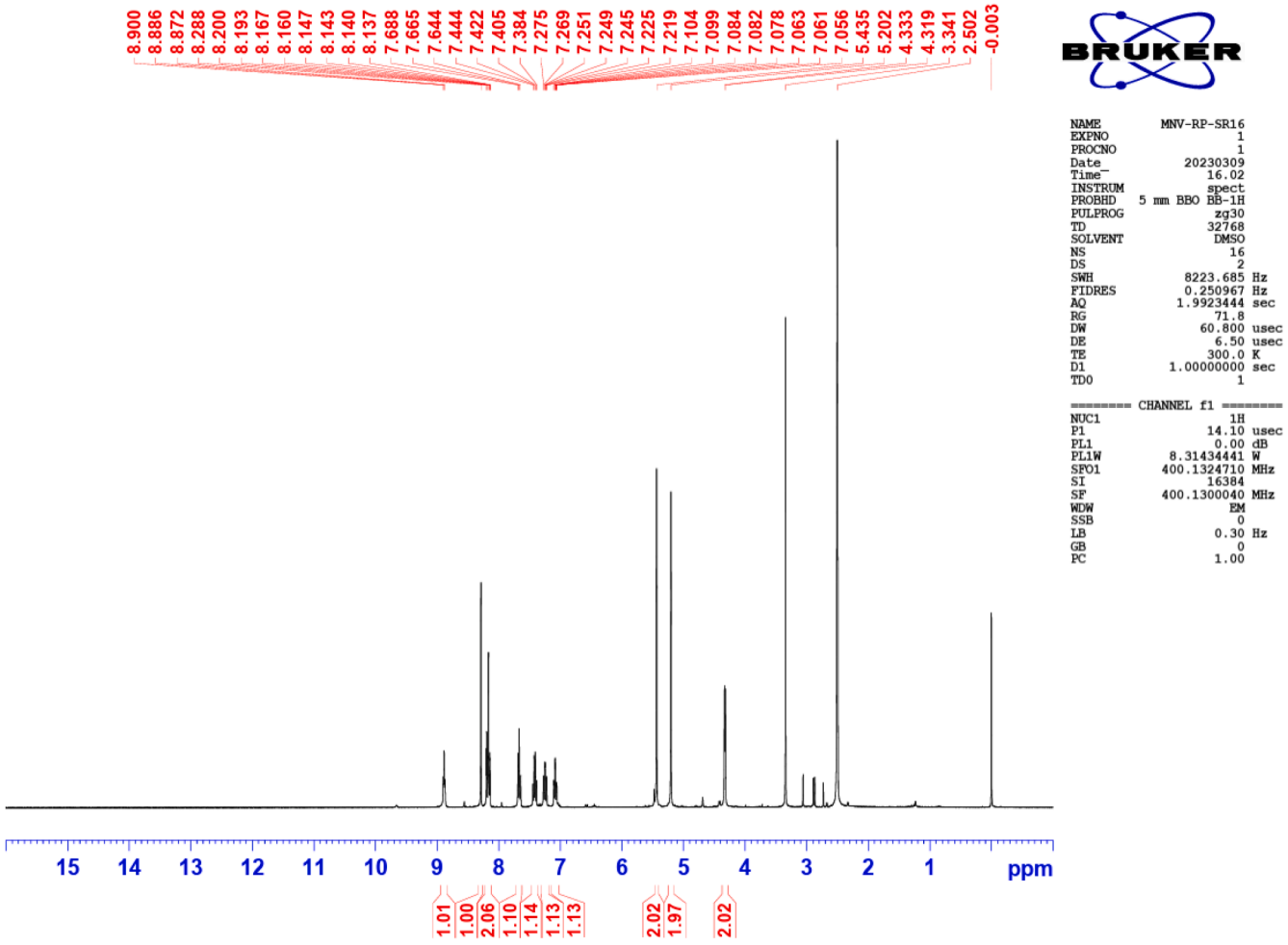

Fig. 40. ^{1}H NMR spectrum of compound SR16.

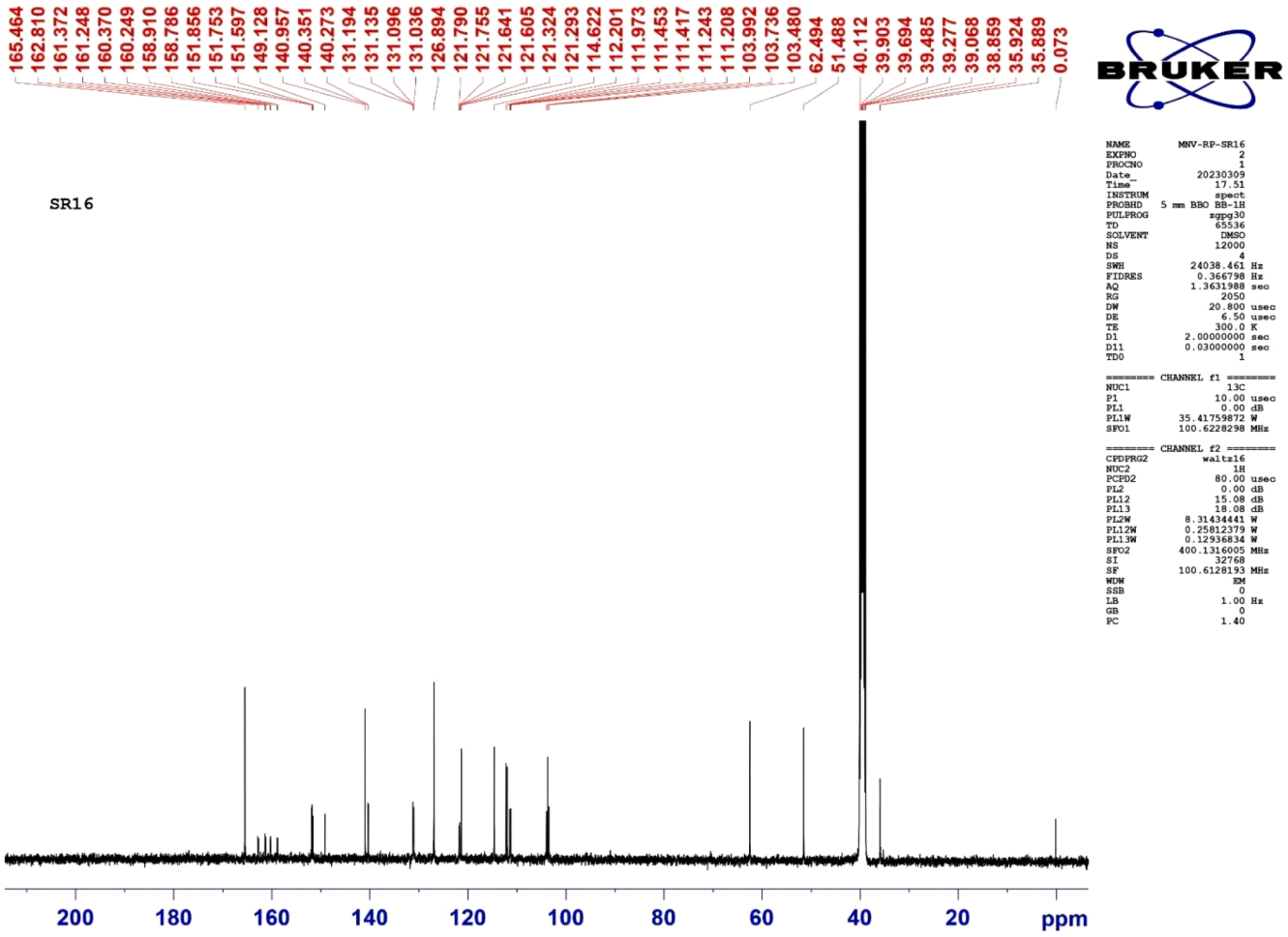

Fig. 41. ^{13}C NMR spectrum of compound SR16.

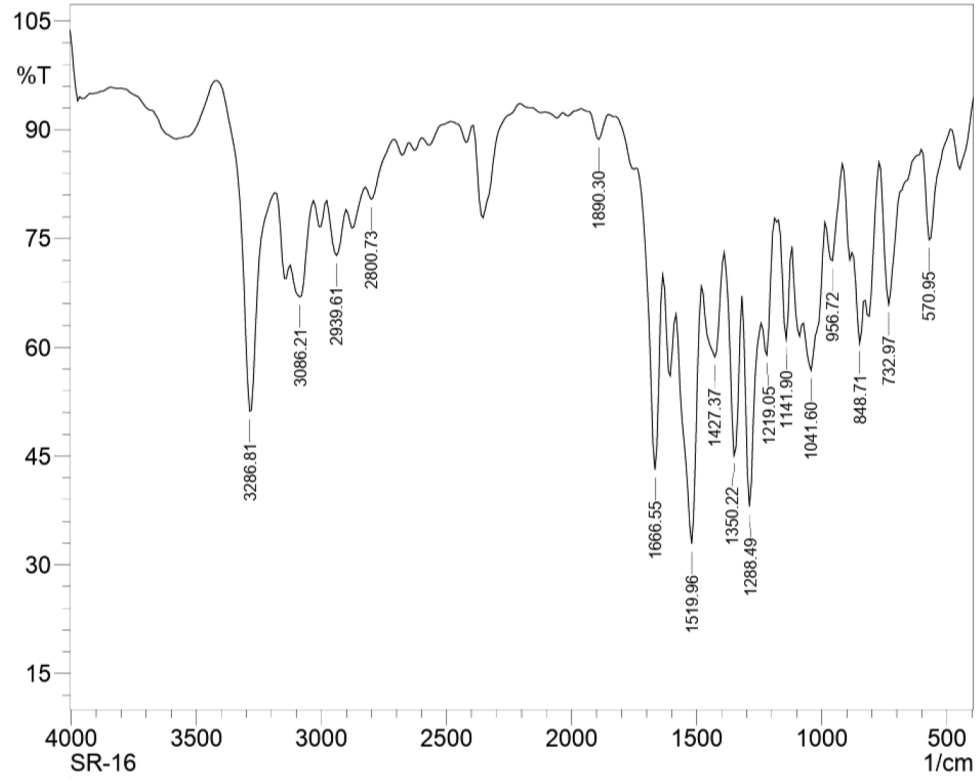

Fig. 42. IR spectrum of compound SR16.

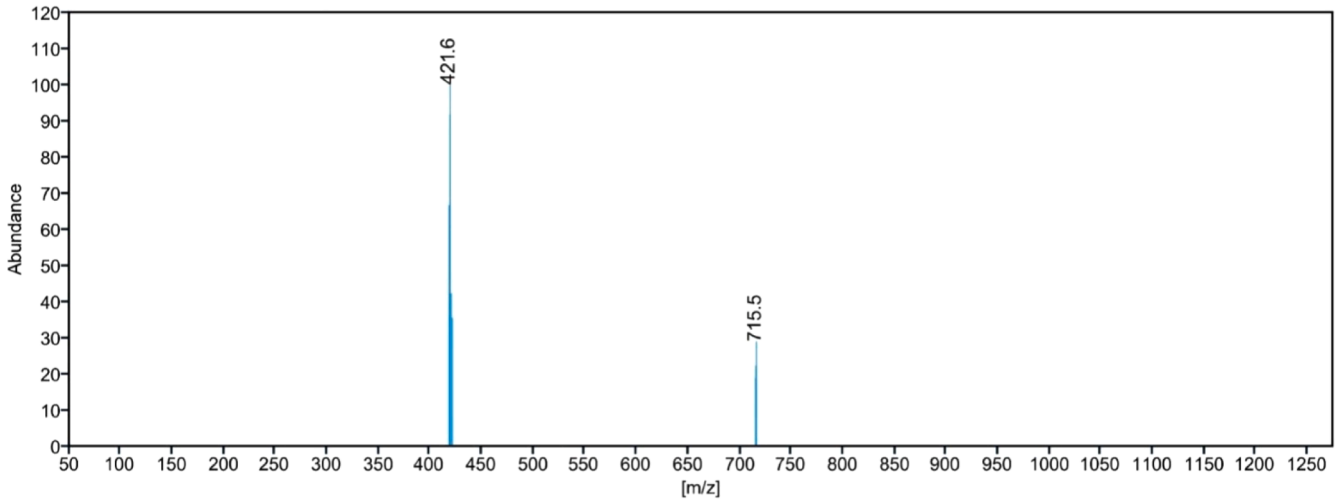

Fig. 43. Mass spectrum of compound SR16.

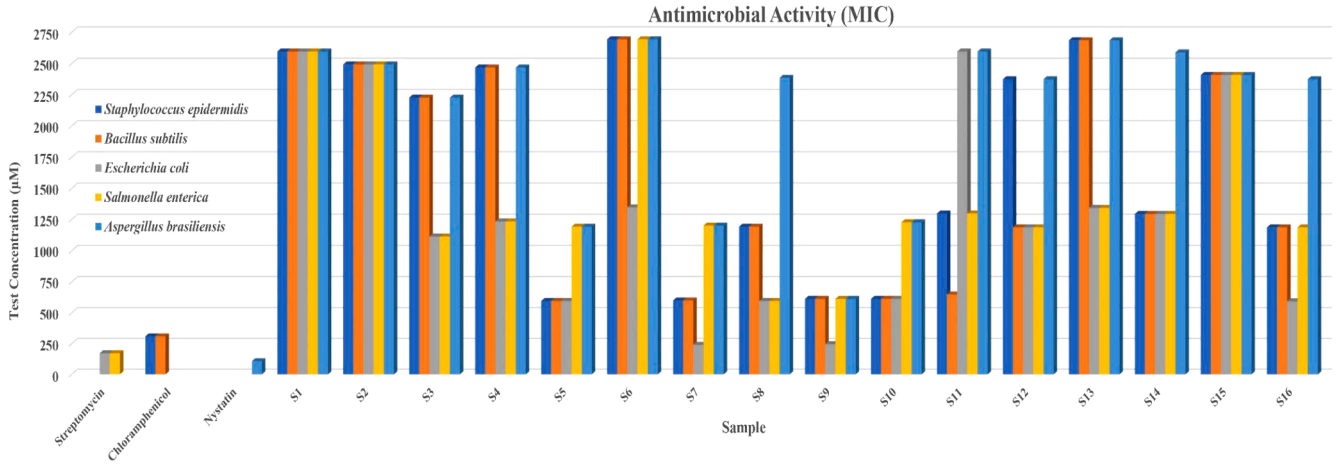

Fig. 44. A comparison of the antimicrobial activities of phenoxy methyl-1,2,3-triazoles derivatives (**SR1** to **SR16**) with standard drugs.

Data availability

Data will be made available on request.

Acknowledgements

We would like to convey our gratitude to the Department of Chemistry, Shri M. & N. Virani Science College (Autonomous), Rajkot (Gujarat), India for providing laboratory facilities to carry out the synthesis and antimicrobial screening of the derivatives. We are also grateful to the Department of Zoology, Biomedical Technology and Human Genetics, University School of Sciences, Gujarat University, Ahmedabad (Gujarat), India for antimalarial activity. The authors are thankful to the "National Facility for Drug Discovery" (NFDD) for instrumentation support.

Supplementary materials

Supplementary material associated with this article can be found, in the online version, at doi:10.1016/j.molstruc.2024.139381.

References

[1] WHO: World Health Organization, World Malaria Report, 2023. (2023).
[2] E.D. Benavente, E. Manko, J. Phelan, M. Campos, D. Nolder, D. Fernandez, G. Velez-Tobon, A.T. Castaño, J.G. Dombrowski, C.R.F. Marinho, Distinctive genetic structure and selection patterns in Plasmodium vivax from South Asia and East Africa, Nat. Commun. 12 (2021) 3160.
[3] K.E. Battle, J.K. Baird, The global burden of Plasmodium vivax malaria is obscure and insidious, PLoS. Med. 18 (2021) e1003799.
[4] R.N. Price, R.J. Commons, K.E. Battle, K. Thriemer, K. Mendis, Plasmodium vivax in the era of the shrinking P. falciparum map, Trends. Parasitol. 36 (2020) 560–570.
[5] Geneva, W.H.O., World Malaria Report 2016, World Heal. Organ., 2017.
[6] B. Aslam, W. Wang, M.I. Arshad, M. Khurshid, S. Muzammil, M.H. Rasool, M. A. Nisar, R.F. Alvi, M.A. Aslam, M.U. Qamar, Antibiotic resistance: a rundown of a global crisis, Infect. Drug Resist. (2018) 1645–1658.
[7] M.A.B. Lucien, M.F. Canarie, P.E. Kilgore, G. Jean-Denis, N. Fénélon, M. Pierre, M. Cerpa, G.A. Joseph, G. Maki, M.J. Zervos, Antibiotics and antimicrobial resistance in the COVID-19 era: perspective from resource-limited settings, Int. J. Infect. Dis. 104 (2021) 250–254.
[8] N. Kerru, L. Gummidi, S. Maddila, K.K. Gangu, S.B. Jonnalagadda, A review on recent advances in nitrogen-containing molecules and their biological applications, Molecules. 25 (2020) 1909.
[9] A. Oubella, A. Bimoussa, A. N'ait Oussidi, M. Fawzi, A. Auhmani, H. Morjani, A. Riahi, M. Esseffar, C. Parish, M.Y. Ait Itto, New 1, 2, 3-triazoles from (R)-carvone: synthesis, DFT mechanistic study and *in vitro* cytotoxic evaluation, Molecules. 27 (2022) 769.
[10] R.V. Parmar, M.S. Vadodaria, Synthesis, characterization and antimicrobial evaluation of novel imidazo [1, 2-a] pyrazine-linked 1, 2, 3-triazole derivatives via a click chemistry approach, Russ. J. Org. Chem. 59 (2023) 1927–1939.

[11] M.M. Alam, 1, 2, 3-Triazole hybrids as anticancer agents: a review, Arch. Pharm. (Weinheim). 355 (2022) 2100158.
[12] R.V. Parmar, M.S. Vadodaria, Click synthesis, characterization, mesomorphic properties, and antimicrobial evaluation of some novel imidazo [1, 2-a] pyrazine derivatives containing a 1, 2, 3-triazole ring, Russ. J. Org. Chem. 59 (2023) 2186–2194.
[13] L. Feng, M. Zheng, F. Zhao, D. Liu, 1, 2, 3-Triazole hybrids with anti-HIV-1 activity, Arch. Pharm. (Weinheim). 354 (2021) 2000163.
[14] L. Kumar, K. Lal, P. Yadav, A. Kumar, A.K. Paul, Synthesis, characterization, α-glucosidase inhibition and molecular modeling studies of some pyrazoline-1H-1, 2, 3-triazole hybrids, J. Mol. Struct. 1216 (2020) 128253.
[15] C.P. Kaushik, M. Chahal, Synthesis, antimalarial and antioxidant activity of coumarin appended 1, 4-disubstituted 1, 2, 3-triazoles, Monatshefte für Chemie-Chemical Mon 152 (2021) 1001–1012.
[16] T. Lengauer, M. Rarey, Computational methods for biomolecular docking, Curr. Opin. Struct. Biol. 6 (1996) 402–406.
[17] A. Kumar, S. Madderla, R. Dharavath, N. Nalaparaju, R. Katta, S. Gundu, V. Thumma, B. Prashanth, D. Ashok, Microwave assisted synthesis of N-substituted acridine-1, 8-dione derivatives: evaluation of antimicrobial activity, J. Heterocycl. Chem. 59 (2022) 1180–1190.
[18] C.M. Venkatachalam, X. Jiang, T. Oldfield, M. Waldman, LigandFit: a novel method for the shape-directed rapid docking of ligands to protein active sites, J. Mol. Graph. Model. 21 (2003) 289–307.
[19] F. Österberg, G.M. Morris, M.F. Sanner, A.J. Olson, D.S. Goodsell, Automated docking to multiple target structures: incorporation of protein mobility and structural water heterogeneity in AutoDock, Proteins Struct. Funct. Bioinforma. 46 (2002) 34–40.
[20] U. Abdulfatai, A. Uzairu, S. Uba, Molecular docking and quantitative structure-activity relationship study of anticonvulsant activity of aminobenzothiazole derivatives Beni-Suef University, J. Basic Appl. Sci. 7 (2018) 204–214.
[21] S. Dallakyan, A.J. Olson, Small-molecule library screening by docking with PyRx, Chem. Biol. methods Protoc. (2015) 243–250.
[22] O. Trott, A.J. Olson, AutoDock Vina: improving the speed and accuracy of docking with a new scoring function, efficient optimization, and multithreading, J. Comput. Chem. 31 (2010) 455–461.
[23] R.V. Parmar, M.S. Vadodaria, P.S. Gajera, Click chemistry" inspired synthesis and antimicrobial evaluation of 1, 2, 4-triazolo [4, 3-a] pyridine linked 1, 4-disubstituted 1, 2, 3-triazole Derivatives with Amide Functionalities, Indian J. Heterocycl. Chem. 34 (2024) 195–203.
[24] A. Daina, O. Michielin, V. Zoete, SwissADME: a free web tool to evaluate pharmacokinetics, drug-likeness and medicinal chemistry friendliness of small molecules, Sci. Rep. 7 (2017) 42717.
[25] J. Yuvaniyama, P. Chitnumsub, S. Kamchonwongpaisan, J. Vanichtanankul, W. Sirawaraporn, P. Taylor, M.D. Walkinshaw, Y. Yuthavong, Insights into antifolate resistance from malarial DHFR-TS structures, Nat. Struct. Mol. Biol. 10 (2003) 357–365.
[26] N.M. O'Boyle, M. Banck, C.A. James, C. Morley, T. Vandermeersch, G. R. Hutchison, Open Babel: an open chemical toolbox, J. Cheminform. 3 (2011) 1–14.
[27] L. George, U. Joshi, D. Jani, S. Guleria, H. Highland, Lantana camara L. aqueous-methanolic extract provides potent red blood cell membrane fortification against plasmodial attack, European J. Med. Plants. 11 (2016) 1–10.
[28] NCCLS (National Committee for Clinical Laboratory Standards) Twelfth Informational Supplement, I. 1-56238-, 454-6 M100-S12 (M7), 2002.
[29] S.T. Dhumal, A.R. Deshmukh, K.R. Kharat, B.R. Sathe, S.S. Chavan, R.A. Mane, Copper fluorapatite assisted synthesis of new 1, 2, 3-triazoles bearing a benzothiazolyl moiety and their antibacterial and anticancer activities, New J. Chem. 43 (2019) 7663–7673.
[30] C. Ferroni, A. Pepe, Y.S. Kim, S. Lee, A. Guerrini, M.D. Parenti, A. Tesei, A. Zamagni, M. Cortesi, N. Zaffaroni, 1, 4-Substituted triazoles as nonsteroidal anti-androgens for prostate cancer treatment, J. Med. Chem. 60 (2017) 3082–3093.
[31] G.N. Forrest, S. Mehta, E. Weekes, D.P. Lincalis, J.K. Johnson, R.A. Venezia, Impact of rapid in situ hybridization testing on coagulase-negative staphylococci positive blood cultures, J. Antimicrob. Chemother. 58 (2006) 154–158.
[32] Y.C. Martin, A bioavailability score, J. Med. Chem. 48 (2005) 3164–3170.
[33] C.A. Lipinski, Lead-and drug-like compounds: the rule-of-five revolution, Drug Discov. today Technol. 1 (2004) 337–341.
[34] P. Ertl, A. Schuffenhauer, Estimation of synthetic accessibility score of drug-like molecules based on molecular complexity and fragment contributions, J. Cheminform. 1 (2009) 1–11.
[35] K. Becker, C. Heilmann, G. Peters, Coagulase-negative staphylococci, Clin. Microbiol. Rev. 27 (2014) 870–926.
[36] H.A. Hong, R. Khaneja, N.M.K. Tam, A. Cazzato, S. Tan, M. Urdaci, A. Brisson, A. Gasbarrini, I. Barnes, S.M. Cutting, Bacillus subtilis isolated from the human gastrointestinal tract, Res. Microbiol. 160 (2009) 134–143.
[37] J.B. Kaper, J.P. Nataro, H.L.T. Mobley, Pathogenic escherichia coli, Nat. Rev. Microbiol. 2 (2004) 123–140.
[38] O. Gal-Mor, E.C. Boyle, G.A. Grassl, Same species, different diseases: how and why typhoidal and non-typhoidal Salmonella enterica serovars differ, Front. Microbiol. 5 (2014) 391.
[39] R.P. de Vries, J. Visser, Aspergillus enzymes involved in degradation of plant cell wall polysaccharides, Microbiol. Mol. Biol. Rev. 65 (2001) 497–522.